

| | |
|---|-----------|
| Time Dependent Evaluation of the Influence of Cadmium and Iron on Their Respective Hepatotoxic Effects In Wistar Rats Obadoni Ashinedu Isabel and Obi Fredrick Otunuya | 01 |
| A Special Family Of Parameter Dependent Nested Hybrid Multistep Methods For Solving Biological And Epidemiological Problems Akhanolu Gilbert Aziegbe & Agbeboh Goddy Ujagbe | 10 |
| Development Of A Fifth Stage, Fourth Order Runge-kutta Method For The Solution Of Initial Value Problems In Ordinary Differential Equations Agbeboh Goddy Ujagbe, Ehiemua Michael Ebhodaghe & Okoruwa Gregory Ogbeide | 19 |
| Two-point Continuous Fourth Derivative Block Methods For Solving Stiff Systems of First Order Ordinary Differential Equations (ODEs) Ukpebor Luke Azeta, Elakhe Ohiomiogue Abraham, Adoghe L. Osa. & Ehapa Precious | 30 |
| A Quartic Based Denominator Of Order Six Rational Integrator Elakhe Ohiomiogue Abraham, Ehika Edith & Ehika Simon | 39 |
| Application Of Electrical Resistivity Tomography For The Delineation Of Deformational Structures: A Case Study Of AAU, Ekpoma, Edo State Airewele Ehizokhale, Ozegin Kesyton Oyamenda, Salufu Samuel Obomheile & Iyoha Abraham | 48 |
| Geophysical Evaluation Of Aquiferous Zone And Its Protective Capacity Rating Using Electrical Resistivity Method Within The Ugbowo Campus Of University Of Benin, Benin City, Edo State, Nigeria. Can-voro O. Amadasun, Salami A. Sikiru, Babafemi E. Muyiwa & Jegede I. Samson | 56 |
| Geological And Geophysical Controls Of Groundwater Occurrence In Ekpoma And Irrua Towns Of Edo State Nigeria Oboh Mathew Edenaruese & Ujuanbi Omeimen | 65 |
| An Evaluation Of The Physico-chemical Properties Affecting The Erodibility Of Soils In Gullies Okojie Usinomen Victor, Isitekhale Harry, Salufu Obomheile Samuel, Ufuah Emmanuel, Akhirevbulu Ojeabu Ehijie, Onogbosele Oziegbe Cyril & Okiti Mohammad Okemukoko | 79 |

AAUJPAS

AMBROSE ALLI UNIVERSITY JOURNAL OF PHYSICAL & APPLIED SCIENCES

ISSN: 2756-3200

AMBROSE ALLI UNIVERSITY JOURNAL OF PHYSICAL & APPLIED SCIENCES



Volume 2, Number 1, July, 2020

International coverage of all aspects of Physical Sciences

Published by the Faculty of Physical Sciences

Ambrose Alli University, Ekpoma

AMBROSE ALLI UNIVERSITY
JOURNAL OF PHYSICAL & APPLIED SCIENCES.
(AAUJPAS)
Volume 2, No 1, July, 2020

AMBROSE ALLI UNIVERSITY JOURNAL OF PHYSICAL & APPLIED SCIENCES. Volume 2, No 1, July, 2020

Editorial Board

Editorial- In Chief/ Chairman

Prof. O. Ujuanbi

Editorial Board Members

Prof. F.M Okoro

Prof. S.O Azi

Prof. Francis Osaigede

Prof. M. O. Osuide

Prof. I. O. Asia

Prof. V. U. Okojie

Prof. G. U. Agbeboh

Prof. C. E. Abhulimen

Prof. I. Aigbedion

Prof. S. E. Iyayi

Prof. C. U. Onianwa

Prof. F. O. Ikpotokin

Prof. I. B. A. Momodu

Editorial Advisers

Emeritus Prof. J. E. A. Osemeikhian

Prof. S. A. Okecha

Prof. E. Ukpebor

Prof. U. S. U. Aashikpelokhai

Prof. F. E. Okieimen

Prof. S. Chiemeke

Prof. S. O. Anigbogun

Business Manager

Dr. O. A. Elakhe

Department of Mathematics

Faculty of Physical Science,

Ambrose Alli University, Ekpoma,

Edo State, Nigeria.

e.mail:drelakheoa@aauekpoma.edu.ng

+2348039611725

Editorial Notice

The Ambrose Alli University Journal of Physical and Applied Science (AAUJPAS), the official publication of the Faculty of Physical Science (FPS), Ambrose Alli University, Ekpoma, Nigeria publishes research papers, review articles, notes and short communications that are of high-quality, original and relevant to fundamental and applied aspects of all areas of physical and applied sciences.

Aim and Scope

The Ambrose Alli University Journal of physical and applied sciences aim to provide a platform for scientist and academics to promote, share and discuss fundamental and applied aspects of all areas of physical sciences and technology provided that there are some advances in knowledge presented by the work. The Journal provides an articulate and formidable platform to drive and actualize the mission and vision of Ambrose Alli University through science and technology.

Correspondence

All correspondence including manuscripts for publication should be addressed to:

Prof. O. Ujuanbi,

Editor-in-chief,

Department of Physics,

Faculty of Physical Sciences

Ambrose Alli University, Ekpoma,

Edo State, Nigeria

e-mail-omiujuanbi@aauekpoma.edu.ng

Instruction to Authors

Submission of Manuscripts

Conditions

Submission of a manuscripts implies that the work described has not been published before (except in the form of an abstract or thesis); that it is not under consideration for publication elsewhere, that its publication has been approved by all authors, if any, as well as by the responsible authorities at the research institute where the work was carried out. The Editor-in-chief reserves the right to modify the style and length of a contribution.

Typing

All manuscripts must be in English Language, original and typeset in Microsoft word in double spacing with 2.5cm margins on all sizes on A4 sizes with a font type of Times New Roman and font size 12, and sent electronically to the editor-in-chief of the Ambrose Alli University Journal of Physical and Applied Sciences (AAUJPAS) by e-mail as attached file to jpas@aauekpoma.edu.ng. First author's surname and sub theme should be used as subject of the mail. The Manuscript must not have been submitted to any other Journal for publication. All equations must be numbered and typed using Equation Editor. The Standard international (SI) system of unit should be used in all the manuscripts. Unusual symbols, abbreviations or notation should be defined

when first mentioned in the text.

Title

The title of a manuscripts should be descriptive, concise and capture the theme as clearly as possible.

Name(s) and Address (es)

The name(s) and the address(es) of the author(s) should be given below the title of each manuscripts. The e-mail address of the corresponding authors must be clearly identified on this page.

Abstract

Each manuscripts should have a single paragraph abstract placed on the first page. This page should carry the title of the manuscript. The abstract should be brief summary of the content and conclusions of the paper not exceeding 250 words.

Text

Text should be organized as follows: introduction, methods, results and discussions. The introduction should describe the purpose of the study and its relation to previous work in the area of study. Methods should be concise but sufficiently detailed to permit replication by other researchers. Results should present relevant positive and negative findings of the study, supported where necessary by references to tables and figures. The discussion should interpret the results of the study with emphasis on their relation to the original concept and to previous studies.

Figures and Table

Titles for figures should be placed below,

AAUJPAS

while that of the tables should be placed above. All tables, figures and references must be cited in the body of the paper. Tables and figures should be numbered in the order in which they are cited in the text. All graphs and figures should be neatly drawn or plotted and bold enough in case of enlargement.

Acknowledgement

Acknowledgement if any, of those who contributed to the research or preparation of the paper should follow text, as well as the acknowledgment of grants and other support.

References

References should be cited using APA style by just writing the name of the author followed by year of publication in brackets, title of the paper (or textbook) and journal where published, volume of the journal and pages. An example is: Asia I. O. (2011). Industrial sludge treatment options. *Journal of Nig. Chemical Soc...*Vol.23. Pp.36-55.

For books, give the authors(s) names, date of publications, title of the book italicized with initial letters capitalized, edition, page references, publishers name and place of publication. An example is BENNET, M.K. (2010). *The world's food 1st ed.* Pp. 55-68. Harper & Brothers, New York.

Acceptance and publication of manuscripts

Authors will be notified via a acceptance letter after the final acceptance of the manuscripts by the Editor. The accepted manuscripts will be immediately copy edited, typeset, paginated and proofread for eventual publication in the next issue of the Journal.

Fees

Authors of accepted manuscripts are required to pay handling and publication fees of twenty thousand naira (N2000.00) only. Five Thousand (N5000.00) naira of the said amount should accompany the manuscript submission. Please note that fully typed work on A4 paper that exceeds ten (10) pages will attract extra charge(s) per extra page.

CONTENTS

| | |
|---|-----------|
| Time Dependent Evaluation of the Influence of Cadmium and Iron on Their Respective Hepatotoxic Effects In Wistar Rats Obadoni Ashinedu Isabel and Obi Fredrick Otunuya | 01 |
| A Special Family Of Parameter Dependent Nested Hybrid Multistep Methods For Solving Biological And Epidemiological Problems Akhanolu Gilbert Aziegbe & Agbeboh Goddy Ujagbe | 10 |
| Development Of A Fifth Stage, Fourth Order Runge–kutta Method For The Solution Of Initial Value Problems In Ordinary Differential Equations Agbeboh Goddy Ujagbe, Ehiemua Michael Ebhodaghe & Okoruwa Gregory Ogbeide | 19 |
| Two–point Continuous Fourth Derivative Block Methods For Solving Stiff Systems of First Order Ordinary Differential Equations (ODEs) Ukpebor Luke Azeta, Elakhe Ohiomioque Abraham, Adoghe L. Osa. & Ehapa Precious | 30 |
| A Quartic Based Denominator Of Order Six Rational Integrator Elakhe Ohiomioque Abraham, Ehika Edith & Ehika Simon | 39 |
| Application Of Electrical Resistivity Tomography For The Delineation Of Deformational Structures: A Case Study Of AAU, Ekpoma, Edo State Airewele Ehizokhale, Ozegin Kesyton Oyamenda, Salufu Samuel Obomheile & Iyoha Abraham | 48 |
| Geophysical Evaluation Of Aquiferous Zone And Its Protective Capacity Rating Using Electrical Resistivity Method Within The Ugbowo Campus Of University Of Benin, Benin City, Edo State, Nigeria. Can-voro O. Amadasun, Salami A. Sikiru, Babafemi E. Muyiwa & Jegede I. Samson | 56 |
| Geological And Geophysical Controls Of Groundwater Occurrence In Ekpoma And Irrua Towns Of Edo State Nigeria Oboh Mathew Edenaruese & Ujuanbi Omeimen | 65 |
| An Evaluation Of The Physico–chemical Properties Affecting The Erodibility Of Soils In Gullies Okojie Usinomen Victor, Isitekhale Harry, Salufu Obomheile Samuel, Ufuah Emmanuel, Akhirevbulu Ojeabu Ehijie, Onogbosele Oziegbe Cyril & Okiti Mohammad Okemukoko | 79 |

TIME DEPENDENT EVALUATION OF THE INFLUENCE OF CADMIUM AND IRON ON THEIR RESPECTIVE HEPATOTOXIC EFFECTS IN WISTAR RATS

Obadoni Ashinedu Isabel and Obi Fredrick Otunuya

Department of Biochemistry, University of Benin, Benin City, Nigeria

Abstract

Heavy metals that pollute the air, water and soil rarely exist in isolation. So, humans and animals are usually exposed to these agents in combinations of two or more concurrently. In this study, the influence of ferrous sulphate (FeSO_4) and cadmium chloride (CdCl_2) on hepatotoxic capacity of each other was examined in rats exposed to these substances via tainted water and feed formulated with iron and cadmium pre-exposed catfish. In both protocols, the exposure was for 1, 2, and 3 months. The concentrations of FeSO_4 and CdCl_2 in the water provided to the rats directly are 1.90 mg Fe and 0.229 mg Cd per liter respectively. In both phases group A served as control while groups B to group D were test groups. At the end of three months of tainted water treatment and the ends of 1, 2 and 3 months of tainted diet treatment, CdCl_2 caused significantly ($p < 0.05$) increased serum alanine and aspartate aminotransferase activities compared to the control, the FeSO_4 only and CdCl_2 plus FeSO_4 groups. Direct and total bilirubin levels were significantly ($p < 0.05$) higher in the serum of CdCl_2 only group exposed via water or feed relative to the control, the FeSO_4 only and combined groups at the end of second and third months. Rats exposed to CdCl_2 only via water or feed had significantly ($p < 0.05$) decreased catalase and superoxide dismutase activities at the ends of 1, 2 and 3 months respectively, relative to the control and FeSO_4 only group but an increase compared to the combined group values. Malondialdehyde level was significantly ($p < 0.05$) increased in the CdCl_2 only group at the end of each exposure duration relative to control, but a decrease in the combined exposed via water at the end of 2 and 3 months and at the end of each exposure duration for those exposed via feed. These results suggest that FeSO_4 ameliorates the hepatotoxic effects of CdCl_2 in rats.

Keywords: cadmium chloride; ferrous sulphate; hepatotoxic effects; antioxidant

Introduction:

Heavy metals are conventionally defined as elements with metallic properties having atomic number >20 and density $> 5 \text{ g/cm}^3$. They are inorganic elements essential for plant growth in trace amounts, toxic in relatively higher concentrations, biologically un-degradable but easily assimilated and bio-accumulated in the protoplasm of aquatic organisms (Egborge, 1994). Humans and other animals interact with their environments on a daily basis and consequently are exposed to a broad spectrum of chemicals present

in the food they eat, the air they breathe and the water they drink (Wade *et al.*, 2002).

Cadmium is a widespread toxic environmental and industrial pollutant. It is unique among the toxic heavy metals because of its toxicity at a very low body burden, long biological half-life (30 years in human) as well as its low rate of excretion from the body (Cuypers *et al.*, 2010). Cadmium is carcinogenic for a number of tissues (Waalkes, 2000). In laboratory animals, acute Cd exposure produces, primarily, hepatic and testicular injury as well as respiratory tract irritation. Chronic exposure on the other hand results in renal damage, anaemia, and immuno- and osteotoxicity (Tim *et al.*, 2008). Although, many studies have reported the toxic and carcinogenic effects of metals in humans and animals (Mahtap and Ethem, 2006); it is also well known that these metals play crucial roles in normal biological functions of cells. Being

Corresponding Author: Obadoni A Isabel
Department of Biochemistry,
University of Benin, Benin City
ashiobadoni@gmail.com

a toxic metal, it is likely that there is no specific transport protein for cadmium. However, because it has similar chemical and physical properties to essential metals such as iron (Fe), zinc (Zn) and calcium (Ca), it can be transported and taken up into the cells by a process referred to as ionic and molecular mimicry (Vesey, 2010). Several essential trace elements like zinc (Zn), copper (Cu), selenium (Se) and iron (Fe) participate in controlling various metabolic and signaling pathways.

In vitro studies suggest there is competition for sites on transport proteins between Cd and some essential trace elements like Zn and Cu (Hakan *et al.*, 2001), Se (Hijova and Nistiar, 2005), Fe (Hakan *et al.*, 2001) in rats, Zn and Se in Japanese quails (Nad *et al.*, 2005) and Ca in suckling rats (Saric *et al.*, 2002). Iron is an essential element for almost all living organisms as it participates in a wide variety of metabolic processes including oxygen transport, DNA synthesis and electron transport. It is also a vital component of other enzymes and proteins. Disorders of iron metabolism are among the most common diseases of humans and encompass a broad spectrum of diseases such as anaemia, iron overload and possibly neurodegenerative diseases (Saric *et al.*, 2002).

Ingestion of water polluted by a mixture of heavy metals and/or the eating of fishes therefrom, amounts to double exposure. The contaminants can augment or antagonize the toxic capacity of one another, which may not be apparent when each is studied in seclusion. Therefore, the need to clearly outline the toxic potential of a heavy metal when examined alone from its toxic ability when it co-exists in an environment with other metallic contaminants is the primary reason for this study.

MATERIALS AND METHODS

Materials

a. Catfish

Two hundred catfish, of mean weight, 120.00 ± 3.15 g were obtained from Diamond Fish Farms by Muritala Mohammed Way, Benin city.

b. Albino rats

Sixty male albino rats (Wistar strain) with an average weight of 172.45 ± 6.23 g were used for the water mediated cadmium exposure while forty eight rats (162.45 ± 7.52 g) were used for the food chain mediated exposure. Rats used were obtained from the Department of Biochemistry's animal

house, University of Benin. Rats were housed in the Department of Biochemistry Animal House under standard laboratory conditions (12-hour light/dark cycle, 22–28°C and 40–60% humidity) and veterinary management. All animal experiments were performed in adherence to the NIH animal guidelines.

3. Salts

The salts were obtained from Pyrex Chemicals, No 65 First East Circular Road, Benin City and Liab Laboratories and Pharmacy, No 48 Apapa Road, Lagos.

Methods

a. Treatment of Experimental Animals.

I. Catfish

All the fishes were acclimatized for twenty one days before the commencement of the studies. The first group (A) was the control. Fishes in this group were kept in uncontaminated water. Group B were maintained in ferrous sulphate contaminated water (equivalent to 1.90 mg Fe/L). Group C were kept in cadmium chloride contaminated water (equivalent to 0.239 mg Cd/L). Group D were maintained in water contaminated with ferrous sulphate and cadmium chloride (equivalent to 1.90 mg Fe/L and 0.239 mg Cd/L). Twenty five fishes were maintained in bowls containing thirty (30) liters of the different solutions. The solutions were changed every twenty four hours. After ninety days, all the fishes were weighed, sacrificed, oven dried, milled and incorporated in the test and control diets respectively, as sources of protein. The compositions of the diets are as shown in Table 1.

II. Albino rats

a. Exposure of rats via drinking water.

Rats were divided randomly into four experimental groups of five rats each, housed in wood-frame cages. Group A rats were maintained on feed (growers mash from Bendel Feeds and Flour Mill, Ewu, Edo State) and untainted water. Group B rats were given a solution of ferrous sulphate (1.90 mg Fe/L) and feed. Group C were given a solution of cadmium chloride (0.239 mg Cd/L) and feed. Group D rats were maintained on a solution of ferrous sulphate and cadmium chloride (1.90 mg Fe/L + 0.239 mg Cd/L) and feed. Rats in each group received the equivalent of 3 litres of the appropriate salt in water /70 kg body weight /day by gavage. Following the administration, all rats were allowed free access to feed and the appropriate solution. Each group had three replicates for the one, two and three month's treatment plan.

b. Exposure of rats via diet

Forty-eight rats used were divided into 4 groups of 4 rats each, housed in wood-framed, iron mesh cages. The duration of the treatments was thirty, sixty and ninety days respectively. The first group of rats, the control (group A) were fed with control diet (CD). Group B rats were fed with ferrous sulphate contaminated diet (TD1). Group C rats were fed with cadmium chloride contaminated diet (TD2). Group D rats were fed with cadmium chloride and ferrous sulphate contaminated diet (TD3). The test and control rats were pair fed, that is, the control rats were fed the same quantity of feed consumed by the corresponding test rat on the previous day. All rats were allowed free access to drinking water. The various combinations are as shown in Table 1. The groups were in three replicates for the different duration of the treatment plan.

Table 1: Composition of control and test diets showing levels of milled fish incorporated

| Ingredients | Percentage Composition (%) | | | |
|---|----------------------------|-------------------|-------------------|-------------------|
| | Control diet (CD) | Test diet 1 (TD1) | Test diet 2 (TD2) | Test diet 3 (TD3) |
| Cadmium chloride and Ferrous sulphate free milled catfish | 22.00 | 0.00 | 0.00 | 0.00 |
| Ferrous sulphate exposed milled catfish | 0.00 | 22.00 | 0.00 | 0.00 |
| Cadmium chloride exposed milled catfish | 0.00 | 0.00 | 22.00 | 0.00 |
| Cadmium chloride and Ferrous sulphate exposed milled fish | 0.00 | 0.00 | 0.00 | 22.00 |
| Corn starch | 53.00 | 53.00 | 53.00 | 53.00 |
| Sugar | 05.00 | 05.00 | 05.00 | 05.00 |
| Palm oil | 07.00 | 07.00 | 07.00 | 07.00 |
| Dried peanut husk | 08.00 | 08.00 | 08.00 | 08.00 |
| ABC multivitamins | 05.00 | 05.00 | 05.00 | 05.00 |

Animal Sacrifice and Sample Collection

After intervals of thirty, sixty and ninety days respectively, each rat was sacrificed and blood was obtained by cardiac puncture using hypodermic syringe and needle. The liver was excised, placed on ice and subsequently weighed.

Preparation of samples

Each blood sample was centrifuged at 3000 rpm for 10 minutes and the serum separated by means of Pasteur pipette and stored in the refrigerator until required for analysis. One gramme of liver was homogenized in ice-cold saline to give a 20% homogenate using ice cooled mortar and pestle. Each homogenate was centrifuged at 3000 rpm for 10 minutes. The supernatant was separated with Pasteur pipette and stored frozen at -20°C until required for biochemical assays.

Digestion of samples

This was done according to the method described by Hernandez *et al.* (2004). One gramme of liver was put in a beaker containing 10 ml of acid mixture ($\text{HNO}_3/\text{HClO}_4$; 4:1 v/v) followed by heating to facilitate digestion. The digests were diluted with deionized water to give a final volume of 100 ml from which aliquots were obtained for AAS analysis of Cd and Fe in the liver.

Biochemical assays

Superoxide dismutase activity was assayed by the method of Misra and Fridovich (1972) and the activity expressed as units/mg tissue. Catalase activity was assayed by using the method of Cohen *et al.* (1970). Each catalase unit specifies the relative logarithmic disappearance of hydrogen peroxide per minute and is expressed as K min^{-1} . The amount of thiobarbituric acid reactive substances (TBARS) which are indicators of lipid peroxidation was assayed by the method of Buege and Aust (1978). Values for TBARS are quantified in terms of Malondialdehyde (MDA) whose molar extinction coefficient is $1.56 \times 10^5 \text{ M}^{-1}\text{cm}^{-1}$. The results are expressed as MDA units per gram tissue. Bilirubin level was assayed for according to the method of Sherlock (1951) and was expressed in mg/dl. Estimation of alanine aminotransferase (ALT) and aspartate aminotransferase (AST) were carried out according to the method described by Reitman and Frankel (1957) and both were expressed in U/I.

Statistical analysis

The results are presented as mean \pm standard error of mean (SEM). Analysis of variance (ANOVA) was carried out using version 21 of SPSS. In order to know which means are significantly different, Duncan multiple range tests was utilized by employing SPSS version 21 computer software. Values were considered significantly different at $p < 0.05$.

RESULTS

Results presented in Figure 1 shows that the cadmium load of the liver of rats exposed to cadmium chloride via tainted water was significantly ($p < 0.05$) elevated in the cadmium chloride only groups when compared to the control and the combined groups, at the end of each of the three periods of study.

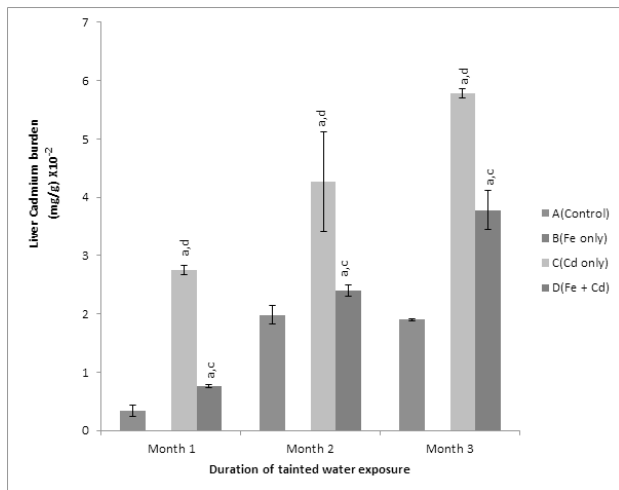


Fig 1: Effects of exposure to cadmium via tainted water on rat liver cadmium burden.

Group bar with a given superscript a, b, c, or d singly or combined is significantly ($p \leq 0.05$) different relative to the value of the group with corresponding uppercase letters, A, B, C and D.

Figures 2 and 3 show that Serum alanine aminotransferase (ALT) and aspartate aminotransferase (AST) activities significantly ($p < 0.05$) increased in the tainted water exposed rats at the end of three months of exposure.

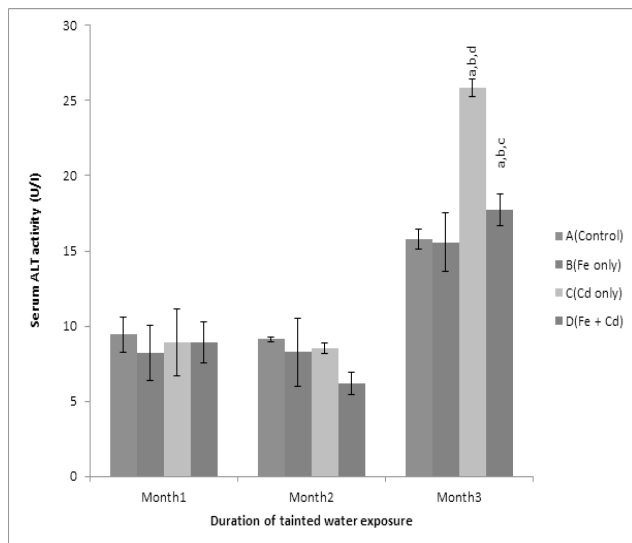


Fig 2: Effects of cadmium and iron on serum ALT activity in tainted water exposed rats.

Group bar with a given superscript a, b, c, or d singly or combined is significantly ($p \leq 0.05$) different relative to the value of the group with corresponding uppercase letters, A, B, C and D.

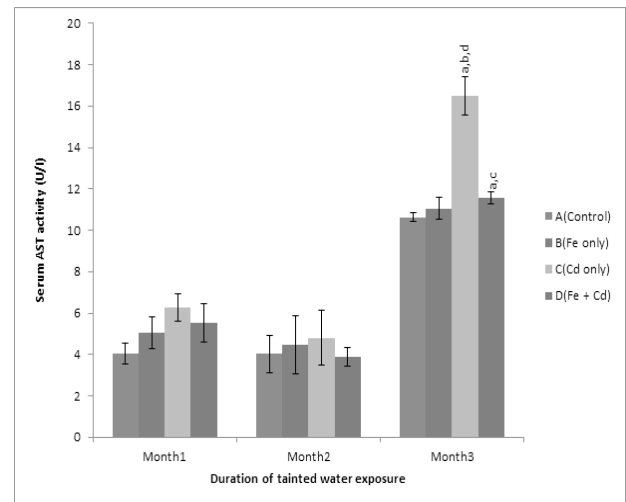


Fig 3: Effects of cadmium and iron on serum AST activity in tainted water exposed rats.

Group bar with a given superscript a, b, c, or d singly or combined is significantly ($p \leq 0.05$) different relative to the value of the group with corresponding uppercase letters, A, B, C and D.

Consistently, serum direct and total bilirubin levels in rats exposed via water were significantly ($p < 0.05$) increased in the cadmium chloride treated group relative to the control and combined groups at the end of 2 and 3 months exposure periods (Figures 4 and 5). Exception are the levels of total bilirubin in rats exposed via tainted water where at the end of the first month there were no significant ($p < 0.05$) difference between the cadmium chloride only and the combined groups.

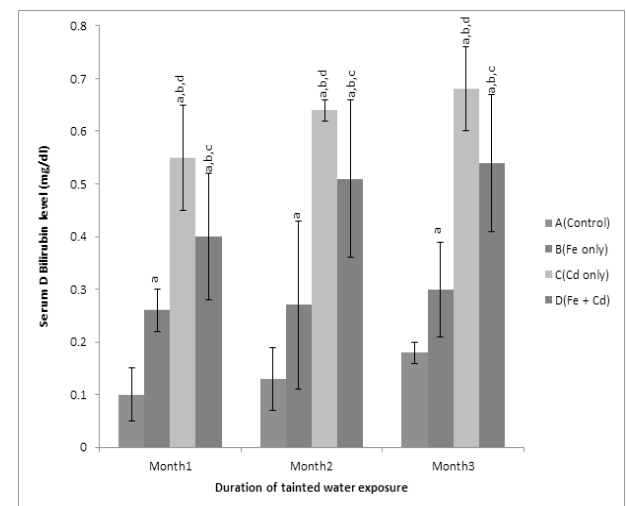


Fig 4: Effects of cadmium and iron on serum direct bilirubin level in tainted water exposed rats.

Group bar with a given superscript a, b, c, or d singly or combined is significantly ($p \leq 0.05$) different relative to the value of the group with corresponding uppercase letters, A, B, C and D.

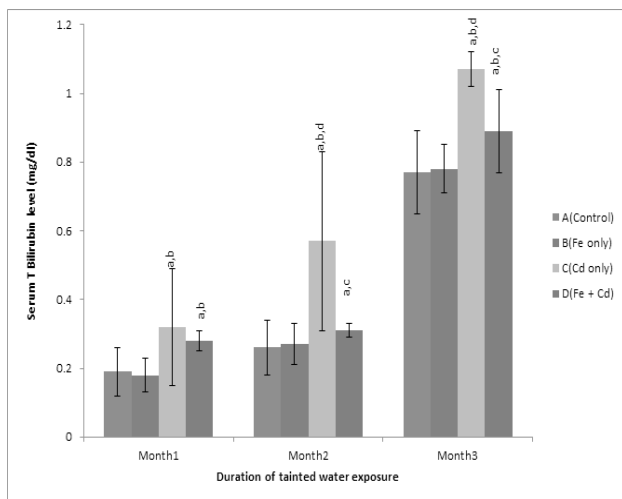


Fig 5: Effects of cadmium and iron on serum total bilirubin level in tainted water exposed rats.

Group bar with a given superscript a, b, c, or d singly or combined is significantly ($p \leq 0.05$) different relative to the value of the group with corresponding uppercase letters, A, B, C and D.

There were significant ($p < 0.05$) decreases in liver catalase and superoxide-dismutase (SOD) activities of the rats exposed to cadmium chloride via tainted at the end of each of the three study intervals, when compared to the control and the combined group values (Figures 6 and 7).

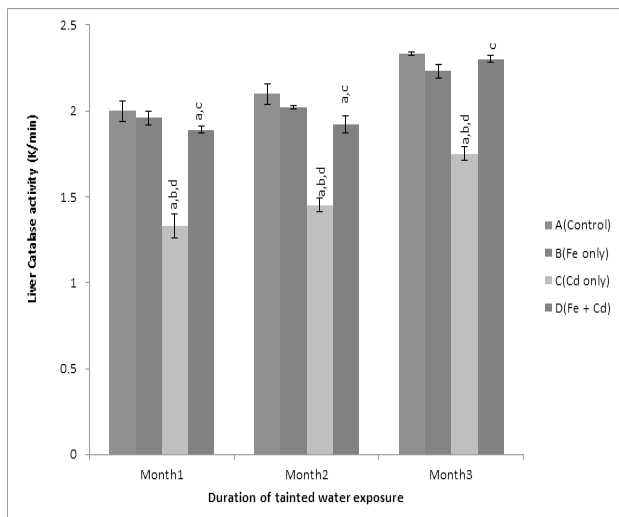


Fig 6: Effects of cadmium and iron on liver catalase activity in tainted water exposed rats.

Group bar with a given superscript a, b, c, or d singly or combined is significantly ($p \leq 0.05$) different relative to the value of the group with corresponding uppercase letters, A, B, C and D.

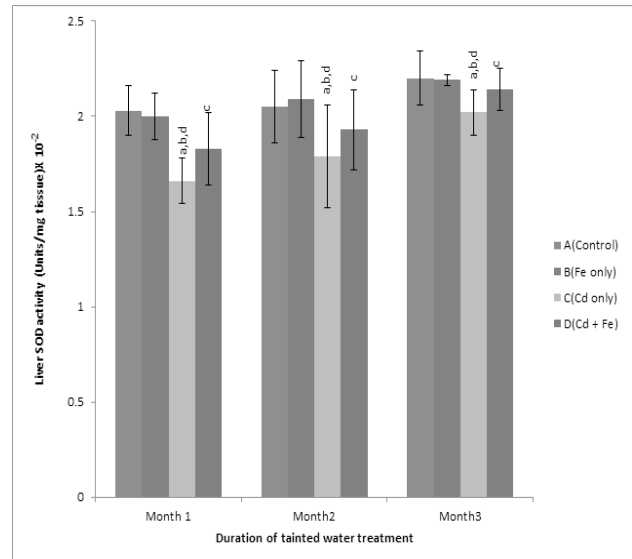


Fig 7: Effects of cadmium and iron on liver superoxide dismutase activity in tainted water exposed rats.

Group bar with a given superscript a, b, c, or d singly or combined is significantly ($p \leq 0.05$) different relative to the value of the group with corresponding uppercase letters, A, B, C and D.

Lipid peroxidation as evidenced by the level of MDA was significantly ($p < 0.05$) increased in the liver of rats exposed to cadmium chloride only, via tainted water at the end of 2 and 3 months exposure interval compared to the control and the combined groups (Figure 8).

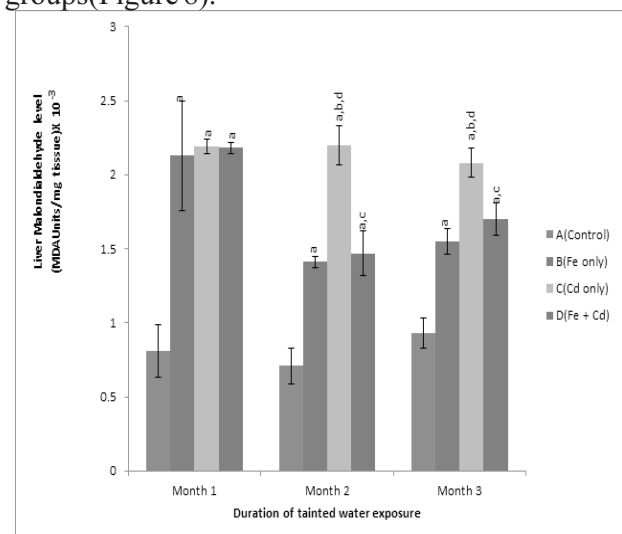


Fig 8: Effects of cadmium and iron on liver malondialdehyde level in tainted water exposed rats.

Group bar with a given superscript a, b, c, or d singly or combined is significantly ($p \leq 0.05$) different relative to the value of the group with corresponding uppercase letters, A, B, C and D.

Results presented in Figure 9 shows that the cadmium load of the liver of rats exposed to cadmium chloride via tainted diet was significantly ($p < 0.05$) elevated in the cadmium chloride only groups when compared to the control and the combined groups, at the end of each of the three periods of study.

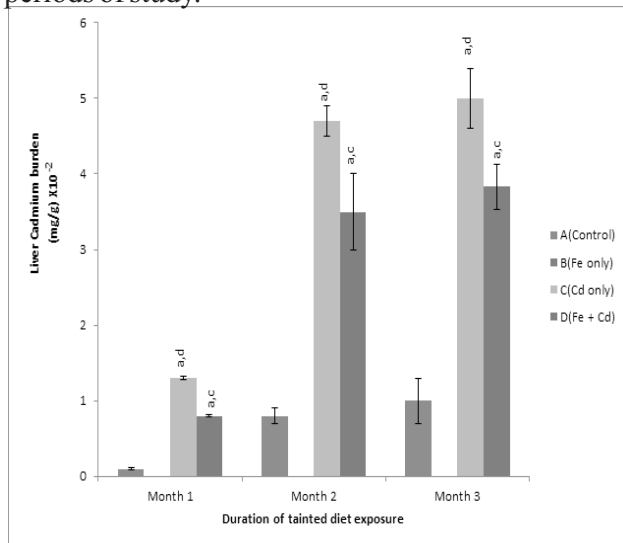


Fig 9: Effects of exposure to cadmium via tainted diet on rat liver cadmium burden.

Group bar with a given superscript a, b, c, or d singly or combined is significantly ($p \leq 0.05$) different relative to the value of the group with corresponding uppercase letters, A, B, C and D.

Serum alanine transferase (ALT) and aspartate transferase (AST) activities significantly ($p < 0.05$) increased in the tainted diet exposed rats at the ends of 1, 2 and 3 months relative to the control, the ferrous sulphate only and the combined groups (Figures 10 and 11).

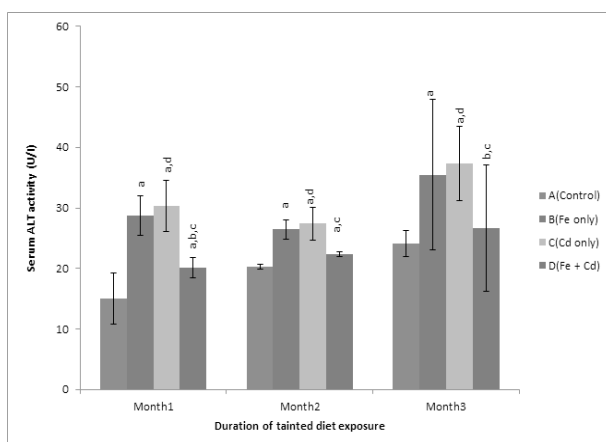


Fig 10: Effects of cadmium and iron on serum ALT activity in tainted diet exposed rats.

Group bar with a given superscript a, b, c, or d singly or combined is significantly ($p \leq 0.05$) different relative to the value of the group with corresponding uppercase letters, A, B, C and D.

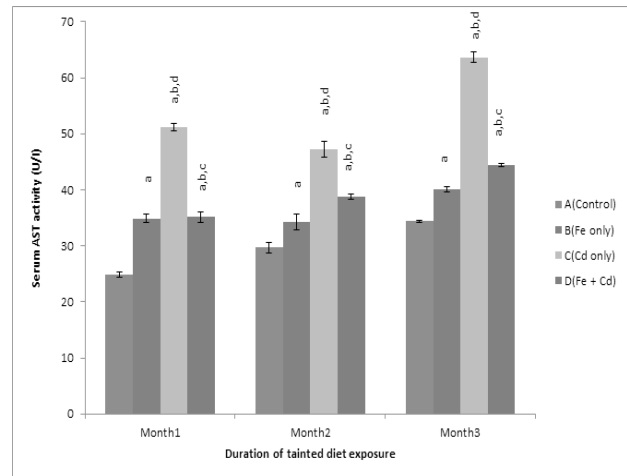


Fig 11: Effects of cadmium and iron on serum AST activity in tainted diet exposed rats.

Group bar with a given superscript a, b, c, or d singly or combined is significantly ($p \leq 0.05$) different relative to the value of the group with corresponding uppercase letters, A, B, C and D.

Consistently, serum direct and total bilirubin levels in rats exposed via diet were significantly ($p < 0.05$) increased in the cadmium chloride treated group relative to the control and combined groups at the end of 2 and 3 months exposure periods (Figures 12 and 13). Exception is the level of direct bilirubin in rats exposed via tainted diet, where at the end of the first month there were no significant ($p < 0.05$) difference between the cadmium chloride only and the combined groups.

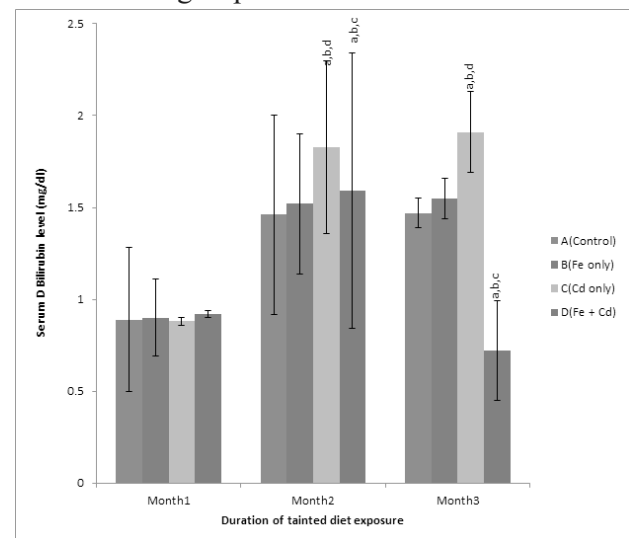


Fig 12: Effects of cadmium and iron on serum direct bilirubin level in tainted diet exposed rats.

Group bar with a given superscript a, b, c, or d singly or combined is significantly ($p \leq 0.05$) different relative to the value of the group with corresponding uppercase letters, A, B, C and D.

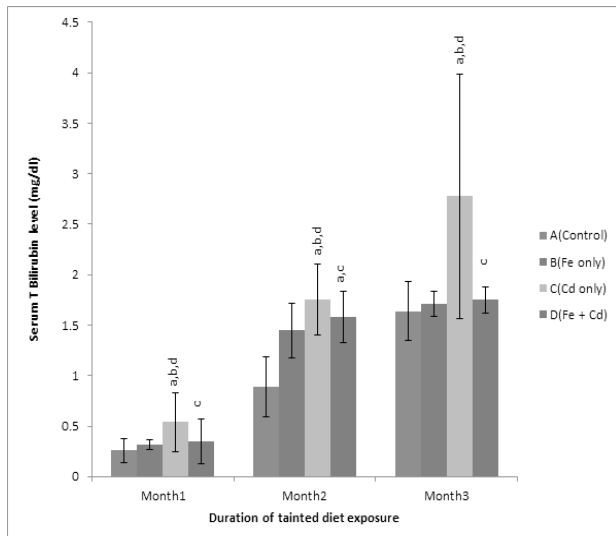


Fig 13: Effects of cadmium and iron on serum total bilirubin level in tainted diet exposed rats.

Group bar with a given superscript a, b, c, or d singly or combined is significantly ($p \leq 0.05$) different relative to the value of the group with corresponding uppercase letters, A, B, C and D.

There were significant ($p < 0.05$) decreases in liver catalase and superoxide-dismutase (SOD) activities of the rats exposed to cadmium chloride via tainted diet at the end of each of the three study intervals, when compared to the control and the combined group values (Figures 14 and 15).

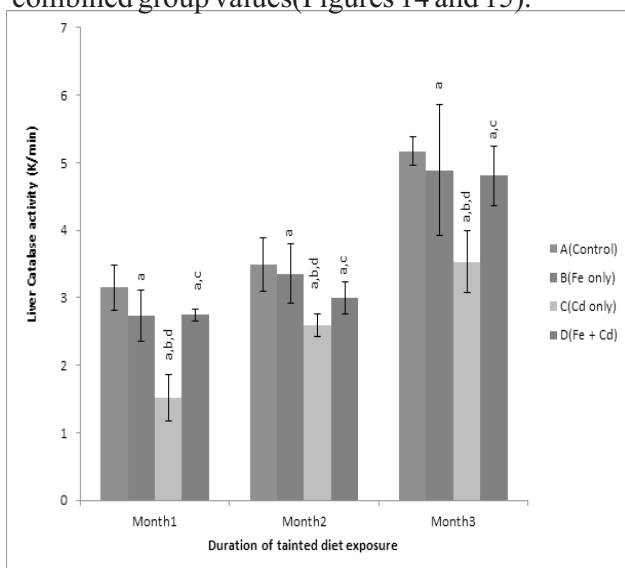


Fig 14: Effects of cadmium and iron on liver catalase activity in tainted diet exposed rats.

Group bar with a given superscript a, b, c, or d singly or combined is significantly ($p \leq 0.05$) different relative to the value of the group with corresponding uppercase letters, A, B, C and D.

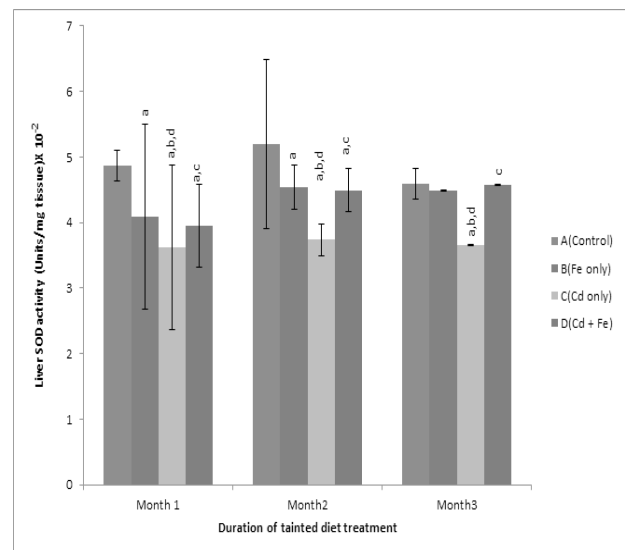


Fig 15: Effects of cadmium and iron on liver superoxide dismutase activity in tainted diet exposed rats.

Group bar with a given superscript a, b, c, or d singly or combined is significantly ($p \leq 0.05$) different relative to the value of the group with corresponding uppercase letters, A, B, C and D.

Lipid peroxidation as evidenced by the level of MDA was significantly ($p < 0.05$) increased in the liver of rats exposed to cadmium chloride only, via tainted diet at the end of 2 and 3 months exposure interval compared to the control and the combined groups (Figure 16).

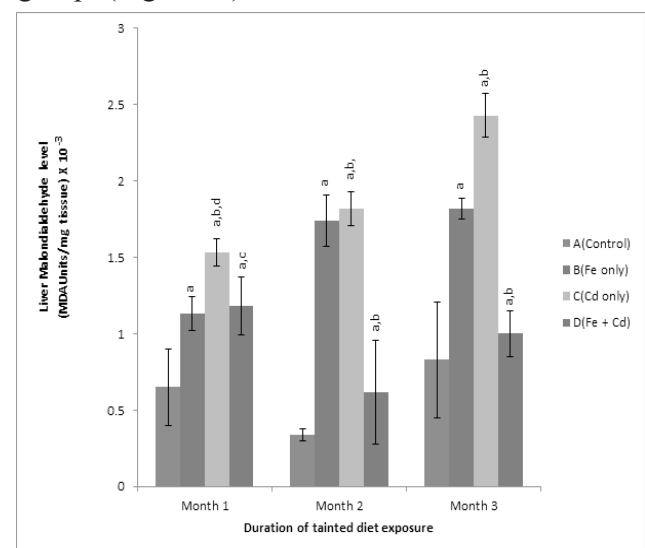


Fig 16: Effects of cadmium and iron on liver malondialdehyde level in tainted diet exposed rats.

Group bar with a given superscript a, b, c, or d singly or combined is significantly ($p \leq 0.05$) different relative to the value of the group with corresponding uppercase letters, A, B, C and D.

Discussion

The serum ALT and AST levels are common markers for hepatic damage. Levels of these enzyme proteins are rapidly increased when the liver is damaged by any cause, including hepatitis or hepatic cirrhosis. The results presented here are in agreement with that of (Al-Attar, 2011) who reported that mixture of heavy metals (Pb, Hg, Cd, and Cu) induced significant increases in plasma ALT, AST, alkaline phosphatase (ALP) and gamma glutamy triansaminase (GGT) and concluded that the increases were evidence of liver damage. Makhoulf and Makhoulf, (2012) also reported significant elevation in serum activities of ALT and AST after Cd exposure. Results obtained in this study also revealed significant decreases in serum ALT and AST activities when cadmium chloride and ferrous sulphate were given simultaneously to rats via tainted water or diet. This finding is similar to that of Al-Attar (2011) who reported that selenium (Se) reversed Pb, Hg, Cd and Cu-induced liver injury as evidenced by the reduced levels of plasma ALT, AST, ALP and GGT. El-Yamany *et al.* (2015) also reported reduced ALT and AST levels in the blood of animals exposed to cadmium and selenium simultaneously. These observations show that cadmium chloride induced liver injury is moderated by ferrous sulphate. Bilirubin arises from the breakdown of the haeme component of haemoglobin present in red blood cells. During normal function, the liver removes bilirubin from the blood and excretes it through bile as bile pigment. Elevated levels of bilirubin in cadmium chloride only treated group of rats is a reflection of the hepatotoxic effects of cadmium chloride. Increases in serum bilirubin in Cd-exposed rats when compared with the control rats values indicates that the capacity of the liver to excrete bilirubin may have been compromised due to either bile duct obstruction (Veena *et al.*, 2012) or impaired liver function. The results obtained agree with the data of (Alhazza, 2008) who reported similar increase in bilirubin level. Concurrent exposure to cadmium chloride and ferrous sulphate significantly reduced the level of bilirubin. So, in the presence of ferrous sulphate, cadmium chloride appears unable to interfere with bilirubin excretion. The results of the present study revealed that cadmium chloride induces oxidative stress as evident by increase in malondialdehyde (MDA) levels and alterations in the activities of catalase and superoxide dismutase enzymes in liver of male albino rat at specific time intervals. Cadmium chloride may induce oxidative damage in different

tissues by altering the antioxidant defence system of the cells. It may also do so by decreasing the absorption of trace elements with antioxidant related functions into the tissues. In the present study, cadmium chloride treated rats showed, not only a significant ($p < 0.05$) increase in MDA levels but also significant ($p < 0.05$) decrease in the activity levels of antioxidant enzymes such as CAT and SOD. These findings are in agreement with earlier reports of Obayah *et al.* (2009), on rats under Cd induced stress. During oxidative stress the CAT activity levels progressively decreases due to high accumulation of H_2O_2 in the tissues, and therefore, more peroxidation of lipids is favoured. This could be the reason for increased MDA levels observed in cadmium chloride intoxicated rats.

The significant ($p < 0.05$) decrease in catalase (CAT) activity may also be due to the decreased absorption of essential trace element, Fe, required for the activity of this enzyme (Jurczuk *et al.*, 2004). The reduction in CAT activity level in cadmium chloride treated rats indicates inefficient scavenging of hydrogen peroxide.

Superoxide dismutase (SOD) is an important antioxidant enzyme that inhibits superoxide radical accumulation and is usually used as a biomarker of oxidative stress (Zhang *et al.*, 2004). The decrease in SOD activity could have caused reactive oxygen species (ROS) to accumulate with attendant rise in lipid peroxidation as evidenced by enhanced MDA level in the present study. Concurrent exposure of rats to cadmium chloride and ferrous sulphate caused profound reversal of the alteration in MDA level brought about by cadmium chloride in the liver. Evidently, there is some degree of antagonism to cadmium chloride induced toxicity by ferrous sulphate. The basis of this antagonism in this study was not investigated but Fe may be competitively absorbed instead of Cd in the gastrointestinal tract (Ryu *et al.*, 2004). The views expressed above with regards to Cd absorption is given credence by the findings in this study that Cd concentrations were significantly ($p < 0.05$) depleted in the liver of rats exposed to ferrous sulphate and cadmium chloride concurrently. This suggests that ferrous sulphate can effectively protect against intestinal absorption of cadmium chloride thereby, decreasing its uptake (Piasek *et al.*, 2004) when they are ingested simultaneously.

Conclusion

Cadmium chloride is hepatotoxic as evidenced by increased levels of hepatic enzymes in the blood of the exposed rats, increased lipid peroxidation as well as decreased SOD and catalase enzyme activities. The study though not new with respect to the individual hepatotoxicity, concurrent exposure of cadmium chloride and ferrous sulphate caused profound reduction in the intensity of the toxic effects. The results presented in this report therefore suggest that ferrous sulphate ameliorates the hepatotoxic effects of cadmium chloride in rats.

References

- Al-Attar, A. M. (2011). Vitamin E attenuates liver injury induced by exposure to lead, mercury, cadmium and copper in albino mice. *Saudi Journal of Biological Sciences*. **18**, 395–401.
- Alhazza, I. M. (2008). Effect of selenium on cadmium induced gonadotoxicity in male rats. *Journal of Biological Science*. **5**, 243–249.
- Buege, J. A., and Aust, S.D., (1978). Microsomal lipid peroxidation. *Methods in enzymology*. Vol LII –Biomembranes. Fleischer and Parker (ed.) Academic Press, New York, pp. 302–310.
- Cohen, G., Denbliec, D., Heiskala, M., Peterson, P.A., Yang, Y., and Marcus, S., (1970). Measurement of catalase activity in tissue extracts. *Annual Review of Biochemistry*. **34**, 30–38.
- Cuyppers, A., Plusquin, M., Remans, T., Jozefczak, M., Keunen, A., and Gielen, H., (2010). Cadmium stress: an oxidative challenge. *Biometals*. **23**(5), 927–940.
- Egborge, A.B.M. (1994). Biodiversity and chemistry of Warri River. In: *Water pollution in Nigeria*. Ben Miller Books Nigeria. pp 275–288
- El-Yamany, I. E., Mahmoud, M. S., Diaa, F. I., and Elsayed, H. D., (2015). Effect of selenium and vitamin E on some physiological parameters of male albino rats subjected to drink polluted water containing mixture of heavy metals. *Report and Opinion*. **7** (6), 113–121.
- Hakan, A. H., Canan, C., and Biltan, E., (2001). *In vivo* interaction between cadmium and essential trace elements copper and zinc in rats. *Turkish Journal of Medical Sciences*. **31**:127–129.
- Hernandez, O. M., Fraga, J.M.G., Jimenez, A.I., Jimenez, F. and Arias, J.J. (2004). Determination of the mineral content by atomic absorption spectrophotometer. *Journal of Food Chemistry*. **93**: 449–458.
- Hijova, E., and Nistiar, F., (2005). Plasma antioxidant changes after acute cadmium intoxication in rats. *Acta Veterinaria Brunensis*. **74**, 565–568.
- Jurczuk, M., Brzoska, M.M., Moniuszko-Jakoniuk, J., Galazyn-Sidorczuk, M., and Eulikowska-Karpinska, E., (2004). Antioxidant enzymes activity and lipid peroxidation in liver and kidney of rats exposed to cadmium and ethanol. *Food Chemistry and Toxicology*. **42**, 429–438.
- Mahtap, K., and Ethem, A., (2006). The effects of chronic cadmium toxicity on the hemostatic system. *Pathophysiology of Haemostasis and Thrombosis*. **35**, 411–416.
- Makhlouf, R., and Makhlouf, I., (2012). Evaluation of the effect of *Spirulina* against Gamma irradiation induced oxidative stress and tissue injury in rats. *International Journal of Applied Science and Engineering Research*. **1**(2), 152–164.
- Misra, H.P., and Fridovich, I., (1972). The role of superoxide anion in the auto oxidation of epinephrine and a simple assay for superoxide dismutase. *Journal of Biological Chemistry*. **247**, 3170–3175.
- Nad, P., Massanyi, P., Skalicka, M., Korenekova, B., and Cigankova, V., (2005). The effect of cadmium in combination with zinc and selenium on ovarian structure in Japanese quails. *Rizilove Factory Potravoveho Refazca*. **5**, 241–247.

A SPECIAL FAMILY OF PARAMETER DEPENDENT NESTED HYBRID MULTISTEP METHODS FOR SOLVING BIOLOGICAL AND EPIDEMIOLOGICAL PROBLEMS

Akhanolu Gilbert Aziegbe

Department of Mathematics,
University of Benin, Benin City, Edo State, Nigeria.

&

Agbeboh Goddy Ujagbe

Department of Mathematics,
Ambrose Alli University, Ekpoma, Edo State, Nigeria,

Abstract

In this paper, a special family of parameter dependent nested hybrid linear multistep methods (PDNHM) tends to address the rising cases of Tuberculosis (TB) in Nigeria. A mathematical model is designed to assess the epidemiological impact of TB transmission in Nigeria using our proposed method which is A-stable, A_0 -stable and $A(\alpha)$ -stable for step number $k \leq 6$. The numerical simulation on biological and epidemiological rising cases of the tuberculosis (TB) dynamical models shows that our method is capable of solving real life problems.

Keywords: a special family, nested hybrid multi-step methods, implicit methods, A-stable, A_0 -stable, $A(\alpha)$ -stability, biological and epidemiological, TB dynamical model.

AMS subject classification: 65L05, 65L06.

Introduction:

Nested formulae have been proposed for the numerical solution of stiff initial value problems in ODEs,

$$y' = f(x, y), \quad x \in [x_0, X], \quad y(x_0) = y_0, \quad f : \mathbb{R} \times \mathbb{R}^m \rightarrow \mathbb{R}^m \quad (1)$$

According to Ekoru et al (2018) and Esuabana et al (2017), such formulae are hybrid multistep formulae with nested hybrid methods. These formulae developed did very well in extensive numerical computations of stiff ODEs. The interest of this paper is to show that a special family of parameter dependent nested hybrid multistep (PDNHLM) methods (1) is capable of solving real life biological and epidemiological problems like the rising cases of the tuberculosis (TB) dynamical models

According to Castillo-Chavez and Song (2004), it is a well known fact that TB has spread through a larger population in the world as it is estimated that a

third of the world's population is infected with *Mycobacterium tuberculosis*; of the 1.7 billion people estimated to be infected with TB, 1.3 billion live in developing countries and it has accounted for a sizeable number of deaths. In 1993, the World Health Organization (WHO) declared TB as a global emergency because of the rising deaths and the rate of infection especially in developing countries with Sub-Saharan Africa having the highest per capital level of incidence. Nigeria has been ranked fourth among the 22 countries Sub-Saharan Africa designated by the WHO as the high-burden countries (HBC) for TB. Nigeria is said to have the highest number of new TB cases in Africa which results to high deaths rate annually. The causes behind the recently observed increase in the number of active TB cases are the subject for many studies (Castillo-Chavez and Song (2004)). According to Blower et al (1996), TB is an airborne transmitted disease. *Mycobacterium tuberculosis* droplets are released in the air by coughing or sneezing infectious individuals. *Tubercle bacillus* contained in such droplets live in the air for a short time (about two hours) and therefore, it is believed that occasional contacts with TB-active persons (infectious individuals) rarely lead to transmission, the most secondary cases are the result of prolonged and constant close contacts with a primary case. According to Feng et al (2000) and Ssematimba et al (2005), latently infected individuals (inactive TB)

Corresponding Author: Akhanolu Gilbert Aziegbe
Department of Mathematics,
University of Benin, Benin City,
Edo State, Nigeria.
merrygil2014@gmail.com

become infectious (active TB) after a variable (typically long) latency period. Latent period is usually months.

A global control strategy adopted by the WHO to help reduce the number of active TB cases as well as promote proper treatment of patients with TB is the Direct Observation Therapy Strategy (DOTS). DOTS have evolved into a strategy that makes it compulsory for patients to complete their treatment and DOTS seems to be highly effective in promoting successful treatment of TB.

The continuous rise in new TB cases in Nigeria motivated this real life biological and epidemiological mathematical model and implementation. The mathematical model is designed and used to assess the epidemiological impact of TB transmission in Nigeria.

The general k -step PDNHLMMs is

$$\begin{cases} Y_0 = \sum_{j=0}^k S_j y_{n+j} + h E_k f_{n+k}; & Y_0 = y_{n+c_0} \\ Y_{i+1} = y_{n+k-1} + \sum_{j=0}^k I_{1j} f_{n+j} + h T_i f(Y_i) & i = 0(1)s-1; Y_{i+1} = y_{n+c_{i+1}} \\ y_{n+k} = y_{n+k-1} + \sum_{j=0}^{k-2} I_{2j} y_{n+j} + h \theta_{s-1} f(Y_{s-1}) + h R_k (f_{n+k} + a f_{n+k-1}) & 0 \leq c \leq k. \end{cases} \quad (2)$$

In (2), the parameters S_j , I_{2j} , I_{1j} , T_i , θ_{s-1} , E_k and R_k with $i = 1, \dots, s-1$, $j = 0, 1, \dots, k$ are all real coefficients. The $f_{n+j} = f(x_{n+j}, y_{n+j})$ is the first derivative function, $h = x_{n+1} - x_n$ denotes the mesh size, k and s represents the step number, and the stage respectively, while $Y_i = y(x_n + c_i h) + O(h^{q_{i+1}})$, $i = 0, \dots, s-1$, and y_{n+k} are the stage and the output point of the methods in (2). The $f(Y_i) = \{f(x_n + c_i h, Y_i)\}_{i=0}^{s-1}$ denotes the derivative of the stages. The stability region of the formulas in (2) depend on the choice of the parameter a . The $c = [c_0, c_1, \dots, c_s]^T$ is the abscissa vector of the input methods. The elements in c are computed from the abscissa generator:

$$c_i = \left\{ c - \frac{1}{2^{k-i}} \right\}_{i=0}^{k-1}, \quad k = 1, 2, \dots, s-1.$$

By Taylor's series technique, the local truncation error of the stage method and the output method in (2) at x_n gives the following order conditions:

$$h^{q_0} : \begin{cases} \sum_{j=0}^k S_j = 1, & q_0 = 0, \\ \sum_{j=1}^k j S_j + E_k = c_0, & q_0 = 1, \\ \frac{1}{q_0!} \sum_{j=1}^k j^{q_0} S_j + \frac{1}{(q_0-1)!} k^{q_0-1} E_k = \frac{c_0^{q_0}}{q_0!}; & q_0 = 2, 3, \dots, \end{cases} \quad (3a)$$

The error constant of the method in (3a) is

$$C_{q_0+1} = \frac{1}{(q_0+1)!} \sum_{j=0}^k j^{q_0+1} S_j + \frac{1}{q_0!} k^{q_0} E_k = \frac{c_0^{q_0+1}}{(q_0+1)!} + O(h^{q_0+1}). \quad (3b)$$

Equations (3a) and (3b) are the order conditions and error constants of the first input method in (2) while the order conditions and error constants of the second input method in (2) are

$$h^{q_i} : \begin{cases} \sum_{j=0}^k I_{1j} + \rho_0 = 4 + c_1, & i = 1, 2, \dots, s, \quad i = 0(1)s-1, \\ \sum_{j=1}^k j I_{1j} + c_0 T_i = 8 - \frac{c_i^2}{2!}, & q_i = 1, \\ \frac{1}{q_i!} \sum_{j=1}^k j^{q_i} I_{1j} + T_0 c_0^{q_i-1} = -\frac{c_0^{q_i}}{q_i!} + \frac{64}{q_i!}; & q_i = 2, 3, \dots, \end{cases} \quad (4a)$$

The error constant of the method in (2) is

$$C_{q_i+1} = \frac{1}{(q_i+1)!} \sum_{j=0}^{k-1} j^{q_i+1} I_{1j} + T_0 c_0^{q_i} = \frac{c_i^{q_i+1}}{(q_i+1)!} + \frac{64}{(q_i+1)!} O(h^{q_i+1}). \quad (4b)$$

For the output method in (2), the order conditions and error constants are

$$h^p : \begin{cases} \sum_{j=0}^{k-1} I_{2j} + R_k = 1, & p = 0, \\ \sum_{j=1}^{k-1} j I_{2j} + R_k(5+a) = c_4, & p = 1, \\ \frac{1}{p!} \sum_{j=1}^{k-1} j^p I_{2j} + \frac{1}{(p-1)!} \theta_{s-1} c_{s-1}^{p-1} + \frac{1}{(p-1)!} ((-1+k)^{p-1} + k^{p-1}) c_k = \frac{k^p}{p!}; & p = 2, 3, \dots, \end{cases} \quad (5a)$$

and

$$C_{p+1} = \frac{1}{(p+1)!} \sum_{j=1}^{k-1} j^{p+1} I_{2j} + \frac{1}{p!} \theta_{s-1} c_{s-1}^p + \frac{1}{p!} ((-1+k)^p + k^p) c_k = \frac{k^{p+1}}{(p+1)!} + O(h^{p+1}) \quad (5b)$$

respectively.

Derivation of the multistep nested hybrid methods

For example, fixing $k = 1$, $s = 1$, $p = q + 1 = 3$ and $c_0 = \frac{1}{2}$ in (3), (4) and (5) respectively and solving the arising system of equations yield,

$$\begin{cases} Y_0 = \frac{1}{4} (y_n + 3y_{n+1}) - \frac{h}{4} f_{n+1}; & q_0 = 2, \quad C_3 = \frac{1}{48}, \\ y_{n+1} = y_n + \left(\frac{1-a}{2 \left(\frac{-1}{2} + \frac{a}{2} \right)} \right) h f(Y_0); & p = 2, \quad C_3 = \frac{1}{24}. \end{cases} \quad (6)$$

Again, when $k = 2$, $s = 2$ $p = q_1 = q_0 + 1$, $c_0 = \frac{7}{4}$ and $c_1 = \frac{3}{2}$ in (2) gives

$$Y_0 = \frac{1}{256}(-3y_n + 28y_{n+1} + 231y_{n+2} - 42hf_{n+2}); \quad C_4 = \frac{7}{2048}, \quad q_0 = 3$$

$$Y_1 = y_{n+1} + \frac{1}{96}(-hf_n + 30hf_{n+1} - 13hf_{n+2} + 32hf(Y_0)); \quad C_5 = \frac{179}{92160}, \quad q_1 = 4,$$

$$y_{n+2} = y_{n+1} + \frac{2}{9}\left(-\frac{1-a}{-2+a}hf_n - \frac{8-5a}{-2+a}hf(Y_1)\right) - \frac{1}{6(-2+a)}h(f_{n+2} + af_{n+1}); \quad C_4 = \frac{1}{84}, \quad p = 3. \quad (7)$$

Setting $k = 3$, $s = 3$, $p = q_2 = q_1 = q_0 + 1 = 5$, $c_0 = \frac{23}{8}$, $c_1 = \frac{11}{4}$, and $c_2 = \frac{5}{2}$, $a = \frac{1}{2}$ into (3), (4) and (5) respectively and solving the arising system equations, gives the method of order five,

$$Y_0 = \frac{1}{49152}(70y_n - 483y_{n+1} + 2070y_{n+2} + 47495y_{n+3} - 4830hf_{n+3}) \quad C_5 = \frac{161}{262144}, \quad q_0 = 4,$$

$$Y_1 = y_{n+2} + \frac{1143}{235520}hf_n - \frac{1983}{51200}hf_{n+1} + \frac{30549}{71680}hf_{n+2} - \frac{4977}{10240}hf_{n+3} + \frac{3396}{824025}hf(Y_0); \quad C_6 = \frac{681}{409600}, \quad q_1 = 5, \quad (8)$$

$$Y_2 = y_{n+2} + \frac{179}{63360}hf_n - \frac{319}{13440}hf_{n+1} + \frac{1979}{5760}hf_{n+2} - \frac{601}{5760}hf_{n+3} + \frac{976}{3465}hf(Y_1); \quad C_6 = \frac{41}{46080}, \quad q_2 = 5,$$

$$y_{n+3} = y_{n+2} - \frac{(1+a)}{30(-3+a)}hf_n - \frac{(1-3a)}{6(-3+a)}hf_{n+1} - \frac{(19-9a)}{15(-3+a)}hf(Y_2) + \frac{1}{3(-3+a)}h(f_{n+3} + af_{n+2}); \quad C_5 = \frac{11}{2880}, \quad p = 4.$$

For $k = 4$, $s = 4$, $p = q_3 = q_2 = q_1 = q_0 + 1 = 6$, $c_0 = \frac{63}{16}$, $c_1 = \frac{23}{8}$, $c_2 = \frac{15}{4}$, and $c_3 = \frac{7}{2}$ into (3), (4) and (5) respectively and solving the arising system of equations gives the method of order six,

$$Y_0 = -\frac{7285}{33554432}y_n + \frac{3255}{2097152}y_{n+1} - \frac{44415}{8388608}y_{n+2} + \frac{30597}{2097152}y_{n+3} + \frac{33197745}{33554432}y_{n+4} - \frac{458955}{8388608}hf_{n+4}; \quad C_6 = \frac{30597}{268435456}, \quad q_0 = 5,$$

$$Y_1 = y_{n+3} - \frac{136493}{53084160}hf_n + \frac{675857}{34652160}hf_{n+1} - \frac{2320297}{30474240}hf_{n+2} + \frac{27461}{55296}hf_{n+3} - \frac{6820457}{5898240}hf_{n+4} + \frac{940562}{590085}hf(Y_0); \quad C_7 = \frac{20953037}{1811939380}, \quad q_1 = 6,$$

$$Y_2 = y_{n+3} - \frac{681}{317440}hf_n + \frac{3867}{235520}hf_{n+1} - \frac{669}{10240}hf_{n+2} + \frac{33273}{71680}hf_{n+3} - \frac{537}{1280}hf_{n+4} + \frac{18876}{24955}hf(Y_1); \quad C_7 = \frac{34537}{36700160}, \quad q_2 = 6,$$

$$Y_3 = y_{n+3} - \frac{41}{34560}hf_n + \frac{589}{63360}hf_{n+1} - \frac{131}{3360}hf_{n+2} + \frac{6347}{17280}hf_{n+3} - \frac{997}{11520}hf_{n+4} + \frac{520}{2079}hf(Y_2); \quad C_7 = \frac{757}{1548288}, \quad q_3 = 6, \quad (9)$$

$$y_{n+4} = y_{n+3} - \frac{1}{4}\frac{(57-59a)}{63(-4+a)}hf_n - \frac{4(-232+23a)}{45(-4+a)}hf_{n+1} - \frac{4(118-119a)}{9(-4+a)}hf_{n+2} - \frac{4(646-25a)}{1575(-4+a)}hf(Y_3) - \frac{179}{36(-4+a)}h(f_{n+4} + af_{n+3}); \quad C_6 = \frac{13}{4140}, \quad p = 5.$$

For $k = 5$, $s = 5$, $p = q_4 = q_3 = q_2 = q_1 = q_0 + 1 = 7$, $c_0 = \frac{159}{32}$, $c_1 = \frac{79}{16}$, $c_2 = \frac{39}{8}$, $c_3 = \frac{19}{4}$, and $c_4 = \frac{9}{2}$ into (3), (4) and (5) respectively and solving the arising system of equations produces the method of order seven,

$$Y_0 = \frac{1570863}{42949672960}y_n - \frac{9833355}{34359738368}y_{n+1} + \frac{4381881}{4294967296}y_{n+2} - \frac{19822795}{8589934592}y_{n+3} + \frac{40285035}{8589934592}y_{n+4}$$

$$+ \frac{171257055123}{171798691840}y_{n+5} - \frac{249767217}{8589934592}hf_{n+5}; \quad C_7 = \frac{11893677}{549755813888}, \quad q_0 = 6,$$

$$Y_1 = y_{n+4} + \frac{151234285}{99589554176}hf_n - \frac{2928519075}{238639120384}hf_{n+1} + \frac{826756935}{17850957824}hf_{n+2} - \frac{2352809825}{19730006016}hf_{n+3}$$

$$+ \frac{31979005155}{58250493952}hf_{n+4} - \frac{4530823545}{1879048192}hf_{n+5} + \frac{1680435380}{582790173}hf(Y_0); \quad C_8 = \frac{21529183055}{26938034880512}, \quad q_1 = 7,$$

$$Y_2 = y_{n+4} + \frac{20953037}{14910750720}hf_n - \frac{19334231}{1698693120}hf_{n+1} + \frac{191274881}{4435476480}hf_{n+2} - \frac{327513697}{2925527040}hf_{n+3}$$

$$+ \frac{302153677}{566231040}hf_{n+4} - \frac{197301587}{188743680}hf_{n+5} + \frac{68317816}{46616715}hf(Y_1); \quad C_8 = \frac{212521897}{289910292480}, \quad q_2 = 7,$$

$$Y_3 = y_{n+4} + \frac{34537}{29818880}hf_n - \frac{670599}{71106560}hf_{n+1} + \frac{951159}{26378240}hf_{n+2} - \frac{21893}{229376}hf_{n+3} + \frac{7971207}{16056320}hf_{n+4}$$

$$\begin{aligned}
& -\frac{858693}{2293760}hf_{n+5} + \frac{1579568}{2270905}hf(Y_2); \quad C_8 = \frac{1217123}{2055208960}, \quad q_3 = 7, \quad (10) \\
Y_4 = & y_{n+4} + \frac{757}{1225728}hf_n - \frac{4933}{967680}hf_{n+1} + \frac{35417}{1774080}hf_{n+2} - \frac{62941}{1128960}hf_{n+3} + \frac{374357}{967680}hf_{n+4} \\
& - \frac{24131}{322560}hf_{n+5} + \frac{63104}{276507}hf(Y_3); \quad C_8 = \frac{13025}{43352064}, \quad q_4 = 7, \\
y_{n+5} = & y_{n+4} - \frac{(53-58a)}{3240(-5+a)}hf_n + \frac{(-90+97a)}{840(-5+a)}hf_{n+1} + \frac{(37-39a)}{120(-5+a)}hf_{n+2} + \frac{589}{1080} + \frac{79}{36(-5+a)}hf_{n+3} \\
& + \frac{8\left(475 + \frac{948}{-5+a}\right)}{2835}hf(Y_4) - \frac{79}{120(-5+a)}h(f_{n+5} + af_{n+4}); \quad C_7 = \frac{373}{362880}, \quad p = 6.
\end{aligned}$$

For $k = 6$, $s = 6$, $p = q_5 = q_4 = q_3 = q_2 = q_1 = q_0 + 1 = 8$, $c_0 = \frac{3839}{64}$, $c_1 = \frac{191}{32}$, $c_2 = \frac{95}{16}$, $c_3 = \frac{47}{8}$, $c_4 = \frac{23}{4}$, and $c_5 = \frac{11}{2}$ into (3), (4) and (5) respectively and solving the arising system of equations produces the method of order eight,

$$\begin{aligned}
Y_0 = & -\frac{920819977}{14073748855328}y_n + \frac{9950051601}{175921860444160}y_{n+1} - \frac{62236597269}{281474976710656}y_{n+2} + \frac{9232305005}{17592186044416}y_{n+3} \\
& - \frac{124963246485}{140737488355328}y_{n+4} + \frac{50382007313}{35184372088832}y_{n+5} - \frac{1406111442098517}{1407374883553280}y_{n+6} - \frac{1058022153573}{70368744177664}hf_{n+6}; \\
C_8 = & \frac{151146021939}{36028797018963968}, \quad q_0 = 7,
\end{aligned}$$

$$\begin{aligned}
Y_1 = & y_{n+5} - \frac{154807620931445}{159180696399642624}hf_n + \frac{63190231095911}{7365628394471424}hf_{n+1} - \frac{135853459989697}{3925256511160320}hf_{n+2} \\
& + \frac{8617444950372269}{99228175627714560}hf_{n+3} - \frac{4888541658041807}{29323975112785920}hf_{n+4} + \frac{22765089824959}{38482906972160}hf_{n+5} \\
& - \frac{9927780212406839}{2078076976496640}hf_{n+6} - \frac{11133442789211}{2116044307146}hf(Y_0); \quad C_9 = \frac{579847204017222941}{1021416395487628492800}, \quad q_1 = 8.
\end{aligned}$$

$$\begin{aligned}
Y_2 = & y_{n+5} - \frac{21529183055}{22969485099008}hf_n + \frac{26368680175}{3186865733632}hf_{n+1} - \frac{510362966625}{15272903704576}hf_{n+2} + \frac{47985404975}{571230650368}hf_{n+3} \\
& - \frac{8342970875}{51539607552}hf_{n+4} + \frac{1087915714125}{1864015806464}hf_{n+5} - \frac{268443523825}{120259084288}hf_{n+6} + \frac{42776282075}{15901846149}hf(Y_1); \\
C_9 = & \frac{537129214325}{985162418487296}, \quad q_2 = 8,
\end{aligned}$$

$$\begin{aligned}
Y_3 = & y_{n+5} - \frac{78297541}{90596966400}hf_n + \frac{607633957}{79524003840}hf_{n+1} - \frac{62270551}{2013265920}hf_{n+2} + \frac{16619460683}{212902871040}hf_{n+3} \\
& - \frac{9466381001}{62411243520}hf_{n+4} + \frac{2851105271}{5033164800}hf_{n+5} - \frac{17453299073}{18119393280}hf_{n+6} + \frac{11822902}{8632725}hf(Y_2); \\
C_9 = & \frac{277769237291}{556627761561600}, \quad q_3 = 8,
\end{aligned}$$

$$\begin{aligned}
Y_4 = & y_{n+5} - \frac{1217123}{1724907520}hf_n + \frac{1493419}{238551040}hf_{n+1} - \frac{28986429}{1137704960}hf_{n+2} + \frac{13694887}{211025920}hf_{n+3} \\
& - \frac{4720003}{36700160}hf_{n+4} + \frac{1926315}{36700160}hf_{n+5} - \frac{2504393}{7340032}hf_{n+6} + \frac{9910172}{15247505}hf(Y_3); \\
C_9 = & \frac{37641013}{93952409600}, \quad q_4 = 8, \quad (11)
\end{aligned}$$

$$Y_5 = y_{n+5} - \frac{13025}{35610624} hf_n + \frac{5351}{1634304} hf_{n+1} - \frac{11621}{860160} hf_{n+2} + \frac{68239}{1935360} hf_{n+3} - \frac{63461}{860160} hf_{n+4} \\ + \frac{173617}{430080} hf_{n+5} - \frac{514019}{7741440} hf_{n+6} + \frac{63104}{276507} hf(Y_4); \quad C_9 = \frac{2961281}{14863564800}, \quad q_4 = 8,$$

$$y_{n+6} = y_{n+5} + \frac{-453 + 533a}{36960(-6+a)} hf_n + \frac{8304 - 9619a}{90720(-6+a)} hf_{n+1} + \frac{9(-263 + 298a)}{7840(-6+a)} hf_{n+2} + \frac{984 - 1079a}{1680(-6+a)} hf_{n+3} + \frac{24487}{30240} \\ + \frac{915}{224(-6+a)} hf_{n+4} + \frac{16\left(19087 + \frac{49410}{-6+a}\right)}{218295} hf(Y_5) - \frac{183}{224(-6+a)} h(f_{n+6} + a f_{n+5}); C_8 = \frac{-1177}{947520}, \quad p = 7.$$

Stability of the Method

Applying the method in (2) to the test equation $y' = \lambda y$, $\text{Re}(\lambda) < 0$, Dahlquist (1965) gives the stability polynomial

$$\pi_s(r, z) = w^k - w^{k-1} - z \sum_{j=0}^{k-2} \delta_j w^j - z \theta_{s-1} (R_s(w, z)) - z \gamma_s (w^k + a w^{k-1}) \quad z = \lambda h, \quad (12)$$

where

$$R_s(w, z) = w^{k-1} + z \sum_{j=0}^k \varphi_j w^j + z \rho_{s-2} (R_{s-1}(w, z) (R_{s-2}(w, z) (R_{s-3}(w, z) (R_{s-4}(w, z) (R_{s-5}(w, z)))))) \quad (13)$$

The boundary locus plot of the stability polynomial for $k=1$ is given below

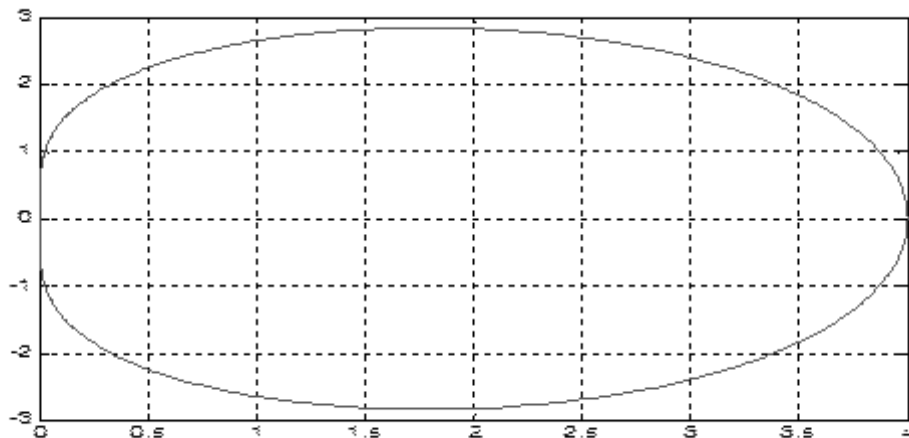


Fig 1: The stability region of the method for $k=1$. The stability region (interior of the closed curves) for the $k=1$ of method (2).

The behavior of the numerical solution of the method will depend on the resulting roots ($w_j(z)$) of $\pi(r, z) = 0$. Adopting the definitions in Castillo and Song (2004), we have:

$$R_0 = \left\{ \pi(w, 0) = 0 \mid \max_{1 \leq j \leq k} |w_j(z)| \leq 1, j = 1, 2, \dots, k \right\} \text{ is called the zero-stability of the methods in (2).}$$

- $R_a = \left\{ \pi(w, z) = 0 \mid \max_{1 \leq j \leq k} |w_j(z)| \leq 1, j = 1, 2, \dots, k \right\}$ is called the absolute stability of the method in (2).
- The methods in (2) with stability polynomial $\pi(w, z)$ is $A(\alpha)$ -stable if $|\pi(w, z)| = 1$ for all $z \in S(\alpha)$, $\alpha \in (0, \pi)$, where α is an angle of absolute stability.
- $R_A = \left\{ \pi(w, z) \leq 1; R(z) \leq 0 \right\}$ is called A -stability of the method (2).

Numerical Simulations

In this section, we first implement our method for the sake of comparison with already existing method in literature by applying the scheme in (6) for $k=1$ to a standard test stiff initial value problems (IVPs). Our aim is to see how our methods compared with the $A(\alpha)$ –stable LMM (Ekoro et al (2018) and Esuabana (2017)) before applying the method to solving real life biological and epidemiological problems.

In order to show the competence and superiority of the new methods compared with the well-known

methods in the scientific literature, we select the works of (Ekoro et al (2018)) for comparison

- PDNHLMM(k_j):the one-step-one-stage method of order 3 derived in (6) of this paper;
- $A(\alpha)$ –stable LMM of (Ekoro et al (2018))

In implementing the method, we solve the standard stiff initial value problems (IVPs)

Problem: Nonlinear chemical problem discussed in (Ekoro et al (2018)) and (Olatunji and Ikhile (2017)).

$$y' = \begin{bmatrix} -0.1 & -199.9 \\ -200 & 0 \end{bmatrix} y, \quad y(0) = \begin{bmatrix} 2 \\ 1 \end{bmatrix} \quad h = 0.0001, \quad x = [0, 1],$$

$$\text{Exact solution : } y_1(x) = \exp^{-0.1x} + \exp^{-200x} \quad \text{and} \quad y_2(x) = \exp^{-200x}$$

Table 1: Results of the solved Problem for comparison

| x | PDNHLMM y_n | $A(\alpha)$ -Stable LMM y_n | Exact Solution $y(x)$ | PDNHLMM Error = $ y(x) - y_n $ | $A(\alpha)$ -Stable LMM Error = $ y(x) - y_n $ |
|-----|---------------------------------|----------------------------------|---------------------------------|-----------------------------------|---|
| 0.2 | $2.2569438502e \times 10^{-9}$ | 2.1190578206 | $2.2779270412e \times 10^{-9}$ | $2.0983190958e \times 10^{-11}$ | $1.9920072216e \times 10^{-16}$ |
| 0.4 | $5.0959769196e \times 10^{-18}$ | 5.1315793862 | $4.6951575726e \times 10^{-18}$ | $4.0081934701e \times 10^{-19}$ | $5.0021074282e \times 10^{-16}$ |
| 0.6 | $1.1506259122e \times 10^{-26}$ | 1.1511722549 | $9.6774410387e \times 10^{-27}$ | $1.8288180836e \times 10^{-27}$ | $9.6663711108e \times 10^{-16}$ |
| 0.8 | $2.5980101770e \times 10^{-35}$ | 2.5960009977 | $1.9946692652e \times 10^{-35}$ | $6.0334091172e \times 10^{-36}$ | $4.7122272259e \times 10^{-16}$ |
| 1.0 | $5.8660741151e \times 10^{-44}$ | 5.8571556981 | $4.1113197817e \times 10^{-44}$ | $1.7547543333e \times 10^{-44}$ | $3.9931006410e \times 10^{-16}$ |

The numerical results in Tables 1 shows that the PDNHLMM for $k=1$ in methods (6) compare favorably well with $A(\alpha)$ -stable LMM in the literature in the solution of stiff IVPs in ODEs.

Model Formulation

From the survey article of Okuonghae and Aihie (2008), Ssematimba et al (2005) and Okuonghae and Korobeinikoy (2007), a typical TB treatment models are usually referred to as the *SEIT* (Susceptible–Exposed–Infected–Treated) models see also Castillo–Chavez and Song (2004). To incorporate the Direct Observation Therapy Strategy (DOTS) implementation into the *SEIT* framework, the infected class was divided into two subclasses with different properties, the undetected

infectious individuals (I_1) and the detected infectious individuals (I_2). Also, a separate class was introduced called the failed treatment class (R), this class monitor individuals who becomes latent after failed treatment and those who become latent due to self-cure from the undetected infectious class.

Let $S(t)$, $E(t)$, $I_1(t)$, $I_2(t)$, $T(t)$, $R(t)$ be the fractions of the susceptible individuals, the exposed (latent) individuals, the undetected and the detected infectious individuals, the treated individuals and the failed treatment individuals respectively at time

t , such that the total population is given by

$$N = S + E + I_1 + I_2 + T + R.$$

$$\dot{S} = \Lambda - \lambda_1 S - \mu S_1, \quad S(0) = 1, \quad (14a)$$

$$\dot{E} = (1 - p)(\lambda_1 S + \lambda_2 T) - \lambda_3 E - (k + \mu + r_0)E, \quad E(0) = 1, \quad (14b)$$

$$\dot{I}_1 = (1 - \omega)(p(\lambda_1 S + \lambda_2 T) + kE + \lambda_3 E) - (\mu + d_1 + r_1)I_1, \quad I_1(0) = 1, \quad (14c)$$

$$\dot{I}_2 = \omega(p(\lambda_1 S + \lambda_2 T) + kE + \lambda_3 E) - (\mu + d_2 + r_2)I_2, \quad I_2(0) = 1, \quad (14d)$$

$$\dot{T} = r_0 E + m r_2 I_2 - \lambda_2 T - \mu T, \quad T(0) = 1, \quad (14e)$$

$$\dot{R} = r_1 I_1 + m r_2 I_2 - \mu R, \quad R(0) = 1, \quad (14f)$$

where $n + m = 1$ and $0 < p < 1$ and the force of infections are given by $\lambda_1 = \beta \frac{I_1 + I_2}{N}$,

$\lambda_2 = \alpha \frac{I_1 + I_2}{N}$ and $\lambda_3 = \gamma \frac{I_1 + I_2}{N}$. Fig. 2 below shows the impact of treatment vaccine on infected persons for a given population (N).

Table 2 below shows the values of the parameters to be used in the model. Moreover, the table gives a brief description of the parameters, the values used as initial estimates for the constants, the range that are used for sampling later in the paper, and the units and references for the constants, also see Okuonghae and Aihie (2008).

Table 2: Parameter information.

| Parameter | Description | Values | Sampling range | Units | Ref. |
|-----------|-------------------------|--------------------|-------------------|------------------------------------|--------------|
| μ | Natural death rate | 0.02041 | (0.0143, 0.04) | year ⁻¹ | 24 |
| Λ | Recruitment rate | $\mu \times 10^5$ | – | year ⁻¹ | 8 |
| B | Transmission. Rate | 8.557 | (4.4769, 15.1347) | year ⁻¹ | Estimated |
| A | Transmission. Rate | $0.9 \times \beta$ | – | year ⁻¹ | Estimated |
| Γ | Trans. Rate | 1.5 | (1.5, 3.5) | year ⁻¹ | Estimated |
| P | Frac. of fast prog. | 0.1 | (0.05, 0.3) | year ⁻¹ | 20, 25 |
| K | Progression Rate | 0.05 | (0.005, 0.04) | year ⁻¹ | 19, 26 |
| r_0 | Recovery rate(latent) | 1.5 | (1.5, 2.5) | Ind ⁻¹ yr ⁻¹ | 1,8,20,23,27 |
| r_1 | Self-cure rate | 0.2 | (0.14, 0.25) | Ind ⁻¹ yr ⁻¹ | 19,21,28 |
| N | Treatment success(det.) | 0.75 | (0.5, 1) | year ⁻¹ | 15 |
| r_2 | Recovery rate(det.) | 1.5 | (1.5, 2.5) | Ind ⁻¹ yr ⁻¹ | 1,8,20,23,27 |
| Ω | Case detection Rate | 0.21 | (0,1) | year ⁻¹ | 15 |
| d_1 | TB-induced death(unde) | 0.365 | (0.22, 0.39) | year ⁻¹ | 19,21,23,28 |
| d_2 | TB-induced death (det.) | 0.3 | (0.22, 0.39) | year ⁻¹ | 19,29,30 |

The full model (14) is now simulated using the parameter estimates in Table 2 by applying the scheme in (6) for $k=1$, this is to assess the potential impact of treatment strategy under DOTS with the implementation parameters as they relate to Nigeria. Figure 2 give the plot of solutions generated by the sets of initial conditions. The DOTS surveillance and implementation in Nigeria was taken for the period of six years. The simulations show the increasing number of the

undetected cases and the effect of these on the fraction of the latent infectious i.e. the primary and the secondary latent individuals. It also shows the growth in the number of latent cases arising from failed treatment and self-cure. The simulations also show an initial drop in the number of primary latent infectious and detected infectious cases. It appears that the high treatment rate accounted for the drop of the disease. In fact, DOTS treatment success rates have been high in Nigeria over the last decade.

However, the continued presence of the huge pool of undetected cases may likely have triggered the sudden rise in the number of latent infectious and active TB cases in Nigeria, especially those who

became latent due to self-cure and failed treatment. The result of the stiffly stable PDNHLMM on the problem above is shown below in Figure 2.

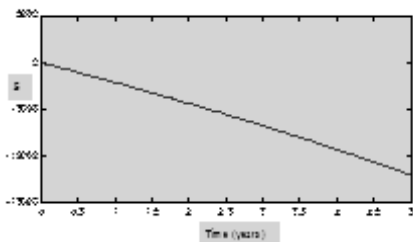


Fig. 2a Susceptible (S)

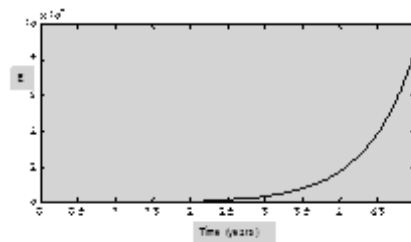


Fig. 2b Exposed (E)

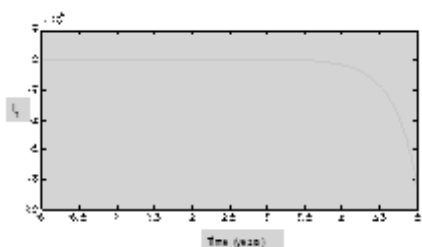


Fig. 2c Infected-undetected (I_1)

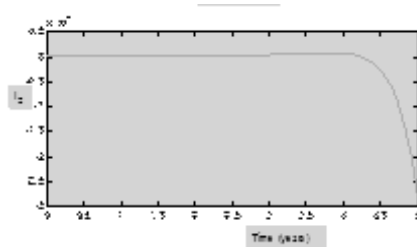


Fig. 2d Infected-detected (I_2)

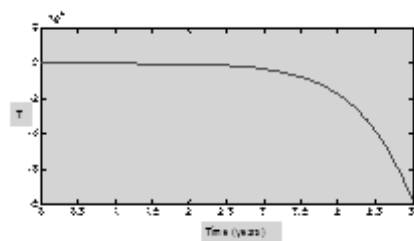


Fig. 2e Treated latent (T)

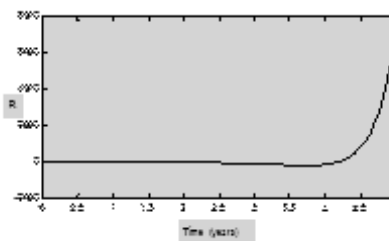


Fig. 2f Failed treatment (R)

Fig. 2: Show the graph of the TB model. (S) Susceptible, (E) Exposed, (I_1) Infected-undetected, (I_2) Infected-detected, (T) Treated latent and (R) Failed treatment classes after the numerical simulation.

Discussion and Conclusion

According to the current clinical data in Nigeria, the results of the numerical simulation in Fig. 2 shows that the incidence of tuberculosis is on the increase as many people are vulnerable and exposed to the disease and among the many factors responsible for this increase is the failure to detect a huge number of active tuberculosis cases which are primarily responsible for the rapid spread of the infection and also, increase in failed treatment cases. In order to effectively control the incidence and spread of

tuberculosis, the issue of S, E, I_1, I_2, T, R with (S) – Susceptible, (E) – Exposed, (I_1) – Infected-undetected, (I_2) – Infected-detected, (T) – Treated latent and (R) – Failed treatment must be addressed.

References

Blower S.M., Small P.M., Hopwell P.C, (1996). Control strategies for tuberculosis epidemics: new models for old problems, *Science* 273: 497 – 500.

Castillo-Chavez, C., Song, B. (2004), Dynamical models of tuberculosis and their applications, *Math Biosci Eng* 1(2): 361-404.

Dahlquist G., (1965) *Convergence and stability in*

the numerical integration of ordinary differential equations. Math. Scand., 4:33–53.

Ekoru, S.E., Esuabana, I.M., **Ikhile, M. N. O**, (2018) Implicit second derivative LMM with nested predictors for ODEs. American scientific Research J. for Engineering Tech. and Science (ASRJETS) Vol. 42 No 1 (2018).

Esuabana, I.M., Ita, M., Ekoru, S.E. and Samson, E. (2017), Hybrid LMMs with nested hybrid predictors for solving linear and non-linear IVPs in ODEs. Mathematical Theory and modeling. Vol 7, No 11 (2017) ISSN 2224–5804.

Feng Z., Castillo-Chavez C., Capurro A.F., (2000) A model for tuberculosis with exogenous reinfection. *Theor Pop Biol* 57: 235–247.

Okuonghae D. and Aihie V., (2008) Case Detection and Direct Observation Therapy Strategy (DOTS) in Nigeria: Its Effect on TB Dynamics. *J. Biological Systems*. Vol. 16, No. 1(2008) 1–31.

Okuonghae, D., Korobeinikov, A., (2007) Dynamics of tuberculosis: the effect of direct observation therapy strategy (DOTS) in Nigeria, *Math. Model Nat. Phenomena*, Vol. 2, No. 1: Epidemiology, pp. 99–111.

Olatunji P.O. and Ikhile M.N.O., (2017) Second derivative backward differentiation formulas with recursively nested hybrid evaluations. *J. Nigerian Mathematical Physics*, 40, pp. 83–90.

Ssematimba, A., Mugisha, J.Y.T., Luboobi, L.S., (2005) Mathematical models for the dynamics of tuberculosis in density-dependent populations: the case of internally displaced D peoples camps (IDPCs) in Uganda. *J Math Stat* 1(3): 217-224.

**DEVELOPMENT OF A FIFTH STAGE, FOURTH ORDER RUNGE-KUTTA METHOD
FOR THE SOLUTION OF INITIAL VALUE PROBLEMS IN ORDINARY
DIFFERENTIAL EQUATIONS**

Agbeboh Goddy Ujagbe, Ehiemua Michael Ebhodaghe and Okoruwa Gregory Ogbeide.
Department of Mathematics,
Ambrose Alli University, Ekpoma Nigeria.

Abstract

Through the traditional method of expansion and comparison with the corresponding Taylor series expansion, a new method is derived. The resulting method was used to solve some selected initial value problems. The results from the new method performed favourably well, when used to compare with those of the existing Classical Runge–Kutta method. The consistency, convergence and stability properties of this method were investigated. Errors involved in the new method and that of classical Runge–Kutta method, were plotted to determine their trajectories.

Keywords: Ordinary Differential Equation, Initial Value Problem, Consistency, Convergence and Absolute Stability

Introduction:

Solutions to real life problems often present themselves through the use of models and sometimes it is difficult to get appropriate model that can handle a problem. This is where differential equation becomes useful since it occurs frequently in several models of mathematical physics, biological sciences, engineering and applied mathematics; and solving these equations arising from the models will not be easy. According to Lambert (2000), numerical treatment is very important and provides a powerful alternative tool for solving the differential equation. There are various classes of methods in this direction. Example is Taylor series method which has a major disadvantage because it requires evaluation of partial derivatives of higher orders manually and this is not possible in any practical application, therefore there is the need for improved methods which do not need evaluation for repeated differentiation of the differential equation

(Butcher; 2000). So in this case, we use the numerical methods to get the approximate solution of a differential equation under a prescribed initial condition or conditions. Many methods have been proposed and used by authors in an attempt to provide accurate solutions to the various types of differential equations. As we already know, differential equation is divided into two parts (ordinary and partial), and we are proposing a scheme that can solve Ordinary Differential Equation (ODE) problems; although many of such methods already exist.

So in this research work, we decided to work within this limitation because as Lambert (2000) puts it, "what was needed was greater insight into the working of existing methods rather than develop new methods". So our focus is to adopt a new method through the traditional expansion approach, which is capable of solving initial value problem in ordinary differential equation given as:

$$y' = f(x, y), \quad y(x_0, y_0), \quad x \in [a, b] \quad (1.1)$$

for the purpose of improving on old stock. This method is expected to be effective for the solutions of non-stiff initial value problems in Ordinary Differential Equation.

In this research paper, we acknowledge that there

Corresponding Author: Agbeboh Goddy Ujagbe
Department of Mathematics,
Ambrose Alli University, Ekpoma Nigeria.
agbebohgoddy@gmail.com

are various one-step methods in existence, but a method becomes useful only when it possesses the inherent properties of consistency, convergence and stability. Here we will establish the consistency property of our method in line with Agbeboh and Ehiemua (2013), which revealed that a one step method is said to be consistent, if the difference equation of the computation formula exactly approximates the differential equation it intends to solve. Moreover, according to Lambert (2000), the traditional criterion for ensuring that a numerical method is absolutely stable, is carried out by subjecting the method to a linear test equation:

$$y' = \lambda h; \quad \lambda \in \mathbb{C}; \quad \text{Re}(\lambda) < 0 \quad (1.2)$$

where λ is complex

Butcher (2003) emphasized that all Runge-Kutta methods, including the implicit ones, when applied to the test equation, reduce to an equation of the form:

Derivation of method:

The general R-stage explicit Runge-Kutta method is defined as;

$$y_{n+1} - y_n = hf(x_n, y_n, h) \quad (2.1)$$

$$\text{where } f(x_n, y_n, h) = \sum_{r=1}^R b_r k_r \quad (2.2)$$

$$k_1 = f(x, y) = f$$

$$k_r = f\left(x_n + hc_r, y + h \sum_{s=1}^{r-1} a_{rs} k_s\right) \quad r = 2, 3, 4 \dots s \quad (2.3)$$

$$c_r = \sum_{s=1}^{r-1} a_{rs} \quad r = 2, 3, 4 \dots s \quad (2.4)$$

Since we are looking for a method with five stages, then we shall adopt the Taylor series to expand (2.3), by setting $r = 1, 2, 3, 4$ and 5 as;

$$\begin{aligned} k_1 &= f(x, y) \\ k_2 &= f(x + c_2 h, y + ha_{21} k_1) \\ k_3 &= f(x + c_3 h, y + h(a_{31} k_1 + a_{32} k_2)) \\ k_4 &= f(x + c_4 h, y + h(a_{41} k_1 + a_{42} k_2 + a_{43} k_3)) \\ k_5 &= f(x + c_5 h, y + h(a_{51} k_1 + a_{52} k_2 + a_{53} k_3 + a_{54} k_4)) \end{aligned} \quad (2.5)$$

$$y_{n+1} = R(\lambda h) y_n$$

where $R(\lambda h)$ is called the stability polynomial function. And so when we write $\mu = \lambda h$ it produces a linear system for the computation of ' k_i 's which will be solved for, and inserted into our method, leading to the equation:

$$\frac{y_{n+1}}{y_n} = R(\mu)$$

In Agbeboh and Esekhaigbe (2015), it was acknowledged that the key issue for understanding the long term dynamics of Runge-Kutta methods, concerns the region where $R(\mu) \leq 1$. The polynomial, for which $R(\mu) \leq 1$,

is known as stability polynomial of the method, and this method is absolutely stable for a given $\mu = \lambda h$ in $R(\mu)$.

But for the purpose of linearity, the above parameters will be transformed to reflect single parameters for $a_{rs} = a_i$ as follows:

$$a_{21} = a_1, a_{31} = a_2, a_{32} = a_3, a_{41} = a_4, a_{42} = a_5, a_{43} = a_6, a_{51} = a_7, a_{52} = a_8, a_{53} = a_9, a_{54} = a_{10}$$

Then (2.5) becomes:

$$\begin{aligned} k_2 &= f(y + ha_1k_1) \\ k_3 &= f(y + h(a_2k_1 + a_3k_2)) \\ k_4 &= f(y + h(a_4k_1 + a_5k_2 + a_6k_3)) \\ k_5 &= f(y + h(a_7k_1 + a_8k_2 + a_9k_3 + a_{10}k_4)) \end{aligned} \quad (2.6)$$

Adopting Taylor series expansion about the point (y_n) , we have:

$$\begin{aligned} k_1 &= f(y_n) \\ k_2 &= \sum_{r=0}^{\infty} \frac{1}{r!} \left(y + ha_1k_1 \frac{d}{dy} \right)^r f(y_n) \\ k_3 &= \sum_{r=0}^{\infty} \frac{1}{r!} \left(y + h(a_2k_1 + a_3k_2) \frac{d}{dy} \right)^r f(y_n) \\ k_4 &= \sum_{r=0}^{\infty} \frac{1}{r!} \left(y + h(a_4k_1 + a_5k_2 + a_6k_3) \frac{d}{dy} \right)^r f(y_n) \\ k_5 &= \sum_{r=0}^{\infty} \frac{1}{r!} \left(y + h(a_7k_1 + a_8k_2 + a_9k_3 + a_{10}k_4) \frac{d}{dy} \right)^r f(y_n) \end{aligned} \quad (2.7)$$

Where k_i^s are expanded individually in (2.7) to obtain the following, while making use of (2.4) as:

$$\begin{aligned} k_1 &:= f(x, y) = f; \\ k_2 &:= f + hc_2ff_y + \frac{1}{2} h^2 c_2^2 f^2 f_{yy} + \frac{1}{6} h^3 c_2^3 f^3 f_{yyy}; \\ k_3 &:= f + fc_3f_y h + h^2 a_3 c_2 f_y^2 + \frac{1}{2} h^2 f^2 c_3^2 f_{yy} + \frac{1}{2} h^3 a_3 c_2 f^2 f_{yy} f_y (c_2 + 2c_3) + \frac{1}{6} h^3 f^3 c_3^3 f_{yyy}; \\ k_4 &:= f + fc_4f_y h + fh^2 f_y^2 (a_5 c_2 + a_6 c_3) + \frac{1}{2} h^2 f^2 c_4^2 f_{yy} + h^3 a_6 a_3 c_2 f_y^3 \\ &\quad + \frac{1}{2} h^3 f_y f_y^2 f_{yy} (a_5 c_2^2 + 2a_5 c_2 c_4 + a_6 c_3^2 + 2a_6 c_3 c_4) + \frac{1}{6} h^3 f^3 c_4^3 f_{yyy}; \\ k_5 &:= f + fc_5f_y h + fh^2 f_y^2 (a_8 c_2 + a_9 c_3 + a_{10} c_4) + \frac{1}{2} h^2 f^2 c_5^2 f_{yy} + \frac{1}{2} h^3 f_y f_y^2 (a_8 c_2^2 \\ &\quad + 2a_8 c_2 c_5 + a_9 c_3^2 + 2a_9 c_3 c_5 + a_{10} c_4^2 + 2a_{10} c_4 c_5) f_{yy} + fh^3 f_y^3 (a_3 a_9 c_2 + a_5 a_{10} c_2 \\ &\quad + a_6 a_{10} c_3) + \frac{1}{6} h^3 f^3 c_5^3 f_{yyy}; \end{aligned} \quad (2.8)$$

Then with (2.2), we obtain;

$$\begin{aligned}
 b_1 \cdot k_1 + b_2 \cdot k_2 + b_3 \cdot k_3 + b_4 \cdot k_4 + b_5 \cdot k_5 = \\
 b_1 f + b_2 \left(f + h c_2 f f_y + \frac{1}{2} h^2 c_2^2 f^2 f_{yy} + \frac{1}{6} h^3 c_2^3 f^3 f_{yyy} \right) + b_3 \left(f + f c_3 f_y h + h^2 a_3 c_2 f f_y^2 \right. \\
 \left. + \frac{1}{2} h^2 f^2 c_3^2 f_{yy} + \frac{1}{2} h^3 a_3 c_2 f^2 f_{yy} f_y (c_2 + 2c_3) + \frac{1}{6} h^3 f^3 c_3^3 f_{yyy} \right) + b_4 \left(f + f c_4 f_y h \right. \\
 \left. + f h^2 f_y^2 (a_5 c_2 + a_6 c_3) + \frac{1}{2} h^2 f^2 c_4^2 f_{yy} + h^3 a_6 a_3 c_2 f f_y^3 + \frac{1}{2} h^3 f_y f^2 f_{yy} (a_5 c_2^2 \right. \\
 \left. + 2a_5 c_2 c_4 + a_6 c_3^2 + 2a_6 c_3 c_4) + \frac{1}{6} h^3 f^3 c_4^3 f_{yyy} \right) + b_5 \left(f + f c_5 f_y h + f h^2 f_y^2 (a_8 c_2 \right. \\
 \left. + a_9 c_3 + a_{10} c_4) + \frac{1}{2} h^2 f^2 c_5^2 f_{yy} + \frac{1}{2} h^3 f_y f^2 (a_8 c_2^2 + 2a_8 c_2 c_5 + a_9 c_3^2 + 2a_9 c_3 c_5 \right. \\
 \left. + a_{10} c_4^2 + 2a_{10} c_4 c_5) f_{yy} + f h^3 f_y^3 (a_3 a_9 c_2 + a_5 a_{10} c_2 + a_6 a_{10} c_3) + \frac{1}{6} h^3 f^3 c_5^3 f_{yyy} \right)
 \end{aligned}$$

Collecting in powers of 'h', we have;

$$\begin{aligned}
 f(b_1 + b_2 + b_3 + b_4 + b_5) + f f_y (b_2 c_2 + b_3 c_3 + b_4 c_4 + b_5 c_5) h + \frac{1}{2} h^2 f^2 (b_2 c_2^2 + b_3 c_3^2 + b_4 c_4^2 + b_5 c_5^2) f_{yy} \\
 + f h^2 f_y^2 (a_3 b_3 c_2 + a_5 b_4 c_2 + a_6 b_4 c_3 + a_8 b_5 c_2 + a_9 b_5 c_3 + a_{10} b_5 c_4) + \\
 \frac{1}{2} h^3 f^2 f_y (a_3 b_3 c_2^2 + 2a_3 b_3 c_2 c_3 + a_5 b_4 c_2^2 + 2a_5 b_4 c_2 c_4 + a_6 b_4 c_3^2 + 2a_6 b_4 c_3 c_4 + a_8 b_5 c_2^2 \\
 + 2a_8 b_5 c_2 c_5 + a_9 b_5 c_3^2 + 2a_9 b_5 c_3 c_5 + a_{10} b_5 c_4^2 + 2a_{10} b_5 c_4 c_5) f_{yy} \quad (2.9)
 \end{aligned}$$

$$f h^3 f_y^3 (a_3 a_6 b_4 c_2 + a_3 a_9 b_5 c_2 + a_5 a_{10} b_5 c_2 + a_6 a_{10} b_5 c_3) + \frac{1}{6} h^3 f^3 (b_2 c_2^3 + b_3 c_3^3 + b_4 c_4^3 + b_5 c_5^3) f_{yyy}$$

This will be used to compare with the Taylor series expansion given as;

$$y_{n+1} - y_n = hf + \frac{1}{2} h^2 f f_y + \frac{1}{6} h^3 (f^2 f_{yy} + f f_y^2) + \frac{1}{24} h^4 (f^3 f_{yyy} + 4f^2 f_y f_{yy} + f f_y^3) \quad (2.10)$$

and we finally get the following seven equations:

$$\begin{aligned}
 (b_1 + b_2 + b_3 + b_4 + b_5) &= 1 \\
 (b_2 c_2 + b_3 c_3 + b_4 c_4 + b_5 c_5) &= \frac{1}{2} \\
 (b_2 c_2^2 + b_3 c_3^2 + b_4 c_4^2 + b_5 c_5^2) &= \frac{1}{3} \\
 (b_2 c_2^3 + b_3 c_3^3 + b_4 c_4^3 + b_5 c_5^3) &= \frac{1}{4} \\
 (a_3 b_3 c_2 + a_5 b_4 c_2 + a_6 b_4 c_3 + a_8 b_5 c_2 + a_9 b_5 c_3 + a_{10} b_5 c_4) &= \frac{1}{6} \\
 (a_3 b_3 c_2^2 + 2a_3 b_3 c_2 c_3 + a_5 b_4 c_2^2 + 2a_5 b_4 c_2 c_4 + a_6 b_4 c_3^2 + 2a_6 b_4 c_3 c_4 + a_8 b_5 c_2^2 \\
 + 2a_8 b_5 c_2 c_5 + a_9 b_5 c_3^2 + 2a_9 b_5 c_3 c_5 + a_{10} b_5 c_4^2 + 2a_{10} b_5 c_4 c_5) &= \frac{1}{3} \quad (2.11)
 \end{aligned}$$

$$(a_3 a_6 b_4 c_2 + a_3 a_9 b_5 c_2 + a_5 a_{10} b_5 c_2 + a_6 a_{10} b_5 c_3) = \frac{1}{24}$$

From the first four equations above, and with the help of MAPLE package, we obtain the following parameters:

$$c_2 := \frac{1}{6}; c_3 := \frac{1}{3}; c_4 := \frac{2}{3}; c_5 := 1; c_1 := 0; b_1 := 0; b_2 := \frac{2}{5}; b_3 := 0; b_4 := \frac{1}{2}; b_5 := \frac{1}{10}$$

The right choice of parameters on the remaining four equations, with the use of MAPLE software package, results to the value given below;

$$a_3 := \frac{1}{2}; a_5 := \frac{2}{3}; a_6 := \frac{1}{3}; a_8 := -2; a_9 := \frac{2}{3}; a_{10} := 1; a_2 := -\frac{1}{6}; a_4 := -\frac{1}{3}; a_7 := \frac{4}{3};$$

So our new method becomes:

$$y_{n+1} = y_n + \frac{h}{10}(4k_2 + 5k_4 + k_5) \quad (2.12a)$$

with

$$\begin{aligned} k_1 &= f(x, y) \\ k_2 &= f\left(x + \frac{1}{6}h, y + \frac{1}{6}hk_1\right) \\ k_3 &= f\left(x + \frac{1}{3}h, y + h\left(-\frac{1}{6}k_1 + \frac{1}{2}k_2\right)\right) \\ k_4 &= f\left(x + \frac{2}{3}h, y + h\left(-\frac{1}{3}k_1 + \frac{2}{3}k_2 + \frac{1}{3}k_3\right)\right) \\ k_5 &= f\left(x + h, y + h\left(\frac{4}{3}k_1 - 2k_2 + \frac{2}{3}k_3 + k_4\right)\right) \end{aligned} \quad (2.12b)$$

Simply put in Butcher's array as:

| | | | | | |
|-----------------|----------------|---------------|---------------|---------------|----------------|
| 00 | | | | | |
| $\frac{11}{66}$ | - | | | | |
| $\frac{1}{3}$ | $-\frac{1}{6}$ | $\frac{1}{2}$ | | | |
| $\frac{2}{3}$ | $-\frac{1}{3}$ | $\frac{2}{3}$ | $\frac{1}{3}$ | | |
| 1 | $\frac{4}{3}$ | -2 | $\frac{2}{3}$ | 1 | |
| | 0 | $\frac{2}{5}$ | 0 | $\frac{1}{2}$ | $\frac{1}{10}$ |

Consistency of the Method

In order to show the consistency of the method (2.12), we prove the following theorem.

Theorem 1: (Consistency and convergence)

We assert here that the method (2.12) is consistent and converges to a known function

$$\text{if: } \lim_{h \rightarrow 0} \frac{y(x_{n+1}) - y(x_n)}{h} = f(y_n) \quad (3.1)$$

Proof: In order to establish the convergence of the method, we show that (2.12) is consistent with the initial value problem (1.1), that is;

$$\phi(x, y, 0) = f(x, y) \quad (3.2)$$

In line with Abadneh, Ahmad and ismail (2009), we prove that our method is consistent by first defining the local truncation error of the one-step method

$$y(x_{n+1}) = y(x_n) + hf(x_n, y_n, h) + T_n(h) \quad (3.3)$$

where $T_n(h)$ is the truncation error.

With (3.3), we proceed by taking the limits as $h \rightarrow 0$ on both sides. i.e.,

$$T_n(h^5) = y_{n+1} - y_n - \frac{1}{10} h (4f(h a_1 k_1 + y_n) + 5f(y_n + h(a_4 k_1 + a_5 f(h a_1 k_1 + y_n) + a_6 k_3)) + f(y_n + h(a_7 k_1 + a_8 f(h a_1 k_1 + y_n) + a_9 k_3 + a_{10} f(y_n + h(a_4 k_1 + a_5 f(h a_1 k_1 + y_n) + a_6 k_3))))))$$

Now divide all through by 'h':

$$T_n(h^4) = \frac{(y_{n+1} - y_n)}{h} - \left(\frac{2}{5} f(h a_1 k_1 + y_n) + \frac{1}{2} f(f(h a_1 k_1 + y_n) h a_5 + h a_4 k_1 + h a_6 k_3 + y_n) + \frac{1}{10} f(y_n + h(a_7 k_1 + a_8 f(h a_1 k_1 + y_n) + a_9 k_3 + a_{10} f(f(h a_1 k_1 + y_n) h a_5 + h a_4 k_1 + h a_6 k_3 + y_n))) \right)$$

Take the limit of both sides as h, we have:

$$0 = \lim_{h \rightarrow 0} \left(\frac{y_{n+1} - y_n}{h} \right) - f(y_n) \quad (3.6)$$

$$\therefore y' = f(y_n)$$

$$\lim_{h \rightarrow 0} T_n(h) = \lim_{h \rightarrow 0} \frac{y(x_{n+1}) - y(x_n)}{h} = f(x_n, y(x_n), h) \text{ and } x_0 + nh = x \in (x_0, \beta)$$

i.e.,

$$y'(x) - f(x, y(x), 0) = 0$$

$$\therefore f(x, y, 0) = f(x, y)$$

$$y = f(x, y)$$

Applying this process to our method, we have that

$$y_{n+1} = y_n + \frac{h}{10} (4k_2 + 5k_4 + k_5)$$

$$k_1 = f(y_n)$$

$$k_2 = f(y_n + a_1 h k_1) \quad (3.4)$$

$$k_3 = f(y_n + h(a_2 k_1 + a_3 k_2))$$

$$k_4 = f(y_n + h(a_4 k_1 + a_5 k_2 + a_6 k_3))$$

$$k_5 = f(y_n + h(a_7 k_1 + a_8 k_2 + a_9 k_3 + a_{10} k_4))$$

Substituting (3.4) into (2.12a), then (3.3) becomes;

$$T_n(h^5) = (y_{n+1} - y_n) - \frac{h}{10} (4k_2 + 5k_4 + k_5) \quad (3.5)$$

And the values of k_1, k_2, k_3, k_4 and k_5 in (3.4) are substituted into (3.5) to get:

ence the method is consistent and therefore converges.

Stability Analysis of the method:

Here we present the stability analysis of the new method, by applying it to the test equation

$y' = \lambda y$, to get:

$$k_1 = \lambda y;$$

$$k_2 := \lambda \cdot y \cdot \left(1 + \frac{1}{6} \cdot \lambda \cdot h\right)$$

$$k_3 := \lambda \cdot y \cdot \left(1 + \frac{1}{3} h \lambda + \frac{1}{12} h^2 \lambda^2\right)$$

$$k_4 := \lambda \cdot y \cdot \left(1 + \frac{2}{3} h \lambda + \frac{2}{9} h^2 \lambda^2 + \frac{1}{36} h^3 \lambda^3\right)$$

(4.4)

Now substituting (4.4) into (2.12a) above, we get:

$$y_{n+1} = y_n + h(b_1 \cdot k_1 + b_2 \cdot k_2 + b_3 \cdot k_3 + b_4 \cdot k_4 + b_5 \cdot k_5)$$

$$y_{n+1} - y_n = h \left(\frac{2}{5} \lambda y \left(\frac{1}{6} h \lambda + 1 \right) + \frac{1}{2} \lambda y \left(1 + \frac{2}{3} h \lambda + \frac{2}{9} h^2 \lambda^2 + \frac{1}{36} h^3 \lambda^3 \right) + \frac{1}{10} \lambda y \left(1 + h \lambda + \frac{5}{9} h^2 \lambda^2 + \frac{5}{18} h^3 \lambda^3 \right) \right)$$

$$y_{n+1} = y_n + h \cdot \lambda \cdot y \cdot \left(1 + \frac{1}{2} h \lambda + \frac{1}{6} h^2 \lambda^2 + \frac{1}{24} h^3 \lambda^3 \right)$$

$$\frac{(y_{n+1} - y_n)}{y_n} = \lambda \cdot h \cdot \left(1 + \frac{1}{2} h \lambda + \frac{1}{6} h^2 \lambda^2 + \frac{1}{24} h^3 \lambda^3 \right)$$

Let $\lambda h = \mu$

$$\frac{y_{n+1}}{y_n} = 1 + \mu + \frac{1}{2} \mu^2 + \frac{1}{6} \mu^3 + \frac{1}{24} \mu^4;$$

$$R(\mu) = 1 + \mu + \frac{1}{2} \mu^2 + \frac{1}{6} \mu^3 + \frac{1}{24} \mu^4; \quad (4.5)$$

To get the roots of the stability polynomial, we equate R.H.S of (4.5) to zero, and using a symbolic manipulation tool (MATLAB) to reduce complexity, we have the following:

$$-0.2706 + 2.5048i$$

$$-0.2706 - 2.5048i$$

$$-1.7294 + 0.8890i$$

$$-1.7294 - 0.8890i$$

So in order to generate the region of stability for our method, we also designed a program in MATLAB code, from which all the roots of the stability polynomial are visible within the stability region as shown in figures 1 and 2 below.

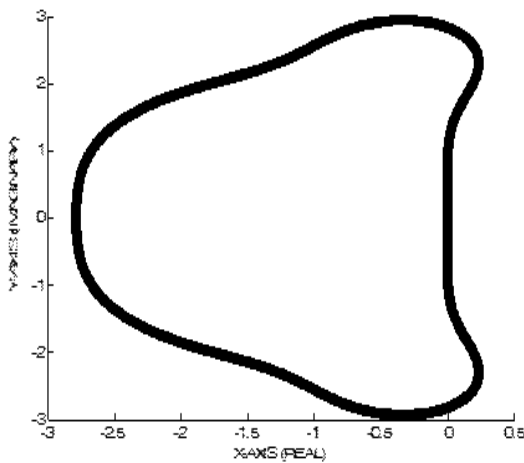


Fig 1: Stability Region Of Method

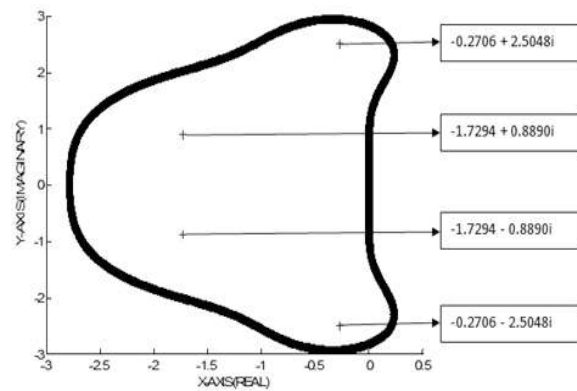


Fig 2: Absolute Stability Of Method

This is a clear indication that the new method so derived is not only A-STABLE, but ABSOLUTELY STABLE.

Implementation of the new method

In order to prove the usefulness of our method, some selected initial value problems were chosen

Problem1. $y' = y, \quad y(0) = 1, \quad 0 \leq x \leq 1$ (Agbeboh and Ehiemua (2014))

With theoretical solution $y(x) = \exp(x)$

Problem2. $y' = 3x + y, \quad y(0) = 1, \quad 0 \leq x \leq 1$ (Agam and Yahaya (2014))

With theoretical solution $y(x) = -3x - 3 + 4\exp(x)$

Problem 3. $y' = \exp(10(x - y)), \quad y(0) = 0.1, \quad 0 \leq x \leq 1$ (Lambert, 2000)

With theoretical solution $y(x) = \frac{1}{10} \log(\exp(10x) + \exp(1) - 1)$

for consideration as shown below. The numerical solution to these initial value problems were generated by using MATLAB package: Below are the selected non-stiff initial value problems for implementation:

Table 1: Numerical Results For Problem 1

| | | NEW METHOD (RKM(5, 4)) | | CLASSICAL METHOD (RKM(4, 4)) | |
|-----|--------------|---------------------------|-----------------|---------------------------------|-----------------|
| XN | TSOL | YN | ERROR | YN | ERROR |
| 0.1 | 1.1051709181 | 1.1051708611 | 5.69645366e-008 | 1.1051708333 | 8.47423145e-008 |
| 0.2 | 1.2214027582 | 1.2214026322 | 1.25911095e-007 | 1.2214025709 | 1.87309475e-007 |
| 0.3 | 1.3498588076 | 1.3498585988 | 2.08729915e-007 | 1.3498584971 | 3.10513466e-007 |
| 0.4 | 1.4918246976 | 1.4918243901 | 3.07576302e-007 | 1.4918242401 | 4.57560585e-007 |
| 0.5 | 1.6487212707 | 1.6487208458 | 4.24905469e-007 | 1.6487206386 | 6.32103290e-007 |
| 0.6 | 1.8221188004 | 1.8221182369 | 5.63511785e-007 | 1.8221179621 | 8.38298576e-007 |
| 0.7 | 2.0137527075 | 2.0137519809 | 7.26572958e-007 | 2.0137516266 | 1.08087370e-006 |
| 0.8 | 2.2255409285 | 2.2255400108 | 9.17699751e-007 | 2.2255395633 | 1.36520015e-006 |
| 0.9 | 2.4596031112 | 2.4596019702 | 1.14099193e-006 | 2.4596014138 | 1.69737688e-006 |
| 1 | 2.7182818285 | 2.7182804274 | 1.40110119e-006 | 2.7182797441 | 2.0843238e-006 |

Problem 1 above is an autonomous linear initial value problem, and the result indicates that the new method performed very well when compared with the Classical Runge-Kutta method as seen from the

error columns. This is expected from the fact that the new method has order five, while that of classical method, is order four.

Table 2: Numerical Results For Problem 2

| | | NEW METHOD (RKM(5, 4)) | | CLASSICAL METHOD (RKM(4,4)) | |
|-----|--------------|---------------------------|-----------------|--------------------------------|-----------------|
| XN | TSOL | YN | ERROR | YN | ERROR |
| 0.1 | 1.1206836723 | 1.1206834444 | 2.27858147e-007 | 1.1206833333 | 3.38969258e-007 |
| 0.2 | 1.2856110326 | 1.2856105290 | 5.03644380e-007 | 1.2856102834 | 7.49237901e-007 |
| 0.3 | 1.4994352303 | 1.4994343954 | 8.34919661e-007 | 1.4994339883 | 1.24205386e-006 |
| 0.4 | 1.7672987906 | 1.7672975603 | 1.23030521e-006 | 1.7672969603 | 1.83024234e-006 |
| 0.5 | 2.0948850828 | 2.0948833832 | 1.69962187e-006 | 2.0948825544 | 2.52841316e-006 |
| 0.6 | 2.4884752016 | 2.4884729475 | 2.25404714e-006 | 2.4884718484 | 3.35319430e-006 |
| 0.7 | 2.9550108299 | 2.9550079236 | 2.90629183e-006 | 2.9550065064 | 4.32349480e-006 |
| 0.8 | 3.5021637140 | 3.5021600432 | 3.67079901e-006 | 3.5021582532 | 5.46080061e-006 |
| 0.9 | 4.1384124446 | 4.1384078807 | 4.56396773e-006 | 4.1384056551 | 6.78950751e-006 |
| 1 | 4.8731273138 | 4.8731217094 | 5.60440475e-006 | 4.8731189765 | 8.33729552e-006 |

Problem 2 above is a non-autonomous linear initial value problem, and similarly the result also indicates that the new method performed well when compared with the Classical Runge-Kutta method

as seen from the error columns. This is also expected from the fact that the new method is of higher order but same stage.

Table 3: Numerical Results For Problem 3

| | | NEW METHOD (RKM(5, 4)) | | CLASSICAL METHOD (RKM(4, 4)) | |
|------|-------------|---------------------------|-----------------|---------------------------------|-----------------|
| XN | TSOL | YN | ERROR | YN | ERROR |
| 0.01 | 0.103796051 | 0.1037960515 | 5.14079196e-011 | 0.1037960519 | 4.42056419e-010 |
| 0.02 | 0.107830229 | 0.1078302293 | 1.14232485e-010 | 0.1078302301 | 9.19280263e-010 |
| 0.03 | 0.112107172 | 0.1121071724 | 1.90114521e-010 | 0.1121071736 | 1.43059001e-009 |
| 0.04 | 0.116630412 | 0.1166304125 | 2.80616294e-010 | 0.1166304142 | 1.97384738e-009 |
| 0.05 | 0.121402306 | 0.1214023065 | 3.87116561e-010 | 0.1214023086 | 2.54577874e-009 |
| 0.06 | 0.126423989 | 0.1264239898 | 5.10696513e-010 | 0.1264239924 | 3.14194973e-009 |
| 0.07 | 0.131695354 | 0.1316953543 | 6.52025406e-010 | 0.1316953575 | 3.75680184e-009 |
| 0.08 | 0.137215050 | 0.1372150504 | 8.11256590e-010 | 0.1372150540 | 4.38375533e-009 |
| 0.09 | 0.142980512 | 0.1429805133 | 9.87944115e-010 | 0.1429805173 | 5.01537623e-009 |
| 0.1 | 0.148988013 | 0.1489880137 | 1.18098972e-009 | 0.1489880182 | 5.64359989e-009 |

The above result again shows that the new method is consistent and converges faster, and gives a favourable result when compared with that of

Classical Runge-Kutta method. Hence the rate and time of convergence is very encouraging.

Representation of the error analysis of the new method

Here we plot the error trajectories of the new method alongside that of the classical method for the reason of comparison:

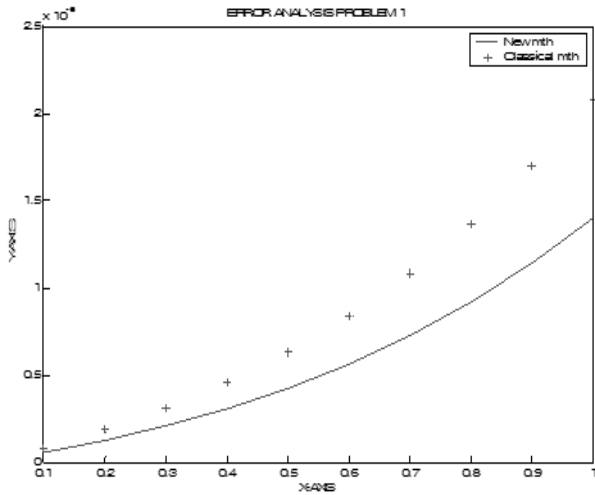


Fig 3: Plot Of Error Analysis Of Problem 1

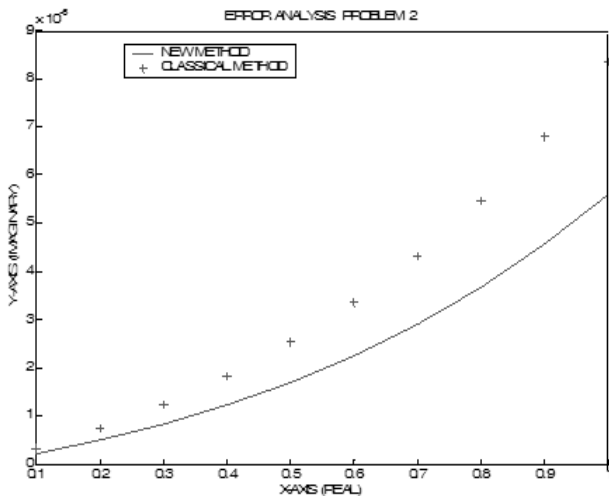


Fig 4: Plot Of Error Analysis Of Problem 2

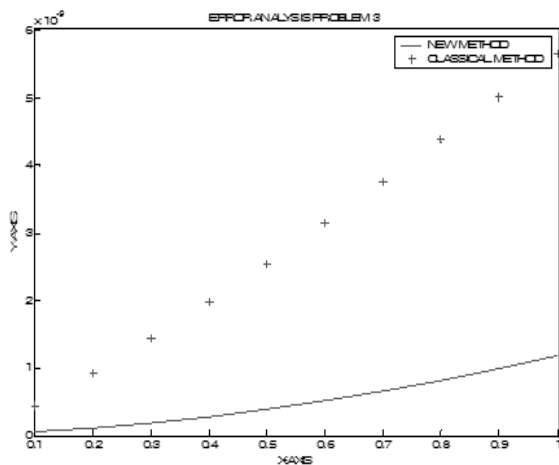


Fig 5: Plot Of Error Analysis Of Problem 3

Discussion and conclusion

The validity of the new method for numerical solution of first order initial value problems has been both theoretical and practically investigated. The results show that the method is consistent, convergent and stable, and the high level of accuracy of the method will therefore be suitable for the solution of real life problems that can possibly be reduced to first order ordinary differential equations.

Our new method has shown a considerable improvement in the solution of the chosen initial value problems when compared with existing order four Runge-Kutta methods. It was observed that the new method performed well especially in the display of error analysis. However, this method was seen to be effective in solving linear and non-stiff problems, as can be seen from the given problems above.

This new method maintains a high degree of accuracy in handling first order initial value problems. This method can also be extended to second order initial value problems with the hope of getting good results. This paper shows the possibility of constructing new Runge-Kutta methods of five-stage, fourth-order which is A-stable and has "absolute stability" properties. From the results obtained via the numerical experiment, it shows that the method is appropriate for the solution of non-stiff initial value problems in Ordinary Differential Equation.

References

- Ababneh O. Y., Ahmad R. and Ismail E. S. (2009), Design of New Diagonally Implicit Runge-Kutta Methods for Stiff Problems, *Applied Mathematical Sciences*, Vol. 3, 2009, no. 45, 2241–2253.
- Agam S.A. and Yahaya Y.A (2014). A highly Implicit Runge-Kutta Method for first order Ordinary differential equation. *African journal of mathematics and Computer Science Research*. Vol. 7, Issue 5, pp 55–60.
- Agbeboh, G.U. and Ehiemua, M.E. (2014). Modified Kutta's Algorithm, *JNAMP*, Vol. 28(1). pp 101–114.
- Agbeboh, G.U. and Ehiemua, M.E. (2013). On the convergence and stability of Modified

Kuta's Algorithm. *Ambrose Alli University post graduate journal*. Vol.1 No.1 pp 70-87.

Agbeboh, G. U. and Esekhaigbe, A. C. (2015). On the Component Analysis and Transformation of an explicit fourth-stage fourth order Runge-Kutta Methods. *Journal of natural Sciences Research*. Vol.5, No. 20, pp 2224-3186.

Butcher, J.C. (2000). *The numerical analysis of Ordinary Differential Equation: Runge-Kutta and General Linear Methods*. New York, John Wiley and sons Ltd.

.Butcher, J.C. (2003). *Numerical Methods for Ordinary Differential Equations*. New York, John Wiley and sons publications.

Lambert, J.D. (2000). *Computational Mathematics in Ordinary Differential Equations*. New York, John Wiley and sons publications, pp 120-133.

TWO-POINT CONTINUOUS FOURTH DERIVATIVE BLOCK METHODS FOR SOLVING STIFF SYSTEMS OF FIRST ORDER ORDINARY DIFFERENTIAL EQUATIONS (ODEs)

Ukpebor Luke Azeta, Elakhe Ohiomiogue Abraham, Adoghe L.Osa. and Ehapa Precious.
Department of Mathematics,
Ambrose Alli University, Ekpoma Nigeria.

Abstract

This paper presents a family of Two-point Continuous Fourth Derivative Block Methods (CFDBM) of order $k + 4$ for the solution of stiff systems of ordinary differential equations. The approach uses the collocation and interpolation technique to generate the main Continuous fourth Derivative method (CFDM) which is then used to obtain the additional methods that are combined as a single block method. Analysis of the methods shows that the method is L-stable up to order eight. Numerical examples are given to illustrate the accuracy and efficiency of the methods.

Keywords: Fourth derivative, Block method, Stiff problems, Continuous,

Introduction:

This study seeks to develop the numerical method for the solving of stiff initial value problems (IVPs) in first order of ordinary differential equations (ODEs) of the form:

$$y' = f(x, y), y(x_0) = y_0 \quad (1)$$

Where $y \in R^m, x \in [a, b]$ in ordinary differential equations. We seek a solution of (1) in the range $a \leq x \leq b$ where a and b are finite, and f satisfies the Lipchitz condition which guarantee that the problem has a unique continuous differentiable solution denoted by $y(x)$.

Equation (1) occurs in several areas of engineering, sciences and social sciences. Many physical problems are modeled into first order problems. Some of these problems have proved to be either difficult to solve or cannot be solved analytically, hence the need for numerical methods for solving such problems. Lambert(1991) and Hairer and Wanner(1996) posited that there are many methods for solving first order ordinary differential equations. One of the popular methods for solving (1) is by Linear Multistep Methods(LMM). This method of solution have been developed in varying form such as discrete linear multistep method and

continuous ones., Continuous linear multistep methods have greater advantages over the discrete methods because they give better error estimation, provide a simplified form of coefficients for further evaluation at different points, and provides solution at all interior points within the interval of integration than the discrete one(see Kayode and Awoyemi (2010), Onumanyi et al(1994)). Second derivative methods have been proposed by Enright (1974), Ismail (1999) and Hojjati et al(2006). Recently Ezzeddine and Hojjati(2012) and Akinfenwa et al (2015) proposed third derivative method of order $k + 3$. These methods were implemented in a step-by-step fashion.

In this paper, Continuous Fourth Derivation Block Methods(CFDBM) that will be self starting and also have better accuracy and stability properties for effectiveness and efficiency is proposed for solving stiff initial value problem in (1).

The paper is organized as follows: Section two considers the material and methods of developing the new method, section three considers the stability properties of the method, section four few provides solution to few numerical examples using the new method and results compared with some existing methods in the literature..

Derivation of the method

We proposed k -step continuous fourth derivative block method of form

Corresponding Author: Ukpebor Luke Azeta
Department of Mathematics,
Ambrose Alli University, Ekpoma Nigeria.

$$y(x) = y_{n+k-1} + h \sum_{j=0}^k \alpha_j(x) f_{n+j} + h^2 \beta_k(x) p_{n+k} + h^3 \eta_k(x) q_{n+k} + h^4 \delta_k(x) r_{n+k} \quad (2)$$

for the solution of (1) on the interval from x_n to x_{n+2} . Interpolation and collocation methods are used in the derivation of CFDBM. We shall consider, the power series polynomial of the form;

$$y(x) = \sum_{j=0}^k a_j x^j \quad (3)$$

as a basis function to approximate solution (1) above), where a_j are the parameters to be determined. where $\alpha_j(x)$, $\beta_k(x)$, $\eta_k(x)$ and $\delta_k(x)$ are the coefficients and k is the step number and h is the step length. We assume that $y_{n+j} = y(x_n + jh)$ is the numerical approximation to the analytical solution y_{n+j} and $y'_{n+j} = f(x_{n+j}, y_{n+j})$, $p_{n+k} = f'(x_{n+k}, y(x_{n+k}))$, $q_{n+k} = f''(x_{n+k}, y(x_{n+k}))$ and $r_{n+k} = f'''(x_{n+k}, y(x_{n+k}))$.

We seek a continuous representation of the CFDBM to approximate the exact solution $y(x)$ by the interpolating function of the form (3)

The first derivative of (3) with respect to x gives

$$f_{n+i} = \sum_{j=0}^{k+4} j a_j x^{j-1}, i = 0(1)k \quad (4)$$

The second derivative of (3) with respect to x gives

$$p_{n+i} = \sum_{j=0}^{k+4} j(j-1) a_j x^{j-2}, i = k \quad (5)$$

The third derivative of (3) with respect to x gives

$$q_{n+i} = \sum_{j=0}^{k+4} j(j-1)(j-2) a_j x^{j-3}, i = k \quad (6)$$

The fourth derivative of (3) with respect to x gives

$$r_{n+i} = \sum_{j=0}^{k+4} j(j-1)(j-2)(j-3) a_j x^{j-4}, i = k \quad (7)$$

Interpolating (3) at $x = x_n$ and Collocating (4), (5), (6) and (7) at $x = x_{n+i}, i = 0(1)k$ results in the system of linear equations

$$\begin{pmatrix} 1 & x_{n+i} & x_{n+i}^2 & x_{n+i}^3 & x_{n+i}^4 & \cdots & x_{n+i}^{k+4} \\ 0 & 1 & 2x_n & 3x_n^2 & 4x_n^3 & \cdots & D'x_{n+i}^{k+3} \\ \vdots & \vdots & \vdots & \vdots & \vdots & \ddots & \vdots \\ 0 & 1 & 2x_{n+k} & 3x_{n+k}^2 & 4x_{n+k}^3 & \cdots & D'x_{n+k}^{k+3} \\ 0 & 0 & 2 & 6x_{n+k} & 12x_{n+k}^2 & \cdots & D''x_{n+k}^{k+2} \\ 0 & 0 & 0 & 6 & 24x_{n+k} & \cdots & D'''x_{n+k}^{k+1} \\ 0 & 0 & 0 & 0 & 24 & \cdots & D''''x_{n+k}^k \end{pmatrix} \begin{pmatrix} a_0 \\ \vdots \\ a_{2k} \\ \vdots \\ a_{2k+1} \end{pmatrix} = \begin{pmatrix} y_{n+i} \\ f_{n+i} \\ p_{n+k} \\ \vdots \\ r_{n+k} \end{pmatrix} \quad (8)$$

where $D' = k + 4$, $D'' = (k + 4)(k + 3)$, $D''' = (k + 4)(k + 3)(k + 2)$, $D'''' = (k + 4)(k + 3)(k + 2)(k + 1)$

Solving equation (8) by Gaussian elimination methods yields values of a_j . Substituting the resulting values a_j into (3) with $x = x_n + jh$ leads to continuous linear multistep method. The resulting continuous scheme is evaluated at different values of t at different nodes.

Construction of Two-point CFDBM

We derive Two-point CFDBM by choosing $k = 2$ in (3), we have a polynomial of Degree $k + 4$ as follows:

$$\sum_{j=0}^{k+4} a_j x^j = y_{n+i}; \quad i = k - 1 \quad (9)$$

$$\sum_{j=0}^{k+4} ja_j x^{j-1} = f_{n+i} ; i = 0, \dots, k \quad (10)$$

$$\sum_{j=0}^{k+4} j(j-1)a_j x^{j-2} = p_{n+i}, i = k \quad (11)$$

$$\sum_{j=0}^{k+4} j(j-1)(j-2)a_j x^{j-3} = q_{n+i}, i = k \quad (12)$$

$$\sum_{j=0}^{k+4} j(j-1)(j-2)(j-3)a_j x^{j-4} = r_{n+i}, i = k \quad (13)$$

Collocating (10), (11), (12) and (13) at $x_{n+j}, j = 0, 1, 2$ and interpolating (9) at $x = x_n$ leads to a system of equations written in a matrix form

$$AX = B \quad (14)$$

$$\begin{pmatrix} 1 & h & (h)^2 & (h)^3 & (h)^4 & (h)^5 & (h)^6 \\ 0 & 1 & 0 & 0 & 0 & 0 & 0 \\ 0 & 1 & 2(h) & 3(h)^2 & 4(h)^3 & 5(h)^4 & 6(h)^5 \\ 0 & 1 & 2(2h) & 3(2h)^2 & 4(2h)^3 & 5(2h)^4 & 6(2h)^5 \\ 0 & 0 & 2 & 6(2h) & 12(2h)^2 & 20(2h)^3 & 30(2h)^4 \\ 0 & 0 & 0 & 6 & 24(2h) & 60(2h)^2 & 120(2h)^3 \\ 0 & 0 & 0 & 0 & 24 & 120(2h) & 360(2h)^2 \end{pmatrix} \begin{pmatrix} a_0 \\ a_1 \\ a_2 \\ a_3 \\ a_4 \\ a_5 \\ a_6 \end{pmatrix} = \begin{pmatrix} y_{n+1} \\ f_n \\ f_{n+1} \\ f_{n+2} \\ p_{n+2} \\ q_{n+2} \\ r_{n+2} \end{pmatrix} \quad (15)$$

Solving equation (15) by Gaussian elimination for the $a_j, j = 0(1)6$ as follows:

$$a_0 = \frac{1}{480}(-129hf_n - 912hf_{n+1} + 561hf_{n+2} - 450h^2p_{n+2} + 154h^3q_{n+2} - 24h^4r_{n+2} + 480y_{n+1})$$

$$a_1 = f_n$$

$$a_2 = -\frac{9f_n - 48f_{n+1} + 39f_{n+2} - 33hp_{n+2} + 12h^2q_{n+2} - 2h^3r_{n+2}}{6h}$$

$$a_3 = -\frac{-21f_n + 192f_{n+1} - 171f_{n+2} + 150hp_{n+2} - 57h^2q_{n+2} + 10h^3r_{n+2}}{18h^2}$$

$$a_4 = -\frac{4f_n - 48f_{n+1} + 44f_{n+2} - 40hp_{n+2} + 16h^2q_{n+2} - 3h^3r_{n+2}}{8h^3}$$

$$a_5 = -\frac{-27f_n + 384f_{n+1} - 357f_{n+2} + 330hp_{n+2} - 138h^2q_{n+2} + 28h^3r_{n+2}}{240h^4}$$

$$a_6 = -\frac{3f_n - 48f_{n+1} + 45f_{n+2} - 42hp_{n+2} + 18h^2q_{n+2} - 4h^3r_{n+2}}{288h^5} \quad (16)$$

On substituting the resulting values of the a_j in (16) into (9) and evaluating at $x = x_n + jh$ yield the continuous scheme

$$hjf_n - \frac{1}{288}hj^6(3f_n - 48f_{n+1} + 45f_{n+2} - 42hp_{n+2} + 18h^2q_{n+2} - 4h^3r_{n+2}) - \frac{1}{8}hj^4(4f_n - 48f_{n+1} + 44f_{n+2} - 40hp_{n+2} + 16h^2q_{n+2} - 3h^3r_{n+2}) - \frac{1}{6}hj^2(9f_n - 48f_{n+1} + 39f_{n+2} - 33hp_{n+2} + 12h^2q_{n+2} - 2h^3r_{n+2}) - \frac{1}{18}hj^3(-21f_n + 192f_{n+1} - 171f_{n+2} + 150hp_{n+2} - 57h^2q_{n+2} + 10h^3r_{n+2}) - \frac{1}{240}hj^5(-27f_n + 384f_{n+1} - 357f_{n+2} + 330hp_{n+2} - 138h^2q_{n+2} + 28h^3r_{n+2}) + \frac{1}{480}(-129hf_n - 912hf_{n+1} + 561hf_{n+2} - 450h^2p_{n+2} + 154h^3q_{n+2} - 24h^4r_{n+2} + 480y_{n+1}) \quad (17)$$

Inserting $j = 1$ and 2 respectively, into the continuous scheme in (17) result in the following formulae:

$$y_n = y_{n+1} - \frac{43hf_n}{160} - \frac{19}{10}hf_{n+1} + \frac{187}{160}hf_{n+2} - \frac{15}{16}h^2p_{n+2} + \frac{77}{240}h^3q_{n+2} - \frac{1}{20}h^4r_{n+2} \quad (18)$$

$$y_{n+2} = y_{n+1} - \frac{hf_n}{480} + \frac{7}{30}hf_{n+1} + \frac{123}{160}hf_{n+2} - \frac{13}{48}h^2p_{n+2} + \frac{13}{240}h^3q_{n+2} - \frac{1}{180}h^4r_{n+2} \quad (19)$$

Inserting $j = 1$ and 2 respectively, into the continuous scheme in (17) result in the following formulae:

The block form of which is given as

$$\begin{pmatrix} 1 & 0 \\ 0 & 1 \end{pmatrix} \begin{pmatrix} y_{n+1} \\ y_{n+2} \end{pmatrix} = \begin{pmatrix} 0 & -1 \\ 0 & 0 \end{pmatrix} \begin{pmatrix} y_{n-1} \\ y_n \end{pmatrix} + \begin{pmatrix} 0 & 0 \\ 1 & 0 \end{pmatrix} \begin{pmatrix} y_{n+1} \\ y_{n+2} \end{pmatrix} + h \begin{pmatrix} 0 & \frac{43}{160} \\ 0 & -\frac{1}{480} \end{pmatrix} \begin{pmatrix} f_{n-1} \\ f_n \end{pmatrix} + \begin{pmatrix} \frac{19}{10} & -\frac{187}{160} \\ \frac{7}{30} & \frac{123}{160} \end{pmatrix} \begin{pmatrix} f_{n+1} \\ f_{n+2} \end{pmatrix} + h^2 \begin{pmatrix} 0 & \frac{15}{16} \\ 0 & -\frac{13}{48} \end{pmatrix} \begin{pmatrix} p_{n+1} \\ p_{n+2} \end{pmatrix} + h^3 \begin{pmatrix} 0 & -\frac{77}{240} \\ 0 & \frac{13}{240} \end{pmatrix} \begin{pmatrix} q_{n+1} \\ q_{n+2} \end{pmatrix} + h^4 \begin{pmatrix} 0 & \frac{1}{20} \\ 0 & -\frac{1}{180} \end{pmatrix} \begin{pmatrix} r_{n+1} \\ r_{n+2} \end{pmatrix} \quad (20)$$

STABILITY ANALYSIS OF THE METHOD

Stability analysis of Two-point CFDBM

In this section, we analysed the order of accuracy, error constant, convergent and region of absolutely stability of the continuous fourth derivative block method (CFDBM).

Order and error constant

Following Lambert (1991) and Fatunla (1991) we define the local truncation error associated with the above methods to be the linear difference operator:

$$L[y(x); h] = \sum_{j=0}^k \varphi_j y(x + jh) - h \sum_{j=0}^k \alpha_j y'(x + jh) + h^2 \beta_k y''(x + jh) + h^3 \eta_k y'''(x + jh) + h^4 \delta_k y''''(x + jh) \quad (21)$$

Assuming that $y(x)$ is sufficiently differentiable, by expanding term in equation (21) in Taylor series about the point x to obtain the expression

$$L[y(x); h] = C_0 y(x) + C_1 h y'(x) + C_2 h^2 y''(x) + C_3 h^3 y'''(x) + \dots + C_p h^p y^{(p)}(x) + \dots$$

Where the constant coefficients C_p , $p = 0, 1, 2, 3, \dots$ are given as follows:

$$\begin{aligned} C_0 &= \sum_{j=0}^k \varphi_j \\ C_1 &= \sum_{j=1}^k j \varphi_j - \sum_{j=0}^k \alpha_j \\ C_2 &= \frac{1}{2!} \sum_{j=0}^k (j^2 \varphi_j - 2\alpha_j) - \beta_k \\ C_3 &= \frac{1}{3!} \sum_{j=0}^k (j^3 - 3j^2 \alpha_j) - k\beta - \lambda_k \\ C_4 &= \frac{1}{4!} \sum_{j=0}^k (j^4 \varphi_j - 4j^3 \alpha_j) - \frac{k^2}{2!} \beta_k - k\lambda_k - \sigma_k \\ C_p &= \frac{1}{p!} \sum_{j=0}^k (j^p \varphi_j - (p-1)\alpha_j) - \frac{k^{p-2}}{(p-2)!} \beta_k - \frac{k^{p-3}}{(p-3)!} \lambda_k - \frac{k^{p-4}}{(p-4)!} \sigma_k \end{aligned} \quad (22)$$

According to Henrici (1962), the method equation (3.1) has the order p if

$$L[y(x):h] = 0(h^{p-1}), \quad C_0 = C_1 = \dots = C_p = 0, \quad C_{p+1} \neq 0.$$

Therefore, C_{p+1} is the error constant and $C_{p+1}h^{p+1}y^{(p+1)}(x_n)$ the local truncation error at the point x_n . It was established from our calculations that the block methods for $k = 2$ have orders and error constants as displays in the table below.

| K | Order p | Error constant(c_{p+1}) |
|-----|-----------|---|
| 2 | 6 | $(-\frac{67}{50400}, -\frac{1}{16800})^T$ |

Linear Stability

The application of the method (20) to the scalar test equations

$$y' = \lambda y, y'' = \lambda^2 y, y''' = \lambda^3 y, y^{(4)} = \lambda^4 y, \operatorname{Re}(\lambda) > 0 \quad (23)$$

yield the stability polynomial

$$Y_{m+1} = M(z)Y_m, \quad z = \lambda h \quad (24)$$

Where the matrix $M(z)$ is the Amplification matrix given by

$$M(z) = -(A_1 - A_2 - B_1 Z - C_1 Z^2 - D_1 Z^3 - E_1 Z^4)^{-1}(A_0 + ZB_0) \quad (25)$$

And $A^{(i)}, B^{(i)}, C^{(i)}, D^{(i)}$ and $E^{(i)}$ are matrices.

The stability function for the method (20) is the polynomial $\pi(w, z)$ given by

$$\pi(w, z) = \operatorname{Det}[I_k w - M(z)] \quad (26)$$

The region of absolute stability (RAS) of CFDBMS (20) is defined by

$$RAS = \{Z \in \mathbb{C}: |p(M(z))| \leq 1\}$$

The Boundary locus is used to determine the region of absolute stability of the continuous fourth derivative block method (CFDBMS).

Consistency

The block method (20) is consistent if it has order at least one

Convergence

The block method (20) is convergent if and only if it is consistent and zero stable

Construction of Continuous Fourth derivative block method

In what follows, the k -step fourth derivative block method can generally be rearranged and rewritten as a matrix finite difference equation of the form:

$$A^{(1)}y_m = A^{(0)}y_{m-1} + A^{(2)}y_{m+1} + h[B^{(0)}f(y_{m-1}) + B^{(1)}f(y_m)] + h^2[C^{(1)}p(y_m)] + h^3[D^{(1)}q(y_m)] + h^4[E^{(1)}r(y_m)] \quad (28)$$

Where the matrix $r(y_m) = f^{(4)}(y_m)$, $q(y_m) = f^{(3)}(y_m)$ and $p(y_m) = f''(y_m)$ the $E^{(1)}, D^{(1)}$ and $C^{(1)}$ are strictly diagonal matrix with dimension $k \times k$

$$A^{(0)} = \begin{pmatrix} 1 & 0 & \dots & 0 \\ 0 & 1 & \dots & 0 \\ \vdots & \vdots & \ddots & \vdots \\ 0 & 0 & \dots & 1 \end{pmatrix}, \quad A^{(1)} = \begin{pmatrix} 0 & 0 & \dots & 0 \\ 0 & 0 & \dots & 1 \\ \vdots & \vdots & \ddots & \vdots \\ 0 & 0 & \dots & 0 \end{pmatrix}, \quad A^{(2)} = \begin{pmatrix} 0 & 1 & \dots & 0 \\ 0 & 0 & \dots & 0 \\ \vdots & \vdots & \ddots & \vdots \\ 0 & 1 & \dots & 0 \end{pmatrix}$$

$$B^{(1)} = \begin{pmatrix} b_{11}^{(1)} & b_{12}^{(1)} & \dots & b_{1k}^{(1)} \\ b_{21}^{(1)} & b_{22}^{(1)} & \dots & b_{2k}^{(1)} \\ \vdots & \vdots & \ddots & \vdots \\ b_{k1}^{(1)} & b_{k2}^{(1)} & \dots & b_{kk}^{(1)} \end{pmatrix}, \quad B^{(0)} = \begin{pmatrix} 0 & 0 & \dots & b_{1k}^{(0)} \\ 0 & 0 & \dots & b_{2k}^{(0)} \\ \vdots & \vdots & \ddots & \vdots \\ 0 & 0 & \dots & b_{kk}^{(0)} \end{pmatrix}, \quad (29)$$

$$C^{(1)} = \begin{pmatrix} 0 & 0 & \dots & c_{1k}^{(1)} \\ 0 & 0 & \dots & c_{2k}^{(1)} \\ \vdots & \vdots & \ddots & \vdots \\ 0 & 0 & \dots & c_{kk}^{(1)} \end{pmatrix}, \quad D^{(1)} = \begin{pmatrix} 0 & 0 & \dots & d_{1k}^{(1)} \\ 0 & 0 & \dots & d_{2k}^{(1)} \\ \vdots & \vdots & \ddots & \vdots \\ 0 & 0 & \dots & d_{kk}^{(1)} \end{pmatrix}, \quad E^{(1)} = \begin{pmatrix} 0 & 0 & \dots & e_{1k}^{(1)} \\ 0 & 0 & \dots & e_{2k}^{(1)} \\ \vdots & \vdots & \ddots & \vdots \\ 0 & 0 & \dots & e_{kk}^{(1)} \end{pmatrix}$$

and the vectors $y_m, y_{m+1}, f_{m+1}, f_m, p_m, q_m$ and r_m defined

$$\begin{aligned}
 y_{m+1} &= \begin{pmatrix} y_{n+1} \\ y_{n+2} \\ y_{n+3} \\ y_{n+4} \\ \vdots \\ y_{n+k-1} \\ y_{n+k} \end{pmatrix}, & y_m &= \begin{pmatrix} y_{n-k+1} \\ y_{n-k+2} \\ y_{n-k+3} \\ y_{n-k+4} \\ \vdots \\ y_{n-1} \\ y_n \end{pmatrix}, & f_{m+1} &= \begin{pmatrix} f_{n+1} \\ f_{n+2} \\ f_{n+3} \\ f_{n+4} \\ \vdots \\ f_{n+k} \end{pmatrix}, \\
 f_m &= \begin{pmatrix} f_{n-k+1} \\ f_{n-k+2} \\ f_{n-k+3} \\ f_{n-k+4} \\ \vdots \\ f_{n-1} \\ f_n \end{pmatrix}, & p_{m+1} &= \begin{pmatrix} p_{n+1} \\ p_{n+2} \\ p_{n+3} \\ p_{n+4} \\ \vdots \\ p_{n+k} \end{pmatrix}, & q_{m+1} &= \begin{pmatrix} q_{n+1} \\ q_{n+2} \\ q_{n+3} \\ q_{n+4} \\ \vdots \\ q_{n+k} \end{pmatrix}, \\
 r_{m+1} &= \begin{pmatrix} r_{n+1} \\ r_{n+2} \\ r_{n+3} \\ r_{n+4} \\ \vdots \\ r_{n+k} \end{pmatrix}
 \end{aligned}$$

Two-point continuous fourth derivative block method

The matrix coefficients of two-point CFDBM of the form (20) is given as

$$\begin{aligned}
 A^{(1)} &= \begin{pmatrix} 1 & 0 \\ 0 & 1 \end{pmatrix}, & A^{(0)} &= \begin{pmatrix} 0 & -1 \\ 0 & 0 \end{pmatrix}, & A^{(2)} &= \begin{pmatrix} 0 & 0 \\ 1 & 0 \end{pmatrix}, \\
 B^{(0)} &= \begin{pmatrix} 0 & \frac{43}{160} \\ 0 & \frac{1}{480} \end{pmatrix}, & B^{(1)} &= \begin{pmatrix} \frac{19}{10} & -\frac{187}{160} \\ \frac{7}{30} & \frac{123}{160} \end{pmatrix}, & C^{(1)} &= \begin{pmatrix} 0 & \frac{15}{16} \\ 0 & -\frac{13}{48} \end{pmatrix}, \\
 D^{(1)} &= \begin{pmatrix} 0 & -\frac{77}{240} \\ 0 & \frac{13}{240} \end{pmatrix}, & E^{(1)} &= \begin{pmatrix} 0 & \frac{1}{20} \\ 0 & -\frac{1}{180} \end{pmatrix}
 \end{aligned} \tag{30}$$

Stability Analysis of Two-point Continuous Fourth Derivative Block Method

The order and error constant of CFDBM of block size $k = 2$ can be obtained in similar manner. Applying CFDBM (20) to the scalar test problem (23) yields the characteristics polynomial equation.

$$\Pi(R, z) = \det(A^{(1)}R - A^{(0)} - A^{(2)}R - ZB^{(0)} - ZRB^{(1)} - Z^2RC^{(1)} - Z^3RD^{(1)} - Z^4RE^{(1)}) = 0 \tag{31}$$

The matrices $A^{(0)}, A^{(1)}$ and $A^{(2)}$ are as specified in CFDBM (30).

Then, k -point CFDBM will be absolutely stable if $|R_j(Z)| < 1, j = 1, 2, \dots, k$ holds.

The method of boundary locus is used to determine the region of absolute stabilities for methods in (2).

The stability analysis of CFDBM (20) leads to the parameters of Table (4.2.3) and the boundary locus plots for CFDBM (20) of block sizes $k = 2$ drawn in figure 1 below using MATLAB

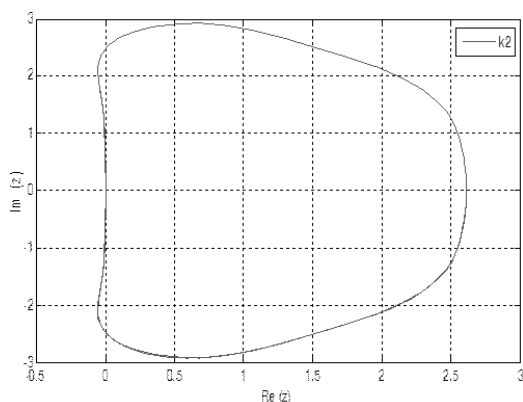


Figure 1: The region of absolute stability of the two point CFDBM

Numerical Experiments

To study the efficiency of the block method, some numerical examples to illustrate the accuracy of the

Problem 1:

$$y_1' = -y_1 + 95y_2, y_1(0) = 1, y_2' = -y_1 - 97y_2, y_2(0) = 1$$

Its exact solution are given as

$$y_1 = \frac{(95e^{-2x} - 48e^{-95x})}{47}, y_2 = \frac{(48e^{-96x} - e^{-2x})}{47}$$

Table (1) :Comparative analysis of result of problem 1 for CFDBM

| h | Methods | y ₁ | y ₂ × 10 ² (/error/) |
|----------|---------------------------------------|---|--|
| 0.0625 | CH4 | 0.2735498 (3.0 × 10 ⁻⁷) | -0.2879471 (4.0 × 10 ⁻⁹) |
| | CH5 | 0.27554005 (3.0 × 10 ⁻⁸) | -0.2879274 (3.0 × 10 ⁻⁹) |
| | J-K | 0.2735523 (1.0 × 10 ⁻⁸) | -0.2879477 (4.0 × 10 ⁻⁹) |
| | F ⁴ | 0.2735503 (3.0 × 10 ⁻⁷) | -0.2879477 (3.1 × 10 ⁻⁷) |
| | F ⁵ | 0.2735503 (6.4 × 10 ⁻⁹) | -0.2879441 (6.7 × 10 ⁻⁹) |
| | OK6 | 0.2735503 (1.3 × 10 ⁻⁶) | -0.28794748 (2.4 × 10 ⁻⁸) |
| | F ⁶ | 0.27354864 (1.3 × 10 ⁻⁹) | -0.28794694 (4.7 × 10 ⁻⁹) |
| | CFDBM2 | 0.27355003 (2.2 × 10 ⁻⁹) | -0.002879474 (2.6 × 10 ⁻¹¹) |
| a0.03125 | CH4 | 0.27355003 (1.0 × 10 ⁻⁸) | -0.28794742 (1.0 × 10 ⁻⁸) |
| | J-K | 0.27355005 (5.0 × 10 ⁻⁷) | -0.28794742 (4.0 × 10 ⁻⁷) |
| | AB7 | 0.273545505 (4.0 × 10 ⁻⁵) | -0.28794751 (6.0 × 10 ⁻⁵) |
| | OK6 | 0.27354657 (3.4 × 10 ⁻⁶) | -0.28355004 (3.7 × 10 ⁻⁸) |
| | F ⁴ | 0.27355005 (1.0 × 10 ⁻⁸) | 0.28794742 (1.0 × 10 ⁻⁸) |
| | F ⁵ | 0.27355004 (6.3 × 10 ⁻¹⁰) | -0.28794740 (1.4 × 10 ⁻¹⁰) |
| | AF5 | 0.27354958 (4.5 × 10 ⁻⁷) | -0.28794694 (4.7 × 10 ⁻⁹) |
| | F ⁶ | 0.27355004 (6.0 × 10 ⁻¹¹) | -0.2879474 (5.0 × 10 ⁻¹⁰) |
| CFDBM2 | 0.27355004 (4.0 × 10 ⁻¹¹) | -0.0028794 (4.2 × 10 ⁻¹³) | |
| 0.05 | OK6 | 0.27354864264 (1.0 × 10 ⁻⁶) | 0.2879459394 (1.0 × 10 ⁻⁴) |
| | AF5 | 0.27354738 (2.7 × 10 ⁻⁶) | -0.28794461 (1.4 × 10 ⁻⁸) |
| | F ⁶ | 0.27355504 (3.7 × 10 ⁻⁸) | -0.2879474 (1.4 × 10 ⁻⁸) |
| | CFDBM2 | 0.27355003 (6.5 × 10 ⁻¹⁰) | -0.0028794 (6.8 × 10 ⁻¹²) |
| | Exact soln | 0.2735004 | -0.287947411 |

Remark: from the table (5.1a), the numerical results revealed that our method of order 6 provides good approximation

methods are presented in this section. Absolute errors of the approximate solution on the partition π_N is found using $|y - y(x)|$. Some problems are solved using CFDBM and their efficiency and results are compared with those of existing methods.

Now, for the purpose of comparative analysis of performance of the new integrator on the various numerical examples, we donate CFDBM2 as new method, F6–Abhulimen and Ukpebor(2017), OK4, and OK6–Okunuga (1997, 1994) methods of Order 4 and 6, CH4, CH5–Cash (1981) method of order 4 and 5 respectively, J–K–Jackson and Kenue (1974), F4–Voss (1988) method of Order 4, AF5–Abhulimen and Okunuga (2008), F5–Abhulimen (2009) method of Order 5, AG6–Abhulimen Omeike (2011) and AB8–Abhulimen (2008) method of order 8.

Problem 2:

$$y'' + 1001y' + 1000y = 0, y(0) = 1, y'(0) = 1 \quad (1)$$

Its exact solution is given as

$$y(x) = \frac{1001}{999} e^{-x} - \frac{2}{999} e^{-1000x}$$

The problem above is a second order problem, but our method is only capable of handling first order problem, hence there is need to convert it to first order system and before applying our method to solve it.

Let $y=y_1$ and $y_1 = y_2$ in equation (1)

Hence (1) become

$$y_2 + 1001y_2 + 1000y_1$$

This can be written in its equivalent system of first order stiff problem as

$$\begin{aligned} y_1' &= y_2, & y_1(0) &= 1 \\ y_2' &= -1001y_2 - 1000y_1, & y_2(0) &= 1 \end{aligned}$$

Its exact solution are given as

$$y_1(x) = \frac{1001}{999} e^{-x} - \frac{2}{999} e^{-1000x}, \quad y_2(x) = -\frac{1001}{999} e^{-x} + \frac{2000}{999} e^{-1000x}$$

Table 2. Comparative analysis of result of problem 2 for CFDBM

Numerical results on second order (ODE) at $x=1$.

| h | Methods | \mathbb{E}_1 | $\mathbb{E}_2 \times 10^2$ (/error/) |
|-------|------------|----------------|--------------------------------------|
| 0.05 | OK6 | 0.367879436 | 5.6×10^{-8} |
| | F5 | 0.367879440 | 5.2×10^{-9} |
| | AG6 | 0.36787846 | 1.4×10^{-8} |
| | AF5 | 0.36787930 | 1.8×10^{-7} |
| | F6 | 0.36787840 | 4.4×10^{-9} |
| | CFDBM2 | 0.368614980 | 9.5×10^{-7} |
| 0.125 | F5 | 0.367879442 | 2.7×10^{-8} |
| | F6 | 0.367879440 | 3.4×10^{-10} |
| | CFDBM2 | 0.36861408 | 1.8×10^{-6} |
| | Exact soln | 0.36789435 | |

Remark: The numerical results in table (2) show that CFDBM compares favourably with method in the literature.

Conclusion

A newly derived family of Continuous Fourth Derivative Block Method has been developed for the solution of stiff systems of ordinary differential equations and used to simultaneously solve (1.1) directly without the need for starting values or predictors. The efficiency of the CFDBM has been demonstrated on some standard numerical examples. Details of the numerical results are displayed in Tables 1 and 2.

References

- Abhulimen, C.E (2008). A class of exponentially – fitted third derivative multistep methods for solving stiff differential equations, International of Physical Sciences(IJPS),(3) 188–193.
- Abhulimen and Omeike (2011); A sixth –order exponentially fitted scheme for the numerical solution of systems of ordinary differential equations, Journal of Appl. Math. Bioinf. (1), 175–186

- Abhulimen, C.E. and Okunuga, S.A.(2008): Exponentially fitted second derivative multistep method for stiff initial value problem for ODEs, *Journal of Engineering Science Applications* (5);36-47
- Akinfenwa.O.A, . Akinnukawe B, Mudasiru S.B(2017): A family of Continuous Third Derivative Block Methods for solving stiff systems of first order ordinary differential equations
- Cash ,J. R.(1981) Second derivative extended backward differential formula for the numerical integration of stiff systems, *SIAM Journal of Numerical Analysis*. Vol.18,21-36
- Enright WH. (1974) Second derivative multistep methods for stiff ordinary differential equations. *SIAM Journal of Numerical Analysis*;11(2):321-31.
- Ezzeddine AK, Hojjati G.(2012) Third derivative multistep methods for stiff systems. *Int J Nonlinear Sci* ;14(4):443-50
- Hairer E, Wanner G(1996). *Solving ordinary differential equations II*. New York: Springer;
- Hojjati G, Rahimi M, Hosseini SM.(2006): New second derivative multistep methods for stiff systems. *Appl Math Model* 2006;30:466-76
- Ismail G, Ibrahim I. New efficient second derivative multistep methods for stiff systems. *Appl Math Model* 1999;23:279-88
- Jackson, L.W. and Kenue, S.K(1974). A fourth-order exponentially fitted method, *SIAM Journal of Numerical Analysis* vol.2, 965-978
- Kayode S.J,and Awoyemi D.O. A multi derivative collocation method for fifth order ordinary differential equation. *J Math Stat* 2010;6(1):60-3
- Lambert, J.D.(1991). *Numerical methods for ordinary differential systems*. New York: John Wiley, U.S.A
- Okunuga, S.A. (1997). Fourth order composite two-step method for stiff problems. *International Journal of Computational Mathematics*,(2), 39-47
- Okunuga, S.A. (1994). *Composite Multiderivative Linear Multistep Method for equations of stiff Ivp in ODEs* (PhD Thesis, Department of Mathematics, University of Lagos, Nigeria)
- Onumanyi .P, Awoyemi D.O, Jator S.N, Sirisena U.W(1994). New linear multistep methods with continuous coefficients for first order initial value Problems. *J Nigerian Math Soc* ; 13:37-51.
- Voss, D.(1988). A fifth-order exponentially fitted formula. *SIAM Journal of Numerical Analysis*. Vol.25(3), 670-678

A QUARTIC BASED DENOMINATOR OF ORDER SIX RATIONAL INTEGRATOR

Elakhe Ohiomiogue Abraham.

Department of Mathematics,
Ambrose Alli University, Ekpoma, Edo State, Nigeria.

Ehika Edith

Department of Mathematics,
Ambrose Alli University, Ekpoma, Edo State, Nigeria.

&

Ehika Simon

Department of Physics,
Ambrose Alli University, Ekpoma, Edo State, Nigeria.

Abstract

There have been several activities among researchers on numerical solution integrated methods for stiff, singular as well as oscillatory systems. This excitement is spurred by real life processes that often lead to initial valued problems that are singular and stiff in nature. This paper presents an order six rational integrator of a quartic based denominator for the solution of initial value problems in ordinary differential equation that are singular, oscillatory or stiff. The analysis of the method shows that the convergence rate is high and that our numerical integrator is A-Stable. Our method compared favourable well with certain Block Hybrid Extended Trapezoidal Multistep Method of the Second kind and hence obtain a good result for real life.

Keywords: Rational Integrator, Initial Value Problems, Convergence, Consistency, quartic based denominator

Introduction:

There have been high levels of interest in the research for numerical integrators that can solve stiff, singular as well as oscillatory systems in ordinary differential equations. Extensive works have been done by scholars in the area of rational integrators, providing encouraging results in the solution of problems arising from mathematical formulation of physical situations in population models, mechanical oscillations, process control, chemical kinetics, biological simulations, radioactivity etc. These Physical situations often lead to initial valued problems (IVPs) in ordinary differential equation (Lambert, 1995; Aashikpelokhai, 1997; Patel, 2000; Abhulimen and Otunta 2007; Osborne and Turner, 2010; Elakhe and Aashikpelokhai 2013; Islam, 2015). This research work is centred on the solution of initial valued problem (IVP) of the form:

$$y' = f(x, y), \quad y(x_0) = y_0, \quad a \leq x \leq b \quad (1)$$

where $f(x, y)$ is defined and continuous in a region $D \subset [a, b]$ of the real line.

This research work was inspired by the work done by Lambert and Shaw (1965) and Aashikpelokhai, (1997). Aashikpelokhai and Momodu (2008) and Elakhe and Aashikpelokhai (2013) extended the work of Lambert and Shaw (1965) whose styles we wish to adopt. Elakhe, Aashikpelokhai and Ebhomien (2011) derived a dynamic Singulo – Stiff numerical rational integrator from a polynomial of degree four based denominator. Subsequently, an order five rational integrator was obtained by Elakhe, Onianwa and Elakhe (2016). In this current work, we wish to extend the work of Elakhe et al., (2016), by deriving a quartic based denominator of order six rational numerical integrator that can handle initial valued problems that are Singular, Stiff or Singulo – Stiff in nature and compare our results with conventional methods. This integrator is a polynomial of degree two in the numerator and a polynomial of degree four based denominator. The polynomial of degree four based denominator gave it the name Quartic. We will also examine its consistency, convergence and stability.

Corresponding Author: Elakhe Ohiomiogue Abraham
Department of Mathematics,
Ambrose Alli University, Ekpoma Nigeria.

DERIVATION OF THE ORDER SIX RATIONALINTEGRATOR

First, we introduce the rational interpolant $U : R \rightarrow R$

$$U(x) = \frac{\sum_{i=0}^2 p_i x_i}{1 + \sum_{i=1}^4 q_i x^i} \quad (2)$$

where p_0, p_1, p_2 and q_1, q_2, q_3, q_4 are called the integrator parameters But

$$U(x) = \sum_{r=0}^{\infty} c_r x^r \quad (3)$$

Hence (2) becomes

$$\sum_{r=0}^{\infty} c_r x^r \left(1 + \sum_{r=1}^4 q_r x^r \right) = \sum_{r=0}^2 P_r x^r \quad (4)$$

On summing and expanding, we have

$$\left. \begin{aligned} p_0 &= c_0 \\ p_1 &= c_0 q_1 + c_1 \\ p_2 &= c_0 q_2 + c_1 q_1 + c_2 \\ p_3 &= c_0 q_3 + c_1 q_2 + c_2 q_1 + c_3 \\ p_4 &= c_0 q_4 + c_1 q_3 + c_2 q_2 + c_3 q_1 + c_4 \\ p_5 &= c_1 q_4 + c_2 q_3 + c_3 q_2 + c_4 q_1 + c_5 \\ p_6 &= c_2 q_4 + c_3 q_3 + c_4 q_2 + c_5 q_1 + c_6 \\ p_7 &= c_3 q_4 + c_4 q_3 + c_5 q_2 + c_6 q_1 + c_7 \\ p_8 &= c_4 q_4 + c_5 q_3 + c_6 q_2 + c_7 q_1 + c_8 \\ p_9 &= c_5 q_4 + c_6 q_3 + c_7 q_2 + c_8 q_1 + c_9 \\ p_{10} &= c_6 q_4 + c_7 q_3 + c_8 q_2 + c_9 q_1 + c_{10} \end{aligned} \right\} \quad (5)$$

Since our numerator is order 2, the integrator parameters

$$p_3 = p_4 = p_5 = p_6 = p_7 = p_8 = p_9 = p_{10} = 0$$

Hence, we have on rearranging and putting in matrix form,

$$\begin{bmatrix} c_5 & c_4 & c_3 & c_2 \\ c_4 & c_3 & c_2 & c_1 \\ c_3 & c_2 & c_1 & c_0 \\ c_2 & c_1 & c_0 & 0 \end{bmatrix} \begin{bmatrix} q_1 \\ q_2 \\ q_3 \\ q_4 \end{bmatrix} = - \begin{bmatrix} C_6 \\ C_5 \\ C_4 \\ C_3 \end{bmatrix} \quad (6)$$

Equation (6) is our governing equation. Hence to solve for q_1, q_2, q_3 and q_4 , we employ the Crammers rule, which is given by

$$q_i = \frac{x_i}{|A|}, \quad \text{where } i=1,2,3,4 \quad (7)$$

First, we construct the following determinants from (6).

$$|A| = \begin{vmatrix} c_5 & c_4 & c_3 & c_2 \\ c_4 & c_3 & c_2 & c_1 \\ c_3 & c_2 & c_1 & c_0 \\ c_2 & c_1 & c_0 & 0 \end{vmatrix} \quad (8)$$

$$x_1 = \begin{vmatrix} -c_6 & c_4 & c_3 & c_2 \\ -c_5 & c_3 & c_2 & c_1 \\ -c_4 & c_2 & c_1 & c_0 \\ -c_3 & c_1 & c_0 & 0 \end{vmatrix} \quad (9)$$

$$x_2 = \begin{vmatrix} c_5 & -c_6 & c_3 & c_2 \\ c_4 & -c_5 & c_2 & c_1 \\ c_3 & -c_4 & c_1 & c_0 \\ c_2 & -c_3 & c_0 & 0 \end{vmatrix} \quad (10)$$

$$x_3 = \begin{vmatrix} c_5 & c_4 & -c_6 & c_2 \\ c_4 & c_3 & -c_5 & c_1 \\ c_3 & c_2 & -c_4 & c_0 \\ c_2 & c_1 & -c_3 & 0 \end{vmatrix} \quad (11)$$

$$x_4 = \begin{vmatrix} c_5 & c_4 & c_3 & -c_6 \\ c_4 & c_3 & c_2 & -c_5 \\ c_3 & c_2 & c_1 & -c_4 \\ c_2 & c_1 & c_0 & -c_3 \end{vmatrix} \quad (12)$$

At the integration point $x = x_{n+1}$, (3) becomes

$$U(x_{n+1}) = \sum_{r=0}^{\infty} c_r x_{n+1}^r \quad (13)$$

we will have on simple Taylor's Series expansion and simplifying

$$c_r = \frac{h^r y_n^{(r)}}{r! x_{n+1}^r}, \quad r = 0, 1, 2, \dots \quad (14)$$

On account of (14), (8) – (12) can be simplified and thus from (7) we obtain our weights as:

$$q_1 x_{n+1} = \frac{h \left[\begin{aligned} &20y_n^2 y_n^{(3)} y_n^{(6)} - 120y_n y_n^{(1)} y_n^{(2)} y_n^{(6)} + 120y_n^{(1)^3} y_n^{(6)} - 30y_n^2 y_n^{(4)} y_n^{(5)} + 150y_n y_n^{(1)} y_n^{(4)^2} \\ &- 1200y_n^{(1)^2} y_n^{(3)} y_n^{(4)} + 120y_n y_n^{(1)} y_n^{(3)} y_n^{(5)} - 400y_n y_n^{(3)^3} + 2400y_n^{(1)} y_n^{(2)} y_n^{(3)^2} + \\ &180y_n y_n^{(2)^2} y_n^{(5)} - 360y_n y_n^{(2)^2} y_n^{(5)} + 900y_n^{(1)} y_n^{(2)^2} y_n^{(4)} - 1800y_n^{(2)^3} y_n^{(3)} \end{aligned} \right]}{5 \left[\begin{aligned} &-24y_n^2 y_n^{(3)} y_n^{(5)} + 144y_n y_n^{(1)} y_n^{(2)} y_n^{(5)} - 144y_n^{(1)^3} y_n^{(5)} + 30y_n^2 y_n^{(4)^2} - 360y_n y_n^{(2)^2} y_n^{(4)} \\ &-240y_n y_n^{(1)} y_n^{(3)} y_n^{(4)} + 720y_n^{(1)^2} y_n^{(2)} y_n^{(4)} + 480y_n y_n^{(2)} y_n^{(3)^2} + 480y_n^{(1)^2} y_n^{(3)^2} \\ &-2160y_n^{(1)} y_n^{(2)^2} y_n^{(3)} + 1080y_n^{(2)^4} \end{aligned} \right]} \quad (15)$$

$$q_2 x_{n+1}^2 = \frac{h^2 \left[\begin{aligned} &6y_n^2 y_n^{(5)^2} - 180y_n y_n^{(2)} y_n^{(3)} y_n^{(5)} - 30y_n y_n^{(1)} y_n^{(4)} y_n^{(5)} + 120y_n^{(1)^2} y_n^{(3)} y_n^{(5)} - 5y_n^2 y_n^{(4)} y_n^{(6)} \\ &+ 30y_n y_n^{(2)^2} y_n^{(6)} + 20y_n y_n^{(1)} y_n^{(3)} y_n^{(6)} - 60y_n^{(1)^2} y_n^{(2)} y_n^{(6)} + 100y_n y_n^{(3)^2} y_n^{(4)} - 400y_n^{(1)} y_n^{(3)^3} \\ &+ 75y_n y_n^{(2)} y_n^{(4)^2} + 180y_n^{(1)} y_n^{(2)^2} y_n^{(5)} + 600y_n^{(2)^2} y_n^{(3)^2} - 450y_n^{(2)^3} y_n^{(4)} \end{aligned} \right]}{5 \left[\begin{aligned} &-24y_n^2 y_n^{(3)} y_n^{(5)} + 144y_n y_n^{(1)} y_n^{(2)} y_n^{(5)} - 144y_n^{(1)^3} y_n^{(5)} + 30y_n^2 y_n^{(4)^2} - 360y_n y_n^{(2)^2} y_n^{(4)} \\ &-240y_n y_n^{(1)} y_n^{(3)} y_n^{(4)} + 720y_n^{(1)^2} y_n^{(2)} y_n^{(4)} + 480y_n y_n^{(2)} y_n^{(3)^2} + 480y_n^{(1)^2} y_n^{(3)^2} \\ &-2160y_n^{(1)} y_n^{(2)^2} y_n^{(3)} + 1080y_n^{(2)^4} \end{aligned} \right]} \quad (16)$$

$$q_3 x_{n+1}^3 = \frac{h^3 \left[\begin{aligned} &20y_n y_n^{(3)^2} y_n^{(5)} - 6y_n y_n^{(1)} y_n^{(5)^2} + 30y_n^{(1)^2} y_n^{(4)} y_n^{(5)} - 25y_n y_n^{(3)} y_n^{(4)^2} + 15y_n y_n^{(2)} y_n^{(4)} y_n^{(5)} \\ &+ 100y_n^{(1)} y_n^{(3)^2} y_n^{(4)} - 150y_n^{(1)} y_n^{(2)} y_n^{(4)^2} + 5y_n y_n^{(1)} y_n^{(4)} y_n^{(6)} - 10y_n y_n^{(2)} y_n^{(3)} y_n^{(6)} \\ &- 20y_n^{(1)^2} y_n^{(3)} y_n^{(6)} + 30y_n^{(1)} y_n^{(2)^2} y_n^{(6)} + 300y_n^{(2)^2} y_n^{(3)} y_n^{(4)} - 200y_n^{(2)} y_n^{(3)^3} - 90y_n^{(2)^3} y_n^{(5)} \end{aligned} \right]}{5 \left[\begin{aligned} &-24y_n^2 y_n^{(3)} y_n^{(5)} + 144y_n y_n^{(1)} y_n^{(2)} y_n^{(5)} - 144y_n^{(1)^3} y_n^{(5)} + 30y_n^2 y_n^{(4)^2} - 360y_n y_n^{(2)^2} y_n^{(4)} \\ &-240y_n y_n^{(1)} y_n^{(3)} y_n^{(4)} + 720y_n^{(1)^2} y_n^{(2)} y_n^{(4)} + 480y_n y_n^{(2)} y_n^{(3)^2} + 480y_n^{(1)^2} y_n^{(3)^2} \\ &-2160y_n^{(1)} y_n^{(2)^2} y_n^{(3)} + 1080y_n^{(2)^4} \end{aligned} \right]} \quad (17)$$

$$q_4 x_{n+1}^4 = \frac{h^4 \left[\begin{aligned} &-960y_n^{(1)} y_n^{(3)^2} y_n^{(5)} + 240y_n y_n^{(3)} y_n^{(4)} y_n^{(5)} + 1440y_n^{(2)^2} y_n^{(3)} y_n^{(5)} - 720y_n^{(1)} y_n^{(2)} y_n^{(4)} y_n^{(5)} \\ &- 72y_n y_n^{(2)} y_n^{(5)^2} + 144y_n^{(1)^2} y_n^{(5)^2} - 1200y_n^{(1)} y_n^{(3)} y_n^{(4)^2} - 150y_n y_n^{(4)^3} - 3600y_n^{(2)} y_n^{(3)^2} y_n^{(4)} \\ &+ 900y_n^{(2)^2} y_n^{(4)^2} + 1600y_n^{(3)^4} + 60y_n y_n^{(2)} y_n^{(4)} y_n^{(6)} - 120y_n^{(1)^2} y_n^{(4)} y_n^{(6)} - 80y_n^{(3)^2} y_n^{(6)} \\ &+ 480y_n^{(1)} y_n^{(2)} y_n^{(3)} y_n^{(6)} - 360y_n^{(2)^3} y_n^{(6)} \end{aligned} \right]}{120 \left[\begin{aligned} &-24y_n^2 y_n^{(3)} y_n^{(5)} + 144y_n y_n^{(1)} y_n^{(2)} y_n^{(5)} - 144y_n^{(1)^3} y_n^{(5)} + 30y_n^2 y_n^{(4)^2} - 360y_n y_n^{(2)^2} y_n^{(4)} \\ &-240y_n y_n^{(1)} y_n^{(3)} y_n^{(4)} + 720y_n^{(1)^2} y_n^{(2)} y_n^{(4)} + 480y_n y_n^{(2)} y_n^{(3)^2} + 480y_n^{(1)^2} y_n^{(3)^2} \\ &-2160y_n^{(1)} y_n^{(2)^2} y_n^{(3)} + 1080y_n^{(2)^4} \end{aligned} \right]} \quad (18)$$

From (2), the rational integrator is expanded to give

$$y_{n+1} = \frac{p_0 + p_1 x_{n+1} + p_2 x_{n+1}^2}{1 + q_1 x_{n+1} + q_2 x_{n+1}^2 + q_3 x_{n+1}^3 + q_4 x_{n+1}^4} \quad (19)$$

From (5) and (19), we have

$$p_0 + p_1 x_{n+1} + p_2 x_{n+1}^2 = y_n + h y_n^{(1)} + \frac{h^2 y_n^{(2)}}{2} + y_n q_1 x_{n+1} + h y_n^{(1)} q_1 x_{n+1} + y_n q_2 x_{n+1}^2 \quad (20)$$

Now, let

$$\{q_1 x_{n+1} = A, q_2 x_{n+1}^2 = B, q_3 x_{n+1}^3 = C \text{ and } q_4 x_{n+1}^4 = D\} \quad (21)$$

On substituting into (19), we obtain (22) which is our quartic based denominator of order six

$$y_{n+1} = \frac{\sum_{r=0}^2 \frac{h^r y_n^{(r)}}{r!} + A \sum_{r=0}^1 \frac{h^r y_n^{(r)}}{r!} + B y_n}{1 + A + B + C + D} \quad (22)$$

where A, B, C, D are as defined by (21) and stated in (15), (16), (17) and (18) respectively.

CONVERGENCE AND CONSISTENCY

For any numerical method to be use, such method must satisfy some basic properties. One-step methods like our new order six numerical integrator with quartic base denominator are normally described symbolically by

$$y_{n+1} = y_n + h\Phi(x_n, y_n; h) \quad (23)$$

where

$\Phi(x_n, y_n; h)$ is called the increment function, x_n the mesh point and h the mesh size. Fatunla (1988) states that a rational integrator is said to be consistent if the increment function is consistent with the IVP that is if

$$\Phi(x, y, 0) = f(x, y) \quad (24)$$

Lambert (1995) went further to conclude that every one-step method is convergent if and only if the one step method is consistent. With these facts, we state and prove the convergence and consistency of the new rational integrator.

Theorem

The Quartic based denominator of order six rational integrator

$$y_{n+1} = \frac{y_n + h y_n^{(1)} + \frac{h^2 y_n^{(2)}}{2} + A y_n + A h y_n^{(1)} + B y_n}{1 + A + B + C + D}$$

where A, B, C and D are as defined by (21) and stated in (15), (16), (17) and (18) respectively is convergent and consistent.

Proof

Subtracting

$$y_{n+1} - y_n = \frac{y_n + h y_n^{(1)} + \frac{h^2 y_n^{(2)}}{2} + A y_n + A h y_n^{(1)} + B y_n}{1 + A + B + C + D} - y_n$$

$$y_{n+1} - y_n = \frac{h y_n^{(1)} + \frac{h^2 y_n^{(2)}}{2} + A h y_n^{(1)} - C y_n - D y_n}{1 + A + B + C + D}$$

Dividing through by h , we have

$$\frac{y_{n+1} - y_n}{h} = \frac{y_n^{(1)} + h y_n^{(2)}/2 + A y_n^{(1)} - (C y_n + D y_n)/h}{1 + A + B + C + D}$$

From (15) – (18) supplemented by (21), we have

$$\lim_{h \rightarrow 0} A = 0, \lim_{h \rightarrow 0} B = 0, \lim_{h \rightarrow 0} C = 0 \text{ and } \lim_{h \rightarrow 0} D = 0.$$

Hence, we have

$$\lim_{h \rightarrow 0} \left(\frac{y_{n+1} - y_n}{h} \right) = \frac{y_n^{(1)} + 0 + 0 - y_n(0+0)}{1+0+0+0+0} = y_n^{(1)} = f(x_n, y_n)$$

Implying that the Quartic based denominator of order six rational integrator is consistent with the IVP. Hence, the integrator is convergent. But the IVP in equation (1) was chosen arbitrarily, therefore our integrator is convergent (Lambert, 1976).

STABILITY CONSIDERATIONS

Lambert (1976) states that a numerical integrator is said to be Absolutely stable in a region, D , of the complex plane if the absolute value of each of the root of the stability polynomial is less than unity in the region. Hence, by employing the integrator to the test equation $y' = \lambda y$ with $h = \lambda h$, we obtain our stability function as

$$\zeta(\bar{h}) = \frac{360 + 120\bar{h} + 12\bar{h}^2}{360 - 240\bar{h} + 72\bar{h}^2 - 12\bar{h}^3 + \bar{h}^4} \quad (24)$$

To analyze the stability formula, we set

$\bar{h} = u + iv$ (where $i^2 = -1$), for our integrator to be Absolutely stable, we must have $|\zeta(\bar{h})| \leq 1 \Leftrightarrow$

$$360 + 120\bar{h} + 12\bar{h}^2 \leq 360 - 240\bar{h} + 72\bar{h}^2 - 12\bar{h}^3 + \bar{h}^4$$

Now, $A(u, v) + iB(u, v) = 360 + 120(u + iv) + 12(u + iv)^2$

And, $C(u, v) + iD(u, v) = 360 - 240(u + iv) + 72(u + iv)^2 - 12(u + iv)^3 + (u + iv)^4$

On expansion and simplification, we get

$$A(u, v) = 360 + 120u + 12u^2 - 12v^2$$

$$B(u, v) = 120v + 24uv$$

$$C(u, v) = 360 - 240u + 72u^2 - 72v^2 - 12u^3 + 36uv^2 + u^4 - 6u^2v^2 + v^4$$

$$D(u, v) = -240v + 144uv - 36u^2v + 12v^3 + 4u^3v - 4uv^3$$

Hence, the inequality becomes

$$|\xi(\bar{h})| \leq 1 \Leftrightarrow |A(u, v) + iB(u, v)| \leq |C(u, v) + iD(u, v)|$$

$$\Leftrightarrow A(u, v)^2 + B(u, v)^2 - C(u, v)^2 - D(u, v)^2 \leq 0$$

Simplifying further, we have

$$A^2 = 129600 + 86400u + 23040u^2 - 8640v^2 + 2880u^3 + 144u^4 - 2880uv^2 - 288u^2v^2 + 144v^4$$

$$B^2 = 1440v^2 + 5760uv^2 + 576u^2v^2$$

$$C^2 = 129600 - 172800u + 109440u^2 - 51840v^2 - 43200u^3 + 60480uv^2 + 11664u^4 \\ - 31968u^2v^2 + 15904v^4 - 2208u^5 + 9792u^3v^2 - 5664uv^4 + 288u^6 - 1872u^4v^2 + \\ 1008u^2v^4 - 144v^6 - 24u^7 + 216u^5v^2 - 456u^3v^4 + 72uv^6 + u^8 - 12u^6v^2 + 38u^4v^4 - 12u^2v^6 + v^8$$

$$D^2 = 51600v^2 - 69120uv^2 + 38016u^2v^2 - 5760v^4 - 12288u^3v^2 + 5376uv^4 + 2448u^4v^2 \\ - 2016u^2v^4 - 2884u^5v^2 + 384u^3v^4 + 144uv^6 - 96uv^6 + 16u^6v^2 - 32u^4v^4 + 16u^2v^6$$

hence the inequality above holds if and only if

$$A^2 + B^2 - (C^2 + D^2) = A^2 + B^2 - C^2 - D^2 = 259200u - 86400u^2 - 12960v^2 + \\ 46080u^3 + 11560uv^2 - 11520u^4 + 6336u^2v^2 + 2208u^5 + 2496u^3v^2 + 288uv^4 - \\ 288u^6 - 576u^4v^2 - 1008u^2v^4 + 244u^7 + 72u^5v^2 + 72u^3v^4 + 24uv^6 - u^8 - 4u^6v^2 \\ - 6u^4v^4 - 4u^2v^6 - v^8 \leq 0$$

Examining values of $u = -1(1) -5$ and $v = 1(1)5$ we have the stability polynomial equality in the table below:

Table 1: Showing Stability Polynomial less than zero

| U | V | $ \zeta(\bar{h}) $ |
|----|---|--------------------|
| -1 | 1 | - 428676 < 0 |
| -2 | 2 | - 1797288 < 0 |
| -3 | 3 | - 7231488 < 0 |
| -4 | 4 | - 28214928 < 0 |
| -5 | 5 | - 95948976 < 0 |

Hence our stability polynomial

$$259200u - 86400u^2 - 12960v^2 + 46080u^3 + 11560uv^2 - 11520u^4 + 6336u^2v^2 + 2208u^5 \\ + 2496u^3v^2 + 288uv^4 - 288u^6 - 576u^4v^2 - 1008u^2v^4 + 244u^7 + 72u^5v^2 + 72u^3v^4 + 24uv^6 \\ - u^8 - 4u^6v^2 - 6u^4v^4 - 4u^2v^6 - v^8 \leq 0$$

holds for any value of v and $u < 0$, hence, the new integrator is Absolutely Stable.

NUMERICAL EXPERIMENTS

In this section, we shall implement our new integrator in solving a number of problems. A sophisticated MATLAB program was written to implement the new rational integrator. Our focus is to select four classes of problems. In the first problem, our rational integrator was compared with the work of Awari (2017) who used Block Hybrid Extended Trapezoidal Multistep Method of Second Kind. Next, we consider three real life problems, where our method is compared with the exact solution arising from these problems. The results obtained in all these comparisons are very positive and encouraging.

Problem 1 (Theoretical)

$$y'(t) = 0.5(1 - y), y(0) = 0.5, h = 0.1$$

(Awari, 2017). The exact solution is

$$y(t) = 1 - 0.5 \exp(-0.5t)$$

Tables 2 shows that our integrator converges quickly to the analytical solution at each corresponding mesh point. It also compares very well with that given by Block Hybrid Extended Trapezoidal Multistep Method of Second Kind of Awari (2017).

Problem 2 (Real life problem)

A new cereal product is introduced through an advertising campaign to a population of 1 million potential customers. The rate at which the population hears about the product is assumed to be proportional to the number of people who are not yet aware of the product. By the end of 1 year, half of the population has heard of the product. How many will have heard of it by the end of 2 years?

The differential equation for this problem is given by

$$\frac{dy}{dt} = k(1 - y); y = 1 - e^{-0.693t}$$

where y represents the number (in millions) of people at time t who have heard of the product. This means that $(1 - y)$ is the number of people who have not heard, and dy / dt is the rate at which the population hears about the product. The exact solution of this problem can easily be obtained as

$y = 1 - e^{-kt}$, where $k = 0.693$. The result which is shown in the numerical solution in Table 3 agrees excellently with the exact result at $t = 2$ years.

Problem 3 (Real life problem)

A population of 20 wolves has been introduced into a national park. The forest service estimates that the maximum population the park can sustain is 200 wolves. After 3 years, the population is estimated to be 40 wolves. If the population follows a Gompertz growth model, how many wolves will there be 10 years after their introduction?

The differential equation for this problem is given by

$$\frac{dy}{dt} = ky \ln\left(\frac{200}{y}\right)$$

where y is the number of wolves at any time t . The exact solution of this problem can easily be obtained as $y = 200 \exp(-2.3026e^{-kt})$, where $k = 0.1194$. The result which is shown in the numerical solution in Table 4 agrees excellently with the exact result at $t = 10$ years.

Problem 4 (Real life problem)

A tank contains 40 gallons of a solution composed of 90% water and 10% alcohol. A second solution containing half water and half alcohol is added to the tank at the rate of 4 gallons per minute. At the same time, the tank is being drained at the rate of 4 gallons per minute. Assuming that the solution is stirred constantly, how much alcohol will be in the tank after 10 minutes?

The differential equation for this problem is given by

$$\frac{dy}{dt} = 4\left(\frac{y}{40}\right) + 2$$

where y is the number of gallons of alcohol in the tank at any time t . The percent of alcohol in the 40-gallon tank at any time is $y/40$. The exact solution of this problem can easily be obtained as $y = 20 - 16e^{-t/10}$. The result which is shown in the numerical solution in Table 5 agrees excellently with the exact result at $t = 10$ minutes.

Table 2: Shows the Results of Problem 1

| Value of t | Analytical solution | Awari (2017) | New Order 6 Rational Integrator | Error Awari (2017) | Error New Order 6 Rational Integrator |
|-----------------|---------------------|-------------------|---------------------------------|--------------------|---------------------------------------|
| 1.000000000e-01 | 5.243852877e-01 | 0.524385287750215 | 5.243852877e-01 | 5.72e-013 | -1.476596623e-14 |
| 2.000000000e-01 | 5.475812910e-01 | 0.547581290982560 | 5.475812910e-01 | 5.40e-013 | -2.853273173e-14 |
| 3.000000000e-01 | 5.696460118e-01 | 0.569646011787959 | 5.696460118e-01 | 4.88e-013 | -4.141131882e-14 |
| 4.000000000e-01 | 5.906346235e-01 | 0.590634623461945 | 5.906346235e-01 | 9.36e-013 | -5.329070518e-14 |
| 5.000000000e-01 | 6.105996085e-01 | 0.610599608465186 | 6.105996085e-01 | 8.88e-013 | -6.450395773e-14 |
| 6.000000000e-01 | 6.295908897e-01 | 0.629590889659952 | 6.295908897e-01 | 8.11e-013 | -7.482903186e-14 |
| 7.000000000e-01 | 6.476559551e-01 | 0.647655955141798 | 6.476559551e-01 | 1.154e-012 | -8.493206138e-14 |
| 8.000000000e-01 | 6.648399770e-01 | 0.664839976983277 | 6.648399770e-01 | 1.097e-012 | -9.447997940e-14 |
| 9.000000000e-01 | 6.811859242e-01 | 0.681185924190118 | 6.811859242e-01 | 1.004e-012 | -1.035838082e-13 |
| 1.000000000e+00 | 6.967346701e-01 | 0.696734670144944 | 6.967346701e-01 | 1.260e-012 | -1.124655924e-13 |

Table 3 Shows the Result of Problem 2

| Time | Exact Result | Numerical Result | Error |
|-----------------|-----------------|------------------|------------------|
| 1.000000000e+00 | 5.000000000e-01 | 5.000000000e-01 | -7.359569577e-05 |
| 1.500000000e+00 | 6.463685465e-01 | 6.464205987e-01 | -5.205216948e-05 |
| 2.000000000e+00 | 7.499263989e-01 | 7.499632157e-01 | -3.681677708e-05 |
| 2.500000000e+00 | 8.231582475e-01 | 8.231842918e-01 | -2.604426038e-05 |
| 3.000000000e+00 | 8.749447951e-01 | 8.749632425e-01 | -1.844737824e-05 |
| 3.500000000e+00 | 9.115661090e-01 | 9.115791473e-01 | -1.303835090e-05 |
| 4.000000000e+00 | 9.374631940e-01 | 9.374724121e-01 | -9.218109353e-06 |
| 4.500000000e+00 | 9.557765461e-01 | 9.557830638e-01 | -6.517715993e-06 |
| 5.000000000e+00 | 9.687269946e-01 | 9.687316031e-01 | -4.608548268e-06 |
| 5.500000000e+00 | 9.778850184e-01 | 9.778882771e-01 | -3.258674348e-06 |
| 6.000000000e+00 | 9.843611957e-01 | 9.843634999e-01 | -2.304212881e-06 |

Table 4 Shows the Result of Problem 3

| Time | Exact Result | Numerical Result | Error |
|-----------------|-----------------|------------------|-----------------|
| 3.000000000e+00 | 4.000000000e+01 | 4.000000000e+01 | 2.966304582e-03 |
| 4.000000000e+00 | 4.794636912e+01 | 4.794321381e+01 | 3.155312617e-03 |
| 5.000000000e+00 | 5.630745376e+01 | 5.630416517e+01 | 3.288589849e-03 |
| 6.000000000e+00 | 6.494102081e+01 | 6.493765479e+01 | 3.366017169e-03 |
| 7.000000000e+00 | 7.370546125e+01 | 7.370207087e+01 | 3.390375926e-03 |
| 8.000000000e+00 | 8.246930129e+01 | 8.246593470e+01 | 3.366587260e-03 |
| 9.000000000e+00 | 9.111575612e+01 | 9.111245517e+01 | 3.300952942e-03 |
| 1.000000000e+01 | 9.954540651e+01 | 9.954220603e+01 | 3.200476220e-03 |
| 1.100000000e+01 | 1.076772682e+02 | 1.076741959e+02 | 3.072305456e-03 |
| 1.200000000e+01 | 1.154485961e+02 | 1.154456728e+02 | 2.923314865e-03 |
| 1.300000000e+01 | 1.228137756e+02 | 1.228110158e+02 | 2.759816996e-03 |
| 1.400000000e+01 | 1.297426212e+02 | 1.297400338e+02 | 2.587389957e-03 |
| 1.500000000e+01 | 1.362183523e+02 | 1.362159415e+02 | 2.410797139e-03 |
| 1.600000000e+01 | 1.422354565e+02 | 1.422332226e+02 | 2.233976417e-03 |
| 1.700000000e+01 | 1.477975906e+02 | 1.477955306e+02 | 2.060077756e-03 |
| 1.800000000e+01 | 1.529156230e+02 | 1.529137315e+02 | 1.891531449e-03 |

Table 5 Shows the Result of Problem 4

| Time | Exact Result | Numerical Result | Error |
|-----------------|-----------------|------------------|------------------|
| 0.000000000e+00 | 4.000000000e+00 | 4.000000000e+00 | 0.000000000e+00 |
| 1.000000000e+00 | 5.522601311e+00 | 5.522601311e+00 | -4.868638825e-11 |
| 2.000000000e+00 | 6.900307951e+00 | 6.900307951e+00 | -8.895018055e-11 |
| 3.000000000e+00 | 8.146908469e+00 | 8.146908469e+00 | -1.222044688e-10 |
| 4.000000000e+00 | 9.274879263e+00 | 9.274879264e+00 | -1.496633928e-10 |
| 5.000000000e+00 | 1.029550944e+01 | 1.029550944e+01 | -1.723741150e-10 |
| 6.000000000e+00 | 1.121901382e+01 | 1.121901382e+01 | -1.912603409e-10 |
| 7.000000000e+00 | 1.205463514e+01 | 1.205463514e+01 | -2.071409710e-10 |
| 8.000000000e+00 | 1.281073657e+01 | 1.281073657e+01 | -2.207904970e-10 |
| 9.000000000e+00 | 1.349488544e+01 | 1.349488544e+01 | -2.329620941e-10 |
| 1.000000000e+01 | 1.411392894e+01 | 1.411392894e+01 | -2.444622282e-10 |
| 1.100000000e+01 | 1.467406266e+01 | 1.467406266e+01 | -2.562501322e-10 |
| 1.200000000e+01 | 1.518089261e+01 | 1.518089261e+01 | -2.696651791e-10 |
| 1.300000000e+01 | 1.563949131e+01 | 1.563949131e+01 | -2.869118276e-10 |
| 1.400000000e+01 | 1.605444858e+01 | 1.605444858e+01 | -3.125997239e-10 |
| 1.500000000e+01 | 1.642991744e+01 | 1.642991744e+01 | -3.602274035e-10 |

Conclusion And Recommendations

We have derived a Quartic-Based Denominator of Order 6 Rational Integrator for solving stiff, singular and oscillatory initial value problems in ordinary differential equations. Our integrator is consistent, and the convergent rate is very high. The stability analysis carried out shows that the method is A-Stable. This current integrator has been used in this work to investigate some real life problems. For instance, it has been used to investigate the rate at which the human population responds to new products introduced into the market by an advertising firm. It has also been used to estimate the rate of growth of certain species of animals introduced into a national park, whose population is governed by the Gompertz growth model. Finally, we have also used our new integrator to calculate how much quantities of a given liquid will be left in a tank, when the rate of flow of the liquid substance per minute is known. In all of these real life investigations, the results obtained by our new integrator agree well with the analytical results.

References

- Aashikpelokhai, U.S.U. (1997): A class of Non Linear One-Step Rational integrators, Pon, Publishing Limited, Agbor, Delta State, 190pp.
- Aashikpelokhai, U.S.U and Momodu, I.B.A (2008): A quadratic based Integration Scheme for the Solution of Singulo-Stiff differential equation. IJPS, 3(4), 97-103.
- Abhulimen, C.E. and Otunta, F.O. (2007): A Family of Two -Step Exponentially Fitted Multiderivable Methods for the Numerical Integration of Stiff IVPs in ODE. International Journal of Numerical Mathematics, Vol.2, pp1-21.
- Awari, Y. S. (2017): Numerical Strategies for the System of First Order IVPs Using Block Hybrid Extended Trapezoidal Multistep Method of Second Kind for Stiff ODEs. Science Journal of Applied Mathematics and Statistics, Vol.5(5): 181-187
- Elakhe, A. O. and Aashikpelokhai U.S.U (2013): Singulo Oscillatory – Stiff rational integrators. International Journal of Physical Sciences, 8 (34), 1703 – 1715, <http://www.academicjournals.org/IJPS>
- Elakhe, A.O., Aashikpelokhai U. S. U. and Ebhomien P.A. (2011): A Dynamical Singulo-Stiff Rational Integrator. IRCAB Journal of Natural Applied Sciences. Vol.1 pp73-79
- Elakhe A.O., Onianwa C.U. and Elakhe S.O. (2016). A new order five numerical rational Rational Integrator. Aiziza Journal of Science and Technology, Vol.1, pp49-63
- Fatunla, S. O. (1988): Numerical Methods for Initial Value Problems in Ordinary Differential Equations. Academic Press, San Diego.
- Islam, Md. A. (2015). A Comparative Study on Numerical Solutions of Initial Value Problems (IVP) for Ordinary Differential Equations (ODE) with Euler and Runge Kutta Methods, American Journal of Computational Mathematics, Vol.5, 393 404
- Lambert, J.D. and Shaw, B. (1965): On the Numerical Solution of $y' = f(x,y)$ by a Class of Formulae based on Rational y' Approximation. Mathematics of Computation 19: 456-462.
- Lambert, J.D. (1976): ‘‘Convergence and Stability’’, (Ed. Hall G. Watt, J.M) Oxford, 20-44.
- Lambert, J.D. (1995): Numerical Methods for Ordinary Differential Systems. John Wiley and Sons Ltd., England, 293 pages.
- Osborne, M. J. and Turner, M. (2010): Cost Benefit Analyses Versus Referenda. Journal of Political Economy 118, pp156-187.
- Patel, S.B. (2000): Nuclear physics: An introduction. New Delhi: New Age International. pp. 62-72.

**APPLICATION OF ELECTRICAL RESISTIVITY TOMOGRAPHY FOR THE
DELINEATION OF DEFORMATIONAL STRUCTURES: A CASE STUDY OF AAU,
EKPOMA, EDO STATE**

Airewele Ehizokhale, Ozegin Kesyton Oyamenda, Salufu Samuel Obomheile and Iyoha Abraham
Department of Physics, Ambrose Alli University, Ekpoma Edo State, Nigeria

Abstract

In this study, Electrical Resistivity Tomography (ERT) technique was used to investigate and delineate the presence of deformational (geologic) structures within the lithological section of the study area as well as the origin of such structures. Three (3) traverses were investigated within the area with traverse 1 taken in the N-S direction measuring 200 m while traverses 2 and 3 were taken in the W-E direction measuring 150 m each. The geographical coordinates of the study area are within 6° 44'19.1" N to 6° 44' 26.1" N and 6° 5'67.6" E to 6° 5'76" E. The two dimensional (2D) ERT data obtained were processed and inverted to generate subsurface model of the study area. Traverse 1 with resistivity distribution values which ranged from 78 - 10713 Ωm has at the centre two significant geologic structures; folds and faults. Traverses 2 and 3 showed only folds. The two structures were restricted to the north eastern part of the study area. The structures which are localized and non expansive must have been formed by unequal loading of the overlying strata, which led to the build up of stress on the underlying rock units. The occurrence of the deformational structures in the study area are indicative of potential hydrocarbon accumulation and surface water.

Keywords: Bende-Ameki Formation, Faults and Folds, Gravity Effect, Sedimentary, Surface Water

Introduction:

Plate tectonics are associated with large scale deformation of the Earth Crust, whereas a smaller scale deformation is related with structural geology. Three main classes of geologic structure caused by deformation in Earth's crust are recognised by geologist: unconformities, faults and fractures, and folds. Moderately deformed sedimentary sequences are commonplace throughout the world (Fityus *et al.*, 2007). Such sequences underlie significant areas of Esan land in the Edo State, Nigeria. The sequence, which displays an upward transition of interbedded succession, comprises conglomerate, kaolin rich sandstones, clayey sandstone, coarse to grained

sandstone, poorly sorted sandstone and Ironstone (Airewele *et al.*, 2020). The occurrence of deformational structures at diverse degrees has had a considerable effect on weathering and rock strength. A good knowledge of deformational structures in situ is a potential target for civil engineering works, hydrocarbons, minerals and groundwater exploration programs.

Geophysical modeling is an approach to get an insight into Earth's crust architecture based on indirect information by means of its physical properties, contributing to classical structural geology evaluations (Jessell and Valenta, 1996, Jessell and Jessell, 2001). The Electrical Resistivity Tomography (ERT) is cost effective, mostly error free, produces results of high resolution, can clearly delineate and give a reliable cross-sectional picture of the entire subsurface lithostructural features, as well as depth to bedrock in the study area. In geophysics, ERT techniques have been used extensively used for mapping subsurface structures

Corresponding Author: Airewele Ehizokhale
Department of Physics
Ambrose Alli University, Ekpoma Nigeria.

(Khalil, 2009), geotechnical and engineering site investigation (Folorunso *et al.*, 2012; Ozegin *et al.*, 2013), as well as geological discontinuities such as faults, drainage channel systems and other structure features (Lebourg *et al.*, 2005; Ozegin *et al.*, 2019) and surface structure failure (Egwuonwu *et al.*, 2011). Electrical resistivity method applies the principle of electrical current flow in investigating subsurface geological structures of the earth.

In the study area, there is no known history of Tectonic events after the deposition of the Bende–Ameki Formation that would have helped expose the lithological section, hence no outcrop exposure. This became a great challenge in understanding the lithostratigraphic unit and the characteristics of the formation of the area. Hence, Two Dimensional Electrical Resistivity Tomography was employed in studying the lithologic section of the subsurface in the study area, with the intention to delineate any deformational structures of the area. This became necessary after a previous work by Salufu and Ujuanbi (2015) on identifying occurrence of deformational structures in Esan Land. This paper deals with distortions of various primary sedimentary structures and deformed bedding that may have taken place at a time of or shortly after deposition of the sediment. Such deformation varies from mildly disturbed layers to those which are closely crumpled. For smaller scale deformations, structural geology operates at a scale ranging from microns to 100 metres (i.e. grains to outcrops).

Site Description and Geology of the Study Area

The study was done within Ambrose Alli University, Ekpoma, Edo Central Senatorial district of Edo State. The area lies within the tropical region between Latitudes 6° 44'19.1" N to 6° 44' 26.1" N and Longitudes 6° 5'67.6" E to 6° 5'76" E with average surface elevation of 343 m (Figure 1). It is well accessible through several road networks within and around the study area. The study area, falls within the Anambra Basin. The basin was formed as a result Santonian tectonic event that affected the floor of the basin. Furthermore, Anambra Basin derives its sediments from the erosion of the Abakaliki Antichorium which had become the major site of deposition in Late Cretaceous – Eocene time. The study area is majorly underlain by Bende–Ameki Formation

which consists of sandstone, clay and shale.

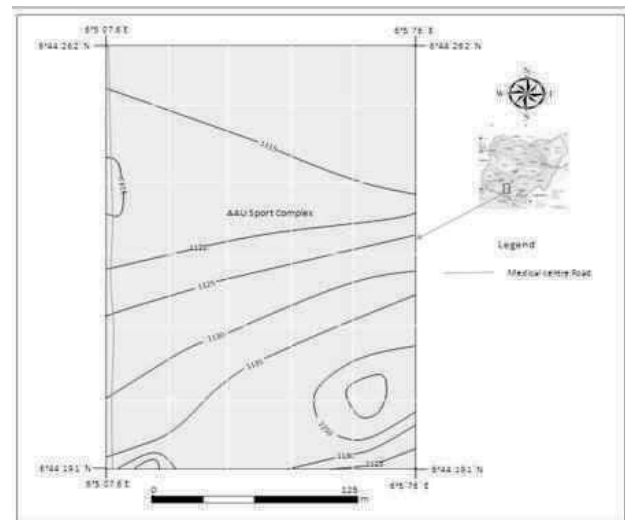


Figure 1: Location Map of the study area

MATERIALS AND METHOD

In Electrical Resistivity measurement, an electric current is injected into the ground through two current electrodes and the voltage difference is measured between two potential electrodes with the intention of mapping the subsurface structure. Electrical Resistivity imaging technique is based on Ohm's law, George Simon Ohm derived empirical relationship between the resistance (R) of a resistor in a simple series circuit, the current passing through the resistor (I) and the corresponding change is potential (ΔV)

$$\Delta V = IR \quad (1)$$

For a given material, resistance is proportional to length (L) and inversely proportional to the cross-sectional area (A) of the conductor. These relationships are expressed in the following equation

$$R = \frac{\rho L}{A} \quad (2)$$

A factor that defines the ease with which electrical circuit flows through the media is known as resistivity (ρ). It is the measurement of how strongly a material resists the flow of electric current (Denchik and Chapellier, 2005).

where inhomogeneity exists in the ground, resistivity is a function of measurement location (Keary *et al.*, 2002). The obtained values of resistivity represent apparent resistivity instead of true resistivity (Lowrie, 2007). In an inhomogeneous area, therefore, the resistivity (ρ) in Equation (2) changes to apparent resistivity (ρ_a)

Considering a continuous current injected into the ground through the current electrodes (C_1 and C_2) as shown in Figure (2), the potential (ΔV) at the centre will be the algebraic sum of the potentials due to current source electrode at point A and the current sink electrode at point B.

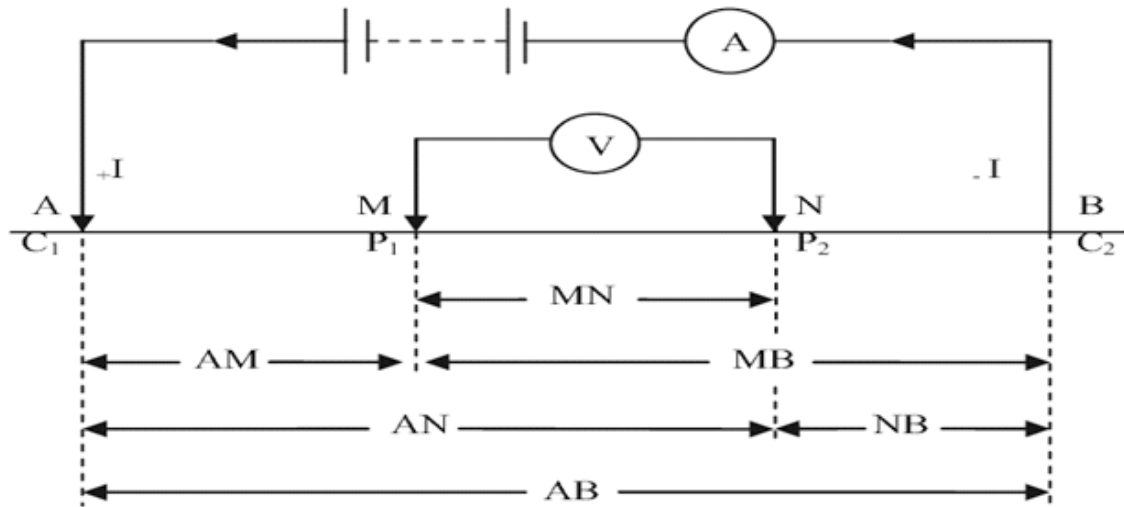


Figure 2: General four electrode configuration for resistivity measurement (Keary and Brooks, 1991)
The potential difference measured at M is given as

$$V_M = \frac{\rho l}{2\pi} \left(\frac{1}{AM} - \frac{1}{MB} \right) \quad (3) \quad \rho_a = \frac{k\Delta V}{I} \quad (7)$$

Similarly, the resultant potential at N is

$$V_N = \frac{\rho l}{2\pi} \left(\frac{1}{AN} - \frac{1}{NB} \right) \quad (4)$$

The potential difference measured by the voltmeter connected between M & N is given as

$$\Delta V = \frac{\rho l}{2\pi} \left[\left(\frac{1}{AM} - \frac{1}{MB} \right) - \left(\frac{1}{AN} - \frac{1}{NB} \right) \right] \quad (5)$$

Therefore,

$$\rho = 2\pi \frac{\Delta V}{I} \frac{1}{\left(\frac{1}{AM} - \frac{1}{MB} \right) - \left(\frac{1}{AN} - \frac{1}{NB} \right)} \quad (6)$$

Where $\frac{\Delta V}{I}$ is the resistance of the ground measured in Ohms. Equation (6) is the basic equation for calculating apparent resistivity (Keary and Brooks, 1991).

Where

$$k = 2\pi \frac{1}{\left(\frac{1}{AM} - \frac{1}{MB} \right) - \left(\frac{1}{AN} - \frac{1}{NB} \right)} \quad (8)$$

The apparent resistivity ρ_a is therefore expressed as equation (7) measured in Ohm-m (Ωm) and k is called the geometric factor of the electrode arrangement.

In data acquisition, the choice of electrode configuration or array has a substantial influence on the resolution, sensitivity and depth of investigation. Some of the common arrays used in investigating subsurface structures are Wenner, Schlumberger, Dipole-Dipole, Pole-Pole and Pole-Dipole. In areas, where there is uncertainty whether both reasonably good horizontal and vertical resolution are required, the Wenner-Schlumberger

array with overlapping data level is the best option and was utilized for this study.

The Pasi Earth Resistivity meter (16 –GL), readily easy to use and characterized by first rate performance, was used for the data collection. The system requires that electric current is injected into the subsurface through a pair of current electrodes and the resulting potential difference measured through a pair of potential electrodes. In addition, two sets of 100m cable reels, P-100N Accumulator – power source, and a set of 21 stainless steel electrodes of 10m spacing were used along with the Pasi Earth Resistivity meter. More so, coordinates and elevations of respective electrode points were taken for the purpose of surface modelling.

During the data acquisition process, the wiring is changed continuously so that the spacing “a”

between the potential electrode remain constant, while that between the “current electrode” increases as a multiple of “n of a” The 2-D resistivity images were generated from the resistivity data acquired from three traverses (T1, T2 and T3) as shown in figure 3, by employing the RES2DINV software. The RES2DINV is a computer program that automatically determines the 2D model of the data obtained. In the interpretation of the 2D resistivity model section, important consideration is given to the electrical resistivity values and not the colour representation because the same colour on each of the profiles represents different resistivity range of values. Variation in the layers is represented by the varying resistivity of formations which is associated with the various colour in the model-sections.

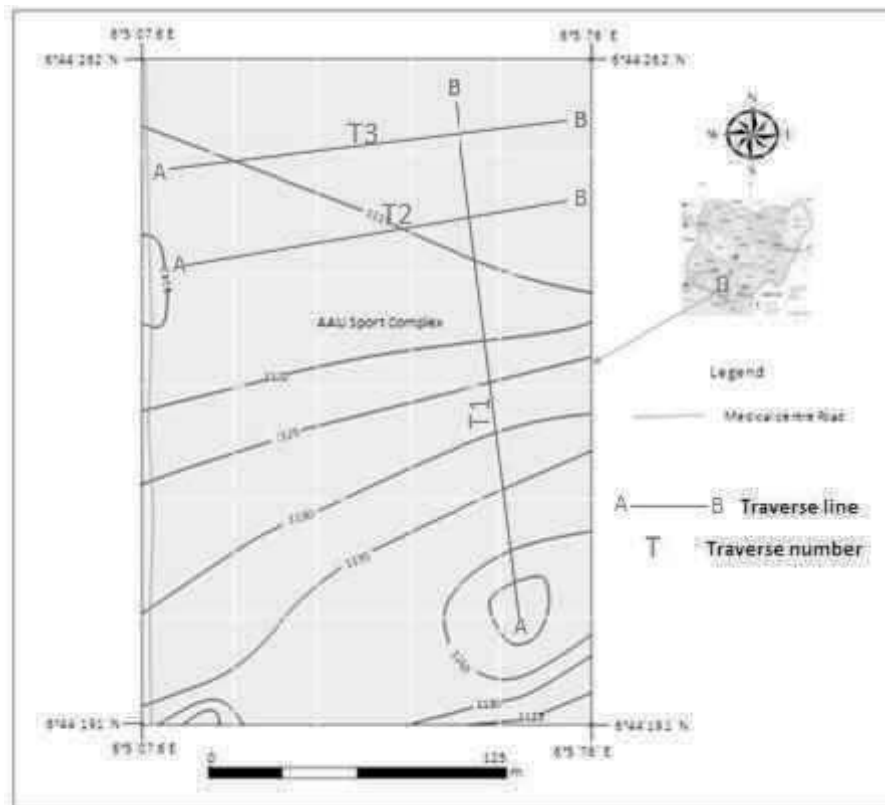


Figure 3: Traverse map of the study area showing the trend of the traverses and location of data acquisition

RESULTS AND DISCUSSION

The inverse resistivity modeled section of the study area showed in figure 4 is characterised by a fold-like structure at the centre and a break in strata on the northern part of the section. The resistivity distribution values for the fold-like structure ranged from 2300 to 11,000.00 Ωm with probed depth of 17.00 m. Towards the extreme southern and northern parts of the section is characterised by sedimentary structures and deformed bedded sequence respectively. The sedimentary structures

include flute casts, extra formational cast of kaolin. The deformed bedded sequence extends from the surface to a depth of 23.00 m. The inverse resistivity model sections of Traverses 2 and 3 are shown in Figs. 5 and 6. These sections showed similar features to that observed in Traverse 1 in terms fold-like structures characteristics. The top layers is characterised by poorly bedded lateritic sandstones, with resistivity ranging from 400 to 3000.00 Ωm and a depth of 15.00 m for T_2 and that of T_3 , resistivity ranged from 200 to 1200.00 Ωm and at a depth of 11.00 m.

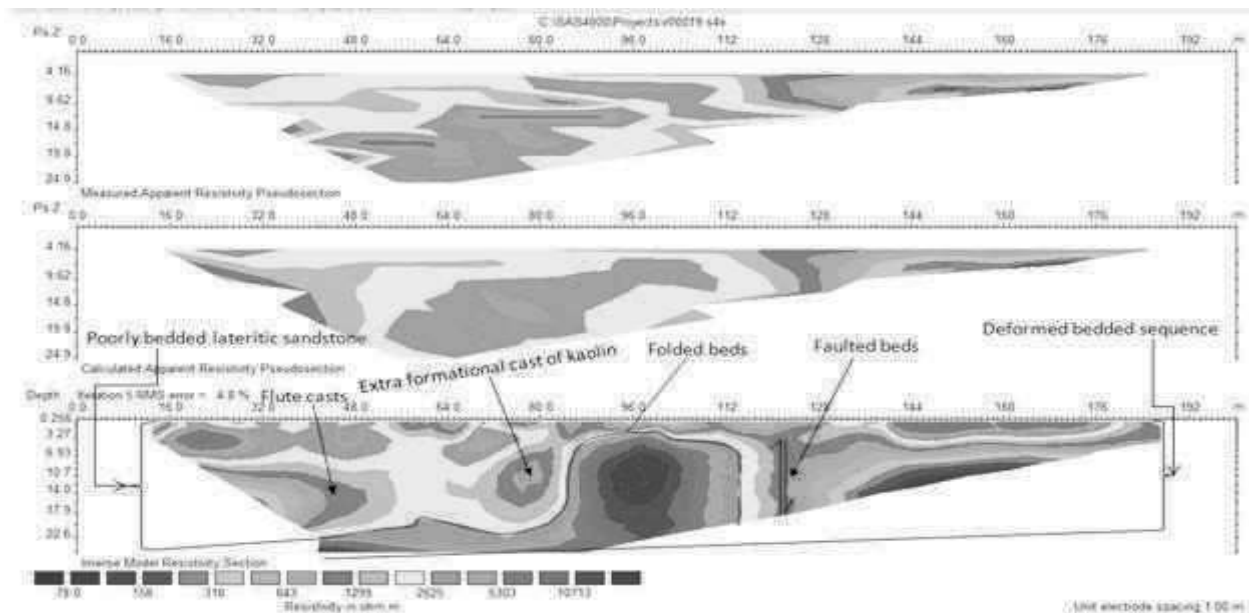


Figure 4: 2D images for Profile 1 with the use of Wenner-Schlumberger array

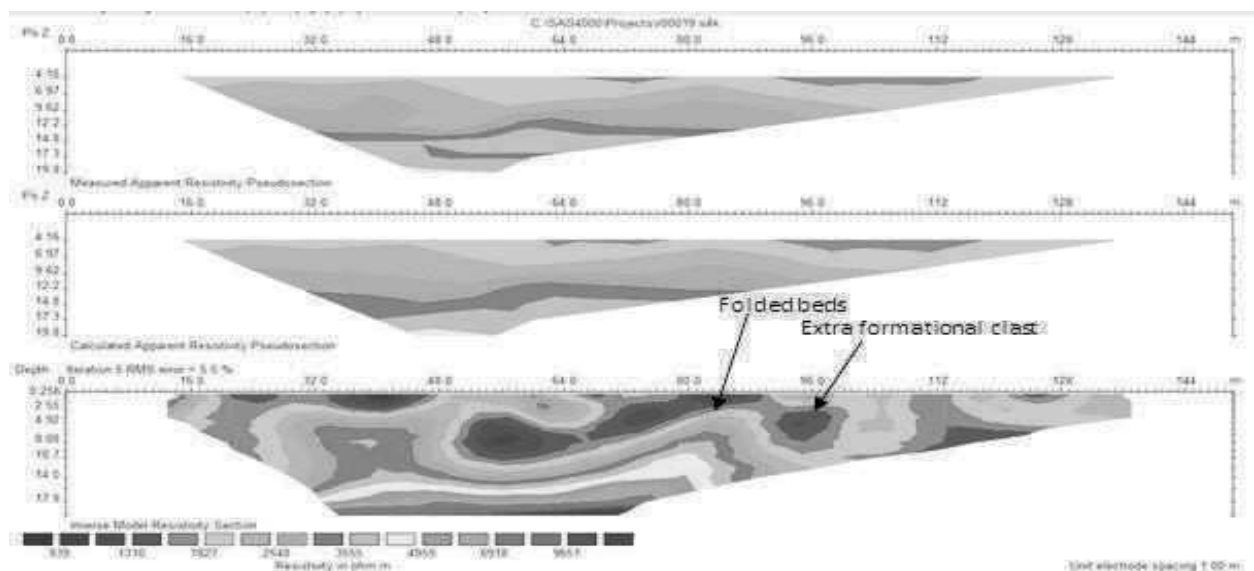


Figure 5: 2D images for Profile 2 with the use of Wenner-Schlumberger array

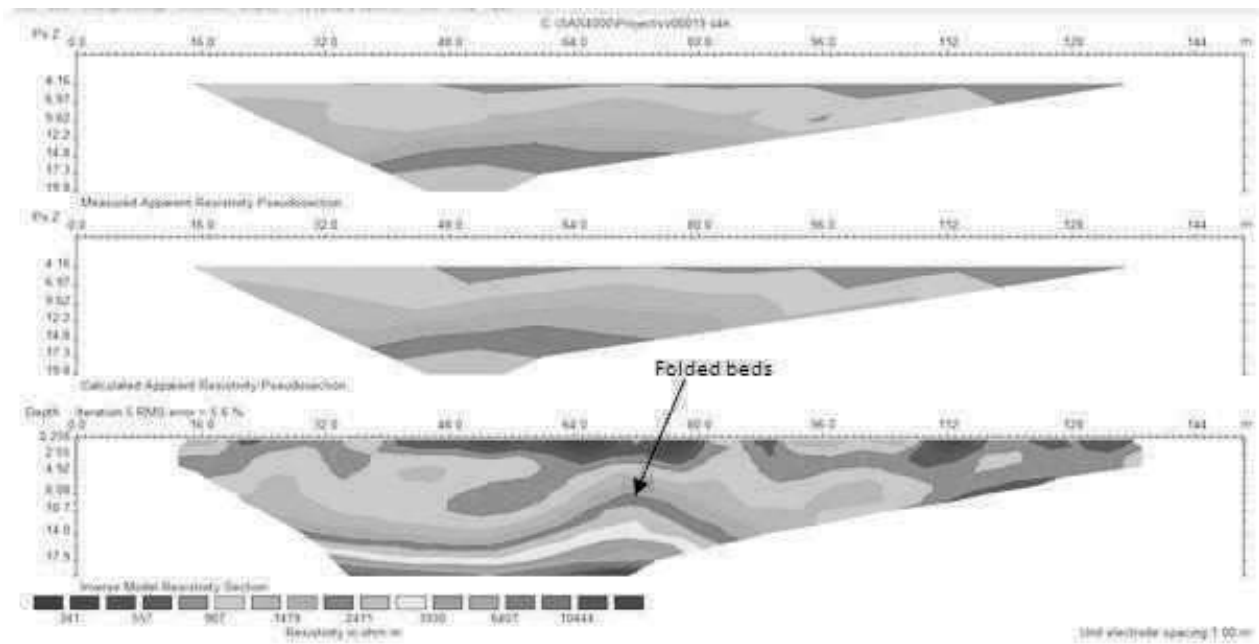


Figure 6: 2D images for Profile 3 with the use of Wenner-Schlumberger array

The two protruding fold-like structures seen in Traverse 2 and Traverse 3 are deformed structures. This is observed between 24.00 and 90.00 m along traverse 2, at a depth of 3 to 17.90 m, with resistivity ranging from 2500.00 – 6000.00 Ωm . While in Traverse 3, resistivity ranged from 1400 – 6000.00 Ωm and structural distance between 50.00 and 85.00 m was also observed. Traverse 1 taken from south to north direction of the study area showed two significant geological structures; folds and faults. However, for Traverses 2 and 3 which runs west to east, only folds were observed. The two geological structures are restricted in the north eastern part of the study area. This observation shows evidence of localized fold and fault which suggests that its occurrence is not from plate tectonism but rather unequal overloading of the underlying bed accompanied with gravity effect – **Non-tectonic structures originate** near the earth's surface, most likely due to **gravitational forces**. As the folding took place, it stretching the beds beyond elastic limit leading to a break in strata consequently the fault evolves. The other part of the structural map reveals sedimentary structures.

3.1 Deformational Structures

The Post-traverse structural map of the study area in some sections along Traverses 1, 2, 3 depicts

imprint of fold and faults. T_1 shows folded unit and faulted unit in the North Eastern part of the study area as presented in figure 7. The fold is seen plunging North west and showing two dips towards the Northern and Southern of 35° . Towards the end of the North East, the deformed unit on exceeded elastic limit resulted into a fault.

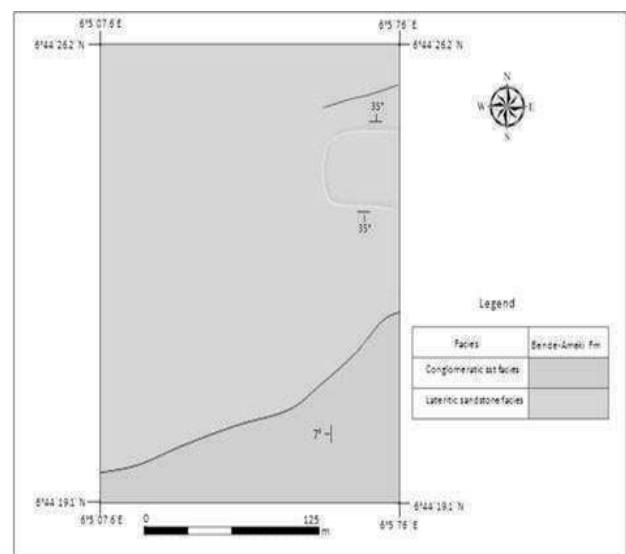


Figure 7: Post-traverse structural Map of the Study Area

4. CONCLUSION

The application of Electrical Resistivity Tomography (ERT) has successfully helped in mapping the deformational structures within the lithological section of the study area. Hence the study has showed the effectiveness of apparent resistivity contrast using Wenner-Schlumberger array as a viable tool for deformational structural mapping. The deformational structures (folds and faults) are not from plate tectonism but due to unequal loading of the underlying strata. The folded beds during the folding process stretches beyond elastic limit resulting in a deformational structure fault. These structures could serve as potential for hydrocarbon accumulation as well as surface water in the area. However, a further study is recommended using other geophysical methods—seismic method to compare the results/ findings from this work. Also a larger spread of electrodes using same 2-D resistivity imaging will probe deeper and provide detailed information of subsurface structures.

REFERENCES

- Airewele, E., Alile, O. M., Ozegin, K.O. and Ataman O.J. (2020). Lithostratigraphic Classification of Subsurface in a Typical Sedimentary Terrain, Southern Nigeria; A Case Study of Ujemen – Ekpoma. *Nigerian journal of Science and Environment*, Vol. 18(1), Pp. 225–236.
- Denchik, N., & Chapellier, D. (2005). 3D electrical resistivity monitoring during rainfalls. Paper presented at the 3rd Swiss Geoscience Meeting.
- Egwuonwu, G. N., S. O. Ibe, and I. B. Osazuwa. (2011). Geophysical Assessment of foundation Depths around a Leaning Superstructure in Zaria Area, Northwestern Nigeria using Electrical Resistivity Tomography. *Pacific Journal of Science and Technology*. Vol. 12(1), Pp. 472–486. <http://www.akamaiuniversity.us/PJST.htm>
- Fityus, S., Török, Á. and Gibson, J. (2007.) The influence of geologic structure on design and construction in a moderately deformed paleozoic sequence in Eastern Australia. *Central European Geology, Vol. 50/4*, Pp. 363 – 380 . DOI : 10.1556/CEuGeol.50.2007.4.6
- Folorunso, A. F., Ayolabi, E. A; Ariyo, S. O., Oyebanjo, I. O. (2012). Fault Presence under a failing Building Complex mapped by electrical resistivity tomography. *Mineral Wealth*. Pp. 47–55.
- Jessell, M W. and Jessell M. (2001). Three-dimensional geological modelling of potential field data. *Computers & Geosciences*, Vol. 27, Pp. 455–465.
- Jessell, M.W. and Valenta, R.K. (1996). Structural geophysics: Integrated structural and geophysical modelling. *Computer Methods in the Geosciences*, Vol. 15, Pp. 303–324. doi: 10.1016/S1874-561X(96)80027-7
- Kearey, P. and Brooks, M. (1991). *An Introduction to Geophysical Exploration*. London: Blackwell Scientific Publication.
- Kearey, P., Brooks, M., and Hill, I., (2002). *An introduction to geophysical exploration (Third Edition)*. Blackwell Publishing, Malden, U.S.A. Pp. 66–67
- Khalil, M. H. (2009) Hydro geophysical assessment of wadi el-sheikh aquifer, Saint Katherine, south Sinai, Egypt. *Journal of Environmental and Engineering Geophysics, JEEG*, Vol. 14(2), Pp. 77–86.
- Lebourg. T., Binet, S., Tric, E., Jomard, H. and El Bedoui, S., (2005). Geophysical survey to estimate the 3D sliding surface and the 4D evolution of the water pressure on part of a deep seated landslide. *Terra Nova*. Vol. 17(5), Pp. 399–406

Lowrie, W. (2007). *Fundamentals of Geophysics*.
Second Edition ed. Zürich: Cambridge
University Press.

Ozegin, K.O., Oseghale, A.O., Audu, A.L,
Ofotokun, E.J. (2013). An Application of
the 2–D D.C. Resistivity Method in
Building Site Investigation – a case study:
Southsouth Nigeria. *Journal of
Environment and Earth Science*, Vol. 3(2),
Pp. 108–112.

Ozegin, K. O., Bawallah, M. A., Ilugbo, S. O.,
Oyedele, A. A. and Oladeji, J. F. (2019).
Effect of Geodynamic Activities on an
Existing Dam: A Case Study of Ojirami
Dam, Southern Nigeria. *Journal of
Geoscience and Environment Protection*,
V o l . 7 , P p . 2 0 0 –
213. <https://www.scirp.org/journal/gep>

Salufu, S. O., and Ujuanbi, O. (2015). Occurrence of
Deformational Structures in the Paleocene–
eocene Sediments in Esan land, Edo State
Nigeria. *Nigerian Annals of Natural
Sciences*, Vol. 15 (1), Pp. 085–093.

GEOPHYSICAL EVALUATION OF AQUIFEROUS ZONE AND ITS PROTECTIVE CAPACITY RATING USING ELECTRICAL RESISTIVITY METHOD WITHIN THE UGBOWO CAMPUS OF UNIVERSITY OF BENIN, BENIN CITY, EDO STATE, NIGERIA.

Can-voro O. Amadasun

Department of Physics,
Ambrose Alli University, Ekpoma. Edo State.

Salami A. Sikiru

Department of Geology,
University of Benin, Benin City, Edo State.

Babafemi E. Muyiwa

Geobabs Integrated Services, Lagos State, Nigeria.

&

Jegede I. Samson

Department of Physics,
Ambrose Alli University, Ekpoma. Edo State.

Abstract

A geophysical work using the Schlumberger array of Electrical resistivity was conducted around the Postgraduates' hostels and the Vice Chancellor's lodge within the Ugbowo campus of the University of Benin, Edo State, Nigeria, with a view to ascertaining the aquiferous zone and the aquifer protective capacity rating (PCR) using the Dar-Zarrouk (D-Z) parameters. Six Vertical Electrical Sounding (VES) points of maximum current spread (AB) of 430m were carried out, and the quantitative interpretation of the VES involved partial-curve matching and computer iteration using the Interpex 1-D sounding inversion software. The results showed five to eight interpreted geo-electric layers but modeled to form six lithologic layers, namely: the topsoil, lateritic sand, clayey sand, dry sand, aquiferous sand and silty/clayey sand. The layer beneath the dry sand constitutes the aquiferous zone in the sounded area and of range 39.55m to 98.26m. The curve types of VES one to six are: KQHKA, KQHAK, KHK, KHAQK, KHAKQH and KQHAK of corresponding aquifer PCR of moderate (VES 1), weak (VES 2) and poor (VES 3 to VES 6). We recommend the location of VES 1 of moderate PCR to be suitable for siting of borehole when compared to the other VES points, numbering 2, 3, 4, 5 and 6, despite the fact that the entire area sounded is viable for borehole water extraction.

Keywords: PCR, Dar-Zarrouk, Aquiferous, Lithologic, Isotropic.

Introduction:

The essence of water to life cannot be over emphasized; neither will it cease to be discussed whether in the political or scientific arena (Miller, 2006). The prosperity of many communities is dependent on the development of new supplies of potable water as demand steadily increases and known supplies of water dwindle. Increased

human population densities and advances in technology over the recent past years, resulted in an exponential increase in the potential number and diversity of viable geophysical applications in the field of groundwater exploration and exploitation (Ayuk *et al.*, 2013). As groundwater becomes more important as a source of uncontaminated water, improved hydrogeological knowledge, new groundwater exploration techniques and data processing methods must be efficient to facilitate investigations and evaluation of groundwater resources (Utom *et al.*, 2012). Under a variety of

Corresponding Author: Can-voro O. Amadasun
Department of Physics,
Ambrose Alli University, Ekpoma. Edo State.
cvoamadasun@aauekpoma.edu.ng

field conditions and geological settings in hydrogeology, environmental geology and geotechnical engineering, surface resistivity techniques are a useful tool routinely used (Beresnev *et al.*, 2002; Vchery and Hobbs, 2003). Ademilua and Ogungbemi (2013) used a non-invasive and less-expensive geoelectric investigation involving VES to estimate the Longitudinal unit conductance (S), Transverse unit resistance (T) and coefficient of Anisotropy (λ) as parameters of aquifer protective capacity. The study and analysis of D-Z parameters deduced from surface VES investigation is also useful in differentiating between saline and fresh water aquifers (Al-Yasi *et al.*, 2013). The main thrust of this research paper is the use of surface resistivity sounding in extrapolating the aquiferous zones, geoelectric and D-Z parameters in evaluating the groundwater potential and aquifer risk to surface filtrations despite the fact that the availability of near surface groundwater within the study area is not much of a concern. Simply put, the ease at which groundwater is exploited in the study area is commendable. As the Earth materials act as a natural sieve to percolating fluids, its protective capacity is the measure of its ability to retard and filter these fluids from the surface from polluting the underground water (Olorunfemi *et. al*, 1999). The first order geoelectric parameters of layer resistivities and thicknesses are used to obtain the Dar-Zarrouk (D-Z) parameters, otherwise called

the secondary geoelectric parameters, which are: the Total Longitudinal Conductance (S), the Transverse unit resistance (T) and the Coefficient of Anisotropy (λ), used to describe a geoelectric section consisting of several (n) layers from surface to bottom (Zohdy *et.al*, 1974; Ademilua and Ogungbemi, 2013). The above D-Z parameters are given by:

$$S = \sum_{i=1}^n \frac{h_i}{\rho_i} \quad 1$$

$$T = \sum_{i=1}^n h_i \rho_i \quad 2$$

$$\lambda = \left(\frac{\rho_T}{\rho_L} \right)^{\frac{1}{2}} \quad 3$$

where

$$H = \sum_{i=1}^n h_i \quad 4$$

$$\rho_T = \frac{T}{H} \quad 5$$

$$\rho_L = \frac{H}{S} \quad 6$$

Such that ρ_L is the longitudinal resistivity, ρ_T is the transverse resistivity, h_i is unit thickness, ρ_i is unit resistivity and H is the total thicknesses. Below is the capacity rating as modified (See Table 1)

Table 1: Modified longitudinal conductance/protective capacity rating.

| LONGITUDINAL CONDUCTANCE (MHOS) | PROTECTIVE CAPACITY RATING (PCR) |
|---------------------------------|----------------------------------|
| < 10 | Excellent |
| 5-10 | Very Good |
| 0.7-4.9 | Good |
| 0.2-0.69 | Moderate |
| 0.1-0.19 | Weak |
| < 0.1 | Poor |

Source: Ademilua and Ogungbemi (2013)

LOCATION OF THE STUDY AREA

The study area (see Figures 1 and 2) was around the Postgraduates' hostels and the Vice Chancellor's lodge within the Ugbowo campus of the University of Benin (UNIBEN), Edo State, Nigeria, of coordinates: $6^{\circ} 20.022$ N and $5^{\circ} 36.009$ E (UNIBEN website, 2019). Edo State

lies within Latitudes $5^{\circ} 44$ N and $7^{\circ} 37$ N and Longitudes $5^{\circ} 34$ E and $6^{\circ} 44$ E sharing common boundaries with Delta State in the east, Anambra State in the north-east, Kogi State in the north and Atlantic ocean in the south (Omorogieva and Imasuen, 2018).



Fig. 1: Location map of the study area showing the Traverse locations for the resistivity survey; the purple location icon shows traverse-1, blue shows traverse-2 while red indicates traverse-3 (Adopted from Google map 2019).



Fig. 2: Arial view of parts of UNIBEN showing area of study (Google Earth, 2019)

LOCAL AND REGIONAL GEOLOGY OF BENIN CITY

Geologically, Benin Formation underlies the study area (Figures 3 and 4) which extends from the West across the whole of the Niger Delta area and southward beyond the present coastline (Reyment, 1965; Kogbe and Assez, 1979). Sediments within the study area is of Miocene to recent and relatively porous and highly

permeable. It is coarse grained, gravelly, locally fine grained, poorly sorted, sub-angular to well-rounded and bears lignite interbeds and wood fragments. Offodile (2002) described the Benin Formation as the most aquiferous formation in Southern Nigeria (Idehai and Egai, 2014). Akujieze and Oteze (2007) summarily put the depth to water level in Benin on an average of 60m.

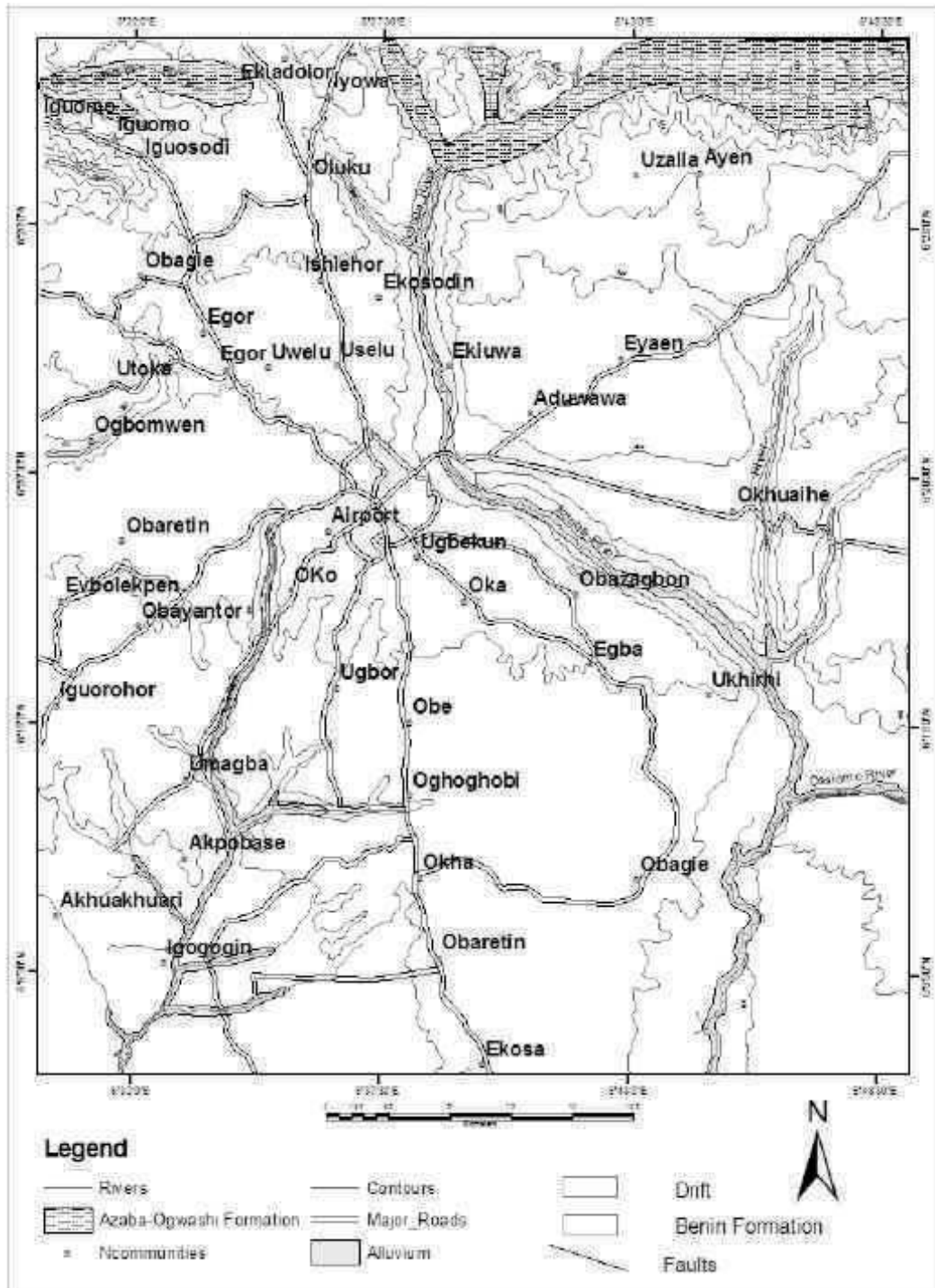


Fig. 3: Geological Map of Some Parts Edo State Showing Various Formations (Akujieze, 2004)

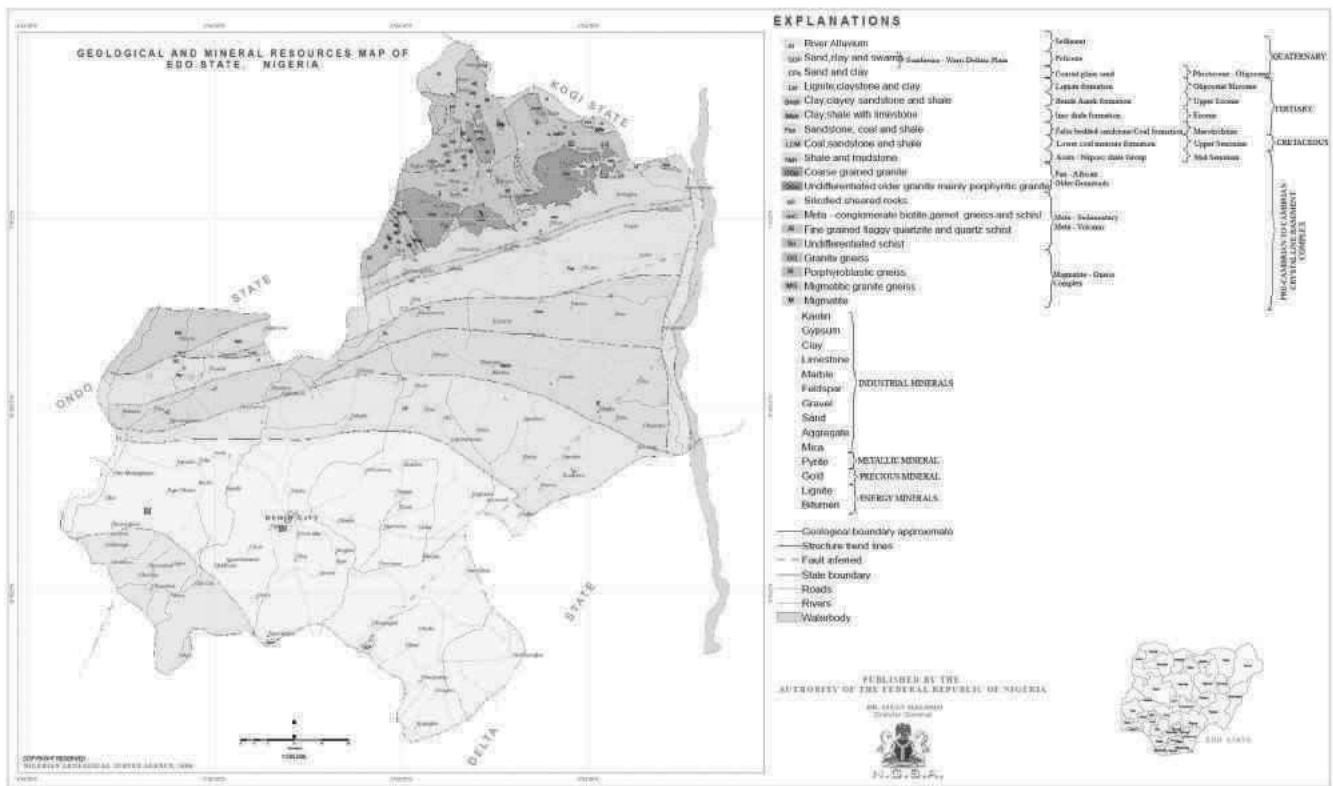


Fig. 4: Geological Map of Edo State Showing Benin City and other Locations (Nigerian Geological Survey Agency, 2006)

RESEARCH METHODOLOGY AND THEORY

The equipment used for the resistivity survey was the ABEM SAS 1000 Terrameter and its accessories. Electrical resistivity using the Schlumberger array was adopted for the study. Three transverses of two VES points each was carried out with a maximum current spread (AB) of 430m. The traditional Earth’s surface four-electrode probing was done and the mathematical inclination is thus cited as follows:

$$V = \frac{I}{r} \tag{7}$$

where ρ is the Earth’s resistivity, V is the Earth’s potential and r the hemispherical surface radius. The potential at any point due to the current flow is equal to the sum of the contributions from the individual current electrodes. Thus,

$$V = \frac{I\rho}{2\pi} \left(\frac{1}{AM} - \frac{1}{MB} - \frac{1}{AN} + \frac{1}{NB} \right) \tag{8}$$

where AM , MB , AN and NB are the distances between corresponding Current and Potential electrodes. From Equation 8,

$$V = \frac{I\rho}{2\pi} G \tag{9}$$

which implies $\rho = \frac{2\pi V}{I} \cdot \frac{1}{G} = K \frac{V}{I} \tag{10}$

where G represents the expression in brackets in equation (8) and $K = \frac{2\pi}{G}$ denotes the geometric

factor of an electrode configuration. The Schlumberger configuration (See Figure 5) was calculated using Equation 11 (Amadasun *et al.*, 2018).

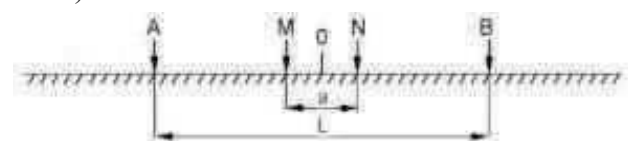


Fig. 5: Schlumberger electrode array.

$$\rho_a = \frac{\pi \Delta V}{I} \left(\frac{(AB/2)^2 - (MN/2)^2}{MN} \right) \quad 11$$

RESULTS

The field results were subjected to quantitative interpretation involving partial-curve matching and computer iteration using the Interpex 1-D sounding inversion software and the summary is as presented in Table 2. Table 3 shows the geo-electric parameters generated for each VES point. Table 4 shows the inferred lithologies of the study area. Figure 7 shows the geo-electric section of the area.

Table 2: The First Geo-electric Parameters for the six VES Points

| | VES 1 | VES 2 | VES 3 | VES 4 | VES 5 | VES 6 |
|------------|------------------|-----------------|------------------|------------------|------------------|-----------------|
| ρ_1 | 294 Ω m | 363 Ω m | 1034 Ω m | 889 Ω m | 506 Ω m | 469 Ω m |
| ρ_2 | 1278 Ω m | 1100 Ω m | 1731 Ω m | 3827 Ω m | 8325 Ω m | 2742 Ω m |
| ρ_3 | 368 Ω m | 421 Ω m | 753 Ω m | 785 Ω m | 682 Ω m | 780 Ω m |
| ρ_4 | 260 Ω m | 230 Ω m | 51675 Ω m | 1374 Ω m | 3713 Ω m | 204 Ω m |
| ρ_5 | 87948 Ω m | 2347 Ω m | 1102 Ω m | 2898 Ω m | 50686 Ω m | 273 Ω m |
| ρ_6 | 2703 Ω m | 5641 Ω m | | 16003 Ω m | 8983 Ω m | 6926 Ω m |
| P_7 | 1135 Ω m | 854 Ω m | | 1948 Ω m | 2753 Ω m | 1485 Ω m |
| P_8 | | | | 536 Ω m | 2771 Ω m | |
| h_1 | 0.84m | 0.41m | 0.69m | 0.72m | 0.35m | 1.54m |
| h_2 | 1.56m | 0.32m | 7.47m | 2.25m | 0.83m | 0.94m |
| h_3 | 0.59m | 1.84m | 7.61m | 4.64m | 2.30m | 0.27m |
| h_4 | 3.53m | 3.26m | 23.78m | 2.14m | 1.41m | 2.72m |
| h_5 | 37.77m | 33.31m | | 2.45m | 9.82m | 17.88m |
| h_6 | 53.97m | 50.97m | | 23.03m | 13.71m | 33.21m |
| h_7 | | | | 17.48m | 34.57m | |
| Σh | 98.26m | 90.12m | 39.55m | 52.72m | 63.00m | 56.54m |

Where ρ_i and h_i are each layer resistivity and thickness.

Applying equations 1-6 to the model parameters as obtained from the software inversion, Table 3 was generated.

Table 3: The Second Geo-electric Parameters

| Profile | VES | S (mhos) | T (Ωm^2) | H (m) | ρ_T (Ωm) | ρ_L (Ωm) | λ |
|---------|-----|----------|--------------------|--------|-------------------------|-------------------------|-----------|
| 1 | 1 | 0.467 | 3470779.5 | 98.256 | 35323.84 | 209.6575 | 12.98 |
| | 2 | 0.158 | 367695.9 | 90.115 | 4080.30 | 570.35 | 2.67 |
| 2 | 3 | 0.016 | 1248047.3 | 39.549 | 31556.99 | 2535.19 | 3.53 |
| | 4 | 0.020 | 93902.5 | 52.716 | 1781.29 | 2619.04 | 0.82 |
| 3 | 5 | 0.019 | 730116.4 | 62.995 | 11590.07 | 3350.80 | 1.86 |
| | 6 | 0.083 | 31112.1 | 56.544 | 550.23 | 681.25 | 0.899 |

Table 4: VES Model Parameters, Inferred Lithologies and Curve Types

| VES Number | Layer Resistivity (Ωm) | Thickness (m) | Depth (m) | Inferred Lithology | Curve Type |
|------------|--|---------------|-----------|--------------------|------------|
| 1 | 294 | 0.84 | 0.84 | Topsoil | KQHKA |
| | 1278 | 1.56 | 2.40 | Lateritic Sand | |
| | 368 | 0.59 | 2.99 | Sand | |
| | 260 | 3.53 | 6.52 | Clayey Sand | |
| | 87948 | 37.77 | 44.29 | Dry Sand | |
| | 2703 | 53.97 | 98.26 | Sand (Aquifer) | |
| | 1135 | – | – | Sand (Aquifer) | |
| 2 | 363 | 0.41 | 0.41 | Topsoil | KQHAK |
| | 1100 | 0.32 | 0.73 | Lateritic Sand | |
| | 421 | 1.83 | 2.57 | Sand | |
| | 230 | 3.26 | 5.83 | Clayey Sand | |
| | 2347 | 33.31 | 39.14 | Dry Sand | |
| | 5641 | 50.97 | 90.11 | Dry Sand | |
| | 854 | – | – | Sand (Aquifer) | |
| 3 | 1034 | 0.69 | 0.69 | Topsoil | KHK |
| | 1731 | 7.47 | 8.07 | Lateritic Sand | |
| | 753 | 7.61 | 15.68 | Sand | |
| | 51675 | 23.78 | 39.46 | Dry Sand | |
| | 1102 | – | – | Sand (Aquifer) | |
| 4 | 889 | 0.72 | 0.72 | Topsoil | KHAACKQ |
| | 3827 | 2.25 | 2.97 | Lateritic Sand | |
| | 785 | 4.64 | 7.61 | Sand | |
| | 1374 | 2.14 | 9.75 | Sand | |
| | 2898 | 2.45 | 12.20 | Dry Sand | |
| | 16003 | 23.03 | 35.23 | Dry Sand | |
| | 1947 | 17.48 | 52.72 | Sand (Aquifer) | |
| | 536 | – | – | Silty Sand | |
| 5 | 506 | 0.35 | 0.35 | Topsoil | KHAKQH |
| | 8325 | 0.83 | 1.18 | Lateritic Sand | |
| | 682 | 2.30 | 3.48 | Sand | |
| | 3713 | 1.41 | 4.89 | Dry Sand | |
| | 50686 | 9.82 | 14.71 | Dry Sand | |
| | 8982 | 13.71 | 28.42 | Dry Sand | |
| | 2753 | 34.57 | 62.99 | Sand (Aquifer) | |
| | 2771 | – | – | Sand (Aquifer) | |
| 6 | 469 | 1.54 | 1.54 | Topsoil | KQHAK |
| | 2742 | 0.94 | 2.48 | Lateritic Sand | |
| | 780 | 0.27 | 2.75 | Sand | |
| | 204 | 2.72 | 5.47 | Clayey Sand | |
| | 273 | 17.88 | 23.35 | Clayey Sand | |
| | 6926 | 33.21 | 56.56 | Dry Sand | |
| | 1485 | – | – | Sand (Aquifer) | |

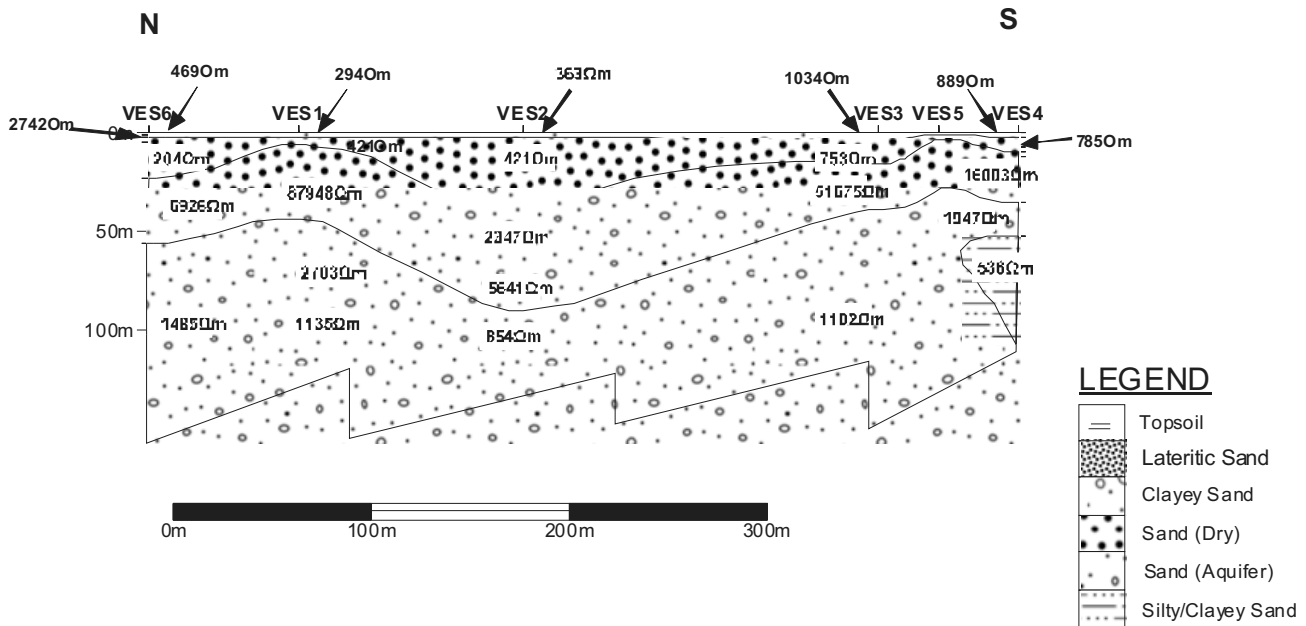


Fig.6: North to south geo-electric sections of the VES points showing the lithologic interpretations beneath each VES station.

DISCUSSION AND RECOMMENDATION

Results of the interpreted data for VES 1 to 6 are as presented in Table 4.

Computer assisted iterative resistivity sounding interpretation (after qualitative interpretation of data using excel software) gave between five and eight geo-electric layers but modeled to six geologic/lithologic layers, viz: the topsoil, lateritic sand, clayey sand, dry sand, aquiferous sand and silty/clayey sand (Figure 7).

The first layer corresponds to the topsoil with resistivity value ranging from 294 Ωm in VES1 to 1034 Ωm in VES 3. The 0.35m to 1.54m thick topsoil consists of loose dry, dark-brown to reddish brown sand.

The second geo-electric layer interpreted to be lateritic sand has a relatively high resistivity value range of 1100 Ωm –8325 Ωm . The thickness of this layer is between 0.32m to 7.47m, and is present beneath all the VES stations.

The lithology beneath the second layer was assigned the sand layer (368 Ωm –785 Ωm) by combining the third and fourth geo-electric layers. This geologic layer consists of sand and a mixture of clayey sand (204 Ωm –421 Ωm). This is present within the third and fourth geo-electric layers of VES 1, 2 and 6, while present only in third geo-electric layer of VES 3, 4 and 5. The thickness of this layer is 2.72m–4.64m for the

clayey sand and 0.27m–7.61m for sand.

The fourth interpreted geologic layer is the high resistivity dry sand with values ranging from 2347 Ωm –87948 Ωm , with thicknesses between 13.71m and 50.97m.

The fourth geologic layer is underlain by the aquiferous sand with resistivity value range of 854 Ωm –2771 Ωm , while the depth to the bottom of the aquifer layer ranges from 39.55m in VES 3 to 98.26m in VES1, which is very much in agreement with the asserted claims by Akujieze and Oteze (2007) and Omorogieva and Imasuen (2018) and an aquifer that can be said to be sandy and highly prolific.

It is noteworthy here that a low resistivity layer beneath the aquifer was delineated in VES4 and assigned silty sand layer, which might also contain some clayey material.

The curve types of VES 1 to 6 are: KQHKA, KQHAK, KHK, KHA AKQ, KHAKQH and KQHAK of corresponding aquifer PCR of moderate (VES1), weak (VES2) and poor (VES3 to VES6), suggestive of the recommendation that VES 1 of moderate PCR is to be considered suitable for siting of borehole compared to the other VES points, despite the fact that the entire area sounded is viable for borehole water extraction.

REFERENCES

- Ademilua, O. L. and Ogungbemi, O. S. (2013). Evaluation of Aquifer Protective Capacity of Groundwater Resources Within Afe-Babalola University, Ado-Ekiti, Southwestern Nigeria. *Transnational Journal of Science and Technology*. 3 (6):1-16.
- Akujieze, C. N. (2004). Effects of Anthropogenic Activities (Sand Quarrying and Waste Disposal) on Urban Groundwater System and Aquifer Vulnerability Assessment in Benin City, Edo State, Nigeria. PhD Thesis, University of Benin, Benin City, Nigeria.
- Akujieze, C. N. and Oteze, G. E. (2007). Deteriorating Quality of Groundwater in Benin City, Edo State. *Journal of Nigerian Association of Hydrogeologists*. Vol.1: 192-196.
- Al-Yasi, A. I.; Alridha, N. A. and Shakir, W. M. (2013). The Exploitation of Dar Zarrouk Parameters to Differentiate Between Fresh and Saline Groundwater Aquifers of Sinjar Plain Area. *Iraqi Journal of Science*. Vol. 54 (2): 358-367.
- Amadasun, C. V. O; Odeh, A. I. and Iguisi, A. E. (2018). Use of Integrated Geophysical Methods for Linear Assessment of a Portion of Siluko Road in Egor Local Government Area of Edo State, Nigeria. *Journal of Physical and Applied Sciences*. Vol. 1, No. 1, Pp. 117-134.
- Ayuk, M. A; Adelusi, A. O. and Adiat, K. A. N. (2013). Evaluation of Groundwater Potential and Aquifer Protective capacity Assessment at Tutugbua-Olugboyega area, Off Owo Road, Akure Southwestern Nigeria. *International Journal of Physical Sciences*. Vol. 8 (1): 37-50.
- Beresnev, I. A; Hruby, C. E. and Davies, C. A. (2002). The Use of Multielectrode Resistivity Imaging in Gravel Prospecting. *Journal of Applied Geophysics*. Vol. 49 (4): 245-254.
- Google Earth/maps (2019) @<https://maps.google.com/maps>.
- Idehai, I. M. and Egai, A. O. (2014). Aspects of Geophysical Exploration for Groundwater Using Vertical Electrical Sounding (VES) in Parts of University of Benin, Benin City, Edo State. *Journal of Applied Sciences and Environmental management (JASEM)*. Vol.18 (1): 19-25.
- Kogbe, C. A, and Assez, L. O. (1979). Geology of Nigeria, the Stratigraphy and Sedimentation of the Niger Delta. Elizabethan Publication, Lagos. 311-323.
- Miller, R (2006). Hydrogeophysics: Introduction to this Special Section. The Leading Edge. Pg. 713.
- Nigerian Geological Survey Agency (2006): <https://ngsa.gov.ng>
- Offordile, M. E. (2002). Groundwater Study and Development in Nigeria. 2nd Edition Published by Mecon Geology and Engineering service Limited, Jos, Nigeria.
- Olorunfemi, M. O.; Ojo, J. S. and Akintunde, O. M. (1999). Hydrogeophysical Evaluation of the Groundwater Potential of Akure Metropolis, Southwestern Nigeria. *Journal of Mineral Geology*. 35(2):207-228.
- Omorogieva, O. M. and Imasuen, O. I. (2018). Litho-stratigraphic and Hydrological Evaluation of Groundwater system in Parts of Benin Metropolis, Benin City, Nigeria: The Key to Groundwater Sustainability. *Journal of Applied Sciences and Environmental management (JASEM)*. Vol.22 (2): 275-280.
- Reyment, R. A. (1965). Aspects of the Geology of Nigeria. University of Ibadan Press, Nigeria
- U N I B E N w e b s i t e (2 0 1 9) : <https://en.m.wikipedia.org/wiki>
- Utom, A. U., Odoh, B. I., Okoro, A. U. (2012). Estimation of Aquifer Transmissivity using Dar Zarrouk Parameters Derived from Surface Resistivity Measurements: A Case history from parts of Enugu town (Nigeria). *Journal of Water Resource and Protection*. 4: 993-1000.
- Vchery, A. and Hobbs, B. (2003). Resistivity Imaging to Determine Clay Cover and Permeable Units at an Ex-Industrial Site. *Near Surface Geophysics*. Vol. 1 (3): 131-137.
- Zohdy, A. A. R; Eaton, G. P. and Mabey, D. R. (1974). Application of Surface Geophysics to Groundwater Investigation. *Techniques of Water Resources Investigation*, US Geological Survey.

GEOLOGICAL AND GEOPHYSICAL CONTROLS OF GROUNDWATER OCCURRENCE IN EKPOMA AND IRRUA TOWNS OF EDO STATE NIGERIA

Oboh Mathew Edenaruese

Department of Physical Science Laboratory Technology,
Auchi Polytechnic, Auchi, Edo State, Nigeria.

meoboh@hotmail.com

&

Ujuanbi Omeimen

Department of Physics,
Ambrose Alli University, Ekpoma, Edo State, Nigeria.

omiujuanbi@aauekpoma.edu.ng

Abstract

Geophysical and geological mapping of some parts of Ekpoma and Irrua towns was carried out to determine the factors responsible for groundwater occurrence in the study area. The geophysical investigation involved the combination of Vertical Electrical Sounding (VES) technique using the Schlumberger configuration and the Electrical Resistivity Tomography (ERT). Available Borehole data were also used to establish the geology of the area. A total of five (5) VES data with a current electrode spacing ($AB/2$) of 400m, were acquired across the study area to determine the occurrence of groundwater and depth to aquifer. The ERT data were obtained along the six (6) profiles of lengths varying from 140m to 220m in order to delineate change in facies. The geophysical field data were inverted using RES1DINV and RES2DINV software respectively. The VES results revealed that the town of Irrua has three aquiferous units with an average depths of 50m, 34m and 295m and thicknesses of 5m, 8m and 30m respectively. However, relative to Irrua, in Ekpoma, there were no shallow aquifers found. Aquifers were only found to occur from an average depth of 300m to 409m. The geoelectric sections obtained shows that the two towns have different geological setting with a sharp transition along the boundary. The ERT result revealed a lateral change in facies from Ekpoma axis to Irrua, except in areas along boundary line within Ekpoma that replicate the same facie as Irrua. The ERT and VES results have shown clearly that the geology of Ekpoma is different from that of Irrua. Whereas, Ekpoma is underlain by Bende-Ameki formation with the nature of the stratigraphic arrangement of geological unit of rock section contributing to the occurrence of deep aquifer, Irrua on the other hand is underlain by the Ogwashi-Asaba formation which extends towards area that fall along the boundary within Ekpoma. The stratigraphic arrangement of the rock units of the Bende-Ameki formation favours shallow occurrence of aquifer that the inhabitants depends on for source of water. The study also revealed that at the centre of Ekpoma town, groundwater occurs within the Imo Shale and Ajali formations.

Keywords: Groundwater, Electrical resistivity tomography (ERT), Vertical Electrical Sounding (VES), Aquiferous unit, Groundwater, Schlumberger configuration, Dipole-dipole configuration.

Introduction:

As a result of rapid population growth and local development, potable water is in short supply and this has led to the usage of groundwater potentials for steady and reliable water (Adagunodoet *al.*,

2018; Anomohanran, 2011).The need for the quality and availability of water resources has always been the primary concern of our societies especially in semi arid and arid regions, and even the areas with abundant rainfall such as tropical region. The problem of gaining an adequate supply of quality water is generally becoming more severe due to growth in population as well as irrigation activities and industrialization. Consequently,

Corresponding Author: Mathew E Oboh
Department of Physical Science
Laboratory Technology,
Auchi Polytechnic Auchi, Edo State, Nigeria
meoboh@hotmail.com

surface water cannot be relied upon throughout the year, hence other alternative sources are needed in order to supplement for surface water. The groundwater is the water that lies under ground and it is the best quality fresh water which the world depends on its availability source. It is the water held in the sub-surface within the saturated zone under hydrostatic pressure below water table. The groundwater can be in the sedimentary terrain where it is less difficult to exploit or in the basement complex terrain in which it can be a bit difficult to locate, especially in areas underlined by crystalline rocks Nejad, *et al.*, (2011).

Nowadays the used of geophysical techniques for groundwater exploration and water quality evaluations has increased due to the rapid advances in computer software and other numerical modeling techniques. The use of Vertical Electrical Sounding (VES) has become very popular with groundwater prospecting due to simplicity of the technique. The essence of electrical survey methods in geophysical prospecting is to detect the surface effects that are produced by the flow of electric current inside the earth. These techniques have been used in wide range of geophysical investigations such as mineral exploration, archeological investigation, engineering studies, geothermal exploration, permafrost mapping and geological mapping.

Previous literature includes those of Adeeko, *et al.*, (2019), Abdullahi, *et al.*, (2015), Nejad, *et al.*, (2011), (2018), Aigbogun, *et al.*, (2018), Layade, *et al.*, (2017), Aluko, *et al.*, (2017), Jassim and Mohammed, (2014), Abudulawal, *et al.*, (2015), Adagunodo, *et al.*, (2018), Abitarin, *et al.*, (2016) . The work of Salufu & Ujuanbi (2015) made use of less data points to make a generalization of the factors affecting groundwater occurrence in the transitional zone within the study area covered, hence this work is aimed at filling the gap in knowledge.

Location and accessibility of the study area

This study was carried out in Ekpoma and Irrua towns, which are respectively situated in Esan West and Esan Central Local Government Areas of Edo State, Nigeria. Both towns lie between latitudes $6^{\circ}42' N - 6^{\circ} 45' N$ and longitudes $6^{\circ} 2' E - 6^{\circ} 13' E$, covering a surface area of about 582 square kilometers. The area shares a common boundary with Agbede to the north, Ewu to the north-west, Ehor to the south-west and Uromi to the south-east. The area is accessible by many roads including the Benin-Auchi and Uromi-Agbor Federal highways.

The location and topographic map of Ekpoma and Irrua and its environs in Esan West and Esan Central Local Government areas showing the accessibility of the area is shown in Figure 1.

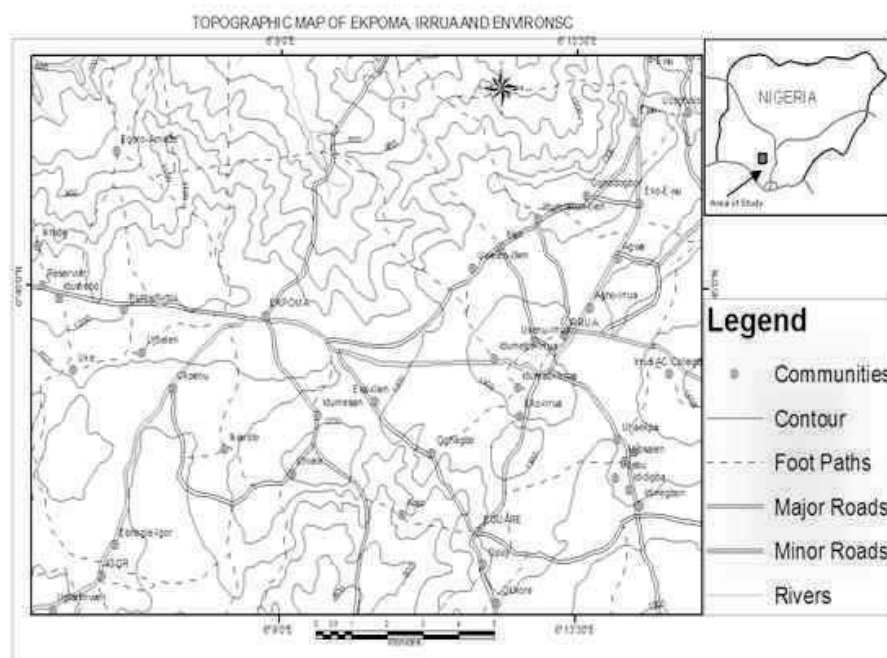


Figure 1: Topographic map of Ekpoma and Irrua and its environs in Esan West and Esan Central Local Government Areas. (Source: Nigeria Geological Survey Agency NGS 2014).

Material and Methods

Integrated geophysical techniques involving 2-dimensional Electrical Resistivity Tomography (ERT) and Electrical Resistivity Sounding (VES) were used to obtain the pseudo-section of the subsurface from which deductions of fracture zones and their thicknesses were made (Loke, 2001).

Vertical electrical sounding which is also called electrical drilling, was carried out at selected moderate resistivity anomalous zones along the 2D-profile. Apart from the selected points along the 2D-profile, other points with favourable features such as ant-hills, big trees, lineaments (e.g.: river channel) were also considered for sounding. The ABEM Terameter SAS 1000 was set-up in the Schlumberger configuration with manual electrode expansion mode to probe up to 100m below ground level. ABEM Terameter SAS 1000 allows one to view the plotted in-situ curve on the field as sounding is in progress, such that values that appear unreasonable could be rejected and sounding repeated at the same spot as deemed necessary to achieve conformity in order to ensure data quality control. The field data was analyzed using RES1DINV and RES2DINV software to produce the VES curves and also to obtain the number of sub-surface geological layers and their corresponding thicknesses, apparent resistivity values and geoelectric sections.

The ABEM Terameter SAS 1000 was connected in 500m spread cable layout with 20m take outs. The

Schlumberger protocol was used throughout the imaging system at all the sites. This protocol was used due to its fair sensitivity to both vertical and lateral geological structures and its good horizontal and vertical resolutions. Electrode test was then carried out to check for each electrode performance and to ensure that each had good ground contact. The electrodes with poor contact were aided with salt solution to enhance their performance. The measurements sequence was carried out within a period of 10 minutes to probe as deep as 75m below ground level with a 500m spread. During the data acquisition, each of the four (4) basic electrodes can either be active or passive (Figure 2) since they are selected concurrently at a time. In the Schlumberger array protocol, C_1 , P_1 , P_2 and C_2 have a as electrode spacing for each measurement sequence at the same level $n=1$. In order to probe deeper, the electrode spacing is then increased to $2a$ among C_1 , P_1 , and P_2 , $-P_2$ while P_1 , $-P_2$ remains a at the new level $n=2$. This was used to take all the measurements sequential and step wisely at the same level. Furthermore, at a deeper level $n=3$ C_1 , $-P_1$, and P_2 C_2 would have electrode spacing to be increased to $3a$ with P_1 , $-P_2$ still remaining a . These processes are automatically chosen and executed from inbuilt program within the ABEM Terameter SAS 1000 during the data acquisition. As the data was being collected, one can view a model pseudo section of the data on the screen of the ABEM Terameter SAS 1000.

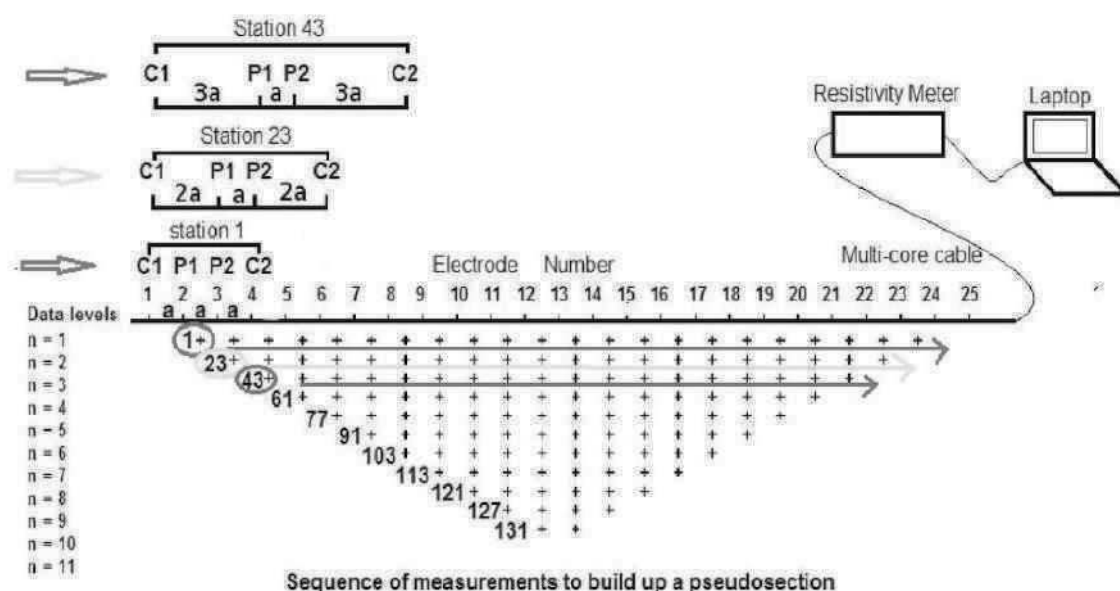


Figure 2: Typical 2D-resistivity data measurement sequence in the Schlumberger array.

The resistivity values were calculated from the field data and modeled against electrode position using RES1DINV and RES2DINV software to obtain a plot of apparent resistivity variation with depth at a potential borehole drilling point. The output model gives a signature curve with specific number of beds of different degrees of weathering as well as their resistivity and thickness (Loke, 2010). Usually, a fracture is associated with decreasing apparent resistivity with expanding current electrode separation. This phenomenon has been used to determine the presence of fractures in the study area (Aluko, *et al.*, 2017).

Data from the geo-electrical survey were processed using mainly RES1DINV and RES2DINV to represent the data in the form that can be easily analyzed and interpreted (Loke, 2001). The field data was downloaded from the ABEM Terameter SAS 1000 equipment in *.dat and *.txt format. The raw data in the *.dat format was read into RES2DINV software and modeled with series of about eight (8) iterations to obtain well refined and colourful model-section of the sub-surface. The elevation along the traverse was introduced into the analysis to obtain the topography of the terrain. The output model-section indicates a plot of apparent resistivity variation with depth along each 500m profile as well as elevation of landscape with position along the traverse.

The inversion routine used for the interpretation of the field data is a Window based programme that is based on the smoothness constrained least square method with the equation (Loke, 2001) as follows;

Where

$$(\mathbf{J}^T \mathbf{J} + \mu \mathbf{F}) \mathbf{d} = \mathbf{J}^T \mathbf{g} - \mathbf{u} \mathbf{F} \mathbf{r} \quad (1)$$

$$\mathbf{F} = \mathbf{f}_x \mathbf{f}_x^T + \mathbf{f}_z \mathbf{f}_z^T$$

\mathbf{F} = a smoothing matrix,

\mathbf{f}_x = horizontal flatness filter,

\mathbf{f}_z = vertical flatness filter,

\mathbf{J} = the Jacobian matrix of partial derivatives,

\mathbf{J}^T = the transpose of \mathbf{J} ,

μ = damping factor,

\mathbf{d} = model perturbation vector,

\mathbf{g} = the discrepancy vector,

\mathbf{r} = a vector containing the logarithm of the model resistivity values.

Theory of resistivity method

Data from resistivity surveys are customarily presented and interpreted in the form of values of apparent resistivity ρ_a . An equation giving the apparent resistivity in terms of applied current, distribution of potential, and arrangement of electrodes can be arrived at through an examination of the potential distribution due to a single current electrode. Consider a single point electrode, located on the boundary of a semi-infinite, electrically homogeneous medium, which represents a fictitious homogeneous earth. If the electrode carries a current I , measured in amperes (A), the potential at any point in the medium or on the boundary is given by:

$$U = \rho \frac{1}{2\pi r}$$

where U = potential, in volts, ρ = resistivity of the medium Ohm-meter, r = distance from the electrode in meter.

For an electrode pair with current I at electrode B (Figure 3), the potential at a point is given by the algebraic sum of the individual contributions given as:

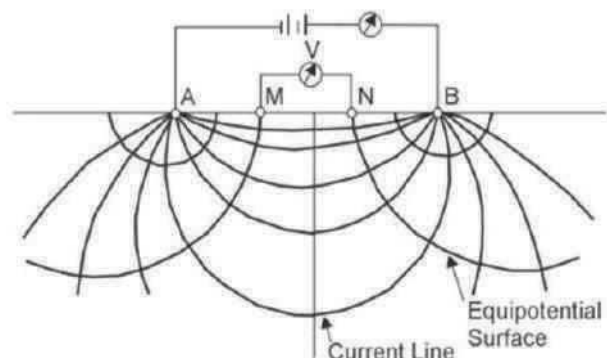


Figure 3: Equipotential and current lines for a pair of current electrodes A and B on a homogeneous half-space

$$U = \frac{\rho I}{2\pi r_A} - \frac{\rho I}{2\pi r_B} = \frac{\rho I}{2\pi} \left[\frac{1}{r_A} - \frac{1}{r_B} \right]$$

where r_A and r_B = distances from the point to electrodes A and B

In addition to current electrodes A and B , Figure 3 shows a pair of electrodes M and N , which carry no current, but between which the potential V may be measured. Following the previous equation, the potential difference V may be written

$$V = U_M - U_N = \frac{\rho I}{2\pi} \left[\frac{1}{AM} - \frac{1}{BM} + \frac{1}{BN} - \frac{1}{AN} \right]$$

where U_M and U_N = Potentials at M and N, AM = distance between electrodes A and M, etc.

These distances are always the actual distances between the respective electrodes, whether or not they lie on a line. The quantity inside the brackets is a function only of the various electrode spacings. The quantity is denoted $1/K$, which allows rewriting the equation as:

$$V = \frac{\rho I}{2\pi K}$$

where K = array geometric factor.

Solving for ρ we obtain

$$\rho = 2\pi K \frac{V}{I}$$

The resistivity of the medium can be found from measured values of V , I , and K , the geometric factor. K is a function only of the geometry of the electrode arrangement.

Schlumberger configuration

For this array (Figure 4), in the limit as a approaches zero, the quantity V/a approaches the value of the potential gradient at the midpoint of the array. In practice, using an finite electrode spacing and equation (3) we can compute the geometric factor.

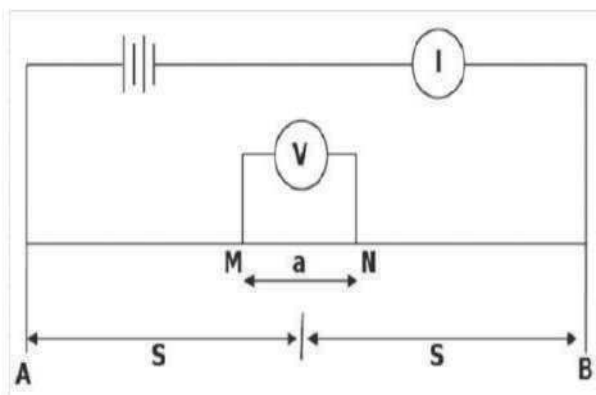


Figure 4. Geometric arrangement of the Schlumberger array configuration.

The apparent resistivity ρ_a is:

$$\rho_a = \pi \left[\left(\frac{s^2}{a} \right) - \frac{a}{4} \right] \frac{V}{I} = \pi a \left[\left(\frac{s^2}{a} \right) - \frac{1}{4} \right]$$

In usual field operations, the inner (potential) electrodes remain fixed, while the outer (current) electrodes are adjusted to vary the distance s . The spacing a is adjusted when it is needed because of decreasing sensitivity of measurement.

ERT (Dipole-dipole) configuration

The dipole-dipole array (Figure 5) is one member of a family of arrays using dipoles (closely spaced electrode pairs) to measure the curvature of the potential field. If the separation between both pairs of electrodes is the same a , and the separation between the centers of the dipoles is restricted to $a(n+1)$, the apparent resistivity is given by:

$$\rho_a = \pi a n(n+1)(n+2) \frac{V}{I}$$



Figure 5: Dipole-dipole configuration.

and the geometric factor is given by

$$K = \pi a n(n+1)(n+2)$$

This array is especially useful for measuring lateral resistivity changes and has been increasingly used in geotechnical applications.

Result and Discussion

The Electrical Resistivity Tomography (ERT) data results (Figures 6 to 10) acquired from the study revealed different colour contrasts varying from blue to deep blue, red, green, purple to green. These colours show the signature of the subsurface geology of the area which is the reflection of the resistivity signature of the subsurface.

The ERT result for all the traverse T2 and T3, acquired in Ekpoma axis of the study area revealed that the apparent resistivity signature of the subsurface ranges from an average of $2500 \Omega m - 10444 \Omega m$ (see Figures 6, and 7). However, the second group of traverses that were acquired across the boundary line from Ekpoma to

Irrua T1 and T4, (Figures 8 and 9) showed two different sets of colour variation from the Ekpoma axis across the boundary to Irrua axis with distinctive colour variation. In some cases, the colour variation type that occurs in Irrua axis extending slightly into the Ekpoma axis across the surface boundary. The resistivity of the portion that falls within the Irrua axis and around the boundary line ranges from an average of 340m –940m. The third category of ERT results obtained from the study area in Irrua is traverse $669 \Omega m - 2214 \Omega m$. The colour contrasts occurs in homogenous manner with the lower inversion model resistivity values compared to those ones in Ekpoma that were extremely high.

The Vertical Electrical Sounding modeling carried out at Irrua at VES stations VES 13, VES 14 and VES 15 revealed that Irrua has three aquiferous units with an average depths and thickness of 50m, 134m, and 295m and 5m, 8m and 30m respectively. In addition, the third aquiferous units have the highest resistivity and yield.

However, the VES results acquired along the boundary between Ekpoma and Irrua (VES 13 and VES 14) revealed similar information as that of the ones acquired in Irrua axis of the study area, while the results from VES 1, VES 2, and VES 3, that were taken far-away from the boundary line within Ekpoma showed different pattern compared to those acquired from Irrua. In Ekpoma, the aquiferous layer occur very deep and there is no shallow aquiferous layers. The aquifer layers occur from an average depth of 300m to 409m with with high resistivity and yield.

In addition to this, the ERT and VES showed clearly that the geology of Ekpoma is different from that of Irrua while Ekpoma is underlain by Bende-Ameki Formation, Irrua is underlain by Ogwashi Asaba Formation. The entire portion of Bende-Ameki Formation is very thick in height but does not carry any aquiferous layer in Ekpoma axis. It is very porous, thus allows rain water to infiltrate easily into the Imo formation that underlies it and therefore serves as a medium of recharge for Imo formation.

The geoelectric sections (Figure 16) extracted from the vertical Electric Sounding results acquired in Irrua and Ekpoma shows that Irrua and Ekpoma have different geological setting. This

dissimilarity in the hydrogeologic settings of the two towns indicates variation in the geological setting of Ekpoma and Irrua while the result of Electric Resistivity Tomography revealed a sharp transition along the boundary between Ekpoma and Irrua. This work further reinforce the work of Salufu & Ujuanbi (2015) This observation in the ERT result indicates lateral change in facies from Ekpoma axis to Irrua except for area along boundary between the two towns. It was also revealed from the ERT results that many areas around Ekpoma, mostly along the boundary have replicate of Irrua being that the same facies in Irrua extends to such areas.

The nature of the stratigraphic arrangement of geological unit of rock sections (Figure 17) in Ekpoma also contributes to occurrence of deep aquifer in Ekpoma. Towards Irrua axis and areas that fall along the boundary with Irrua, the stratigraphic arrangement of rock units (Figure 18) favours shallow occurrence of aquiferous units which majority of the inhabitants depend on for source of water. These results correlate with the borehole data obtained from both areas where the study was conducted.

Conclusion

The electrical resistivity method which involves Schlumberger and ERT (Dipole-Dipole arrays) were used to determine the factors controlling the occurrence of groundwater in Ekpoma and Irrua towns. From this investigation; it was revealed from the VES results that the town of Irrua has three aquiferous units with an average depths and thicknesses of 50m, 134m, and 295m and 5m, 8m and 30m respectively. On the other hand, in the Ekpoma axis at the boundary line between Ekpoma and Irrua, it was revealed that they have similar information with those ones acquired in Irrua, whereas, far-away from the boundary line within Ekpoma showed different patterns compared to those data acquired from Irrua. In Ekpoma, the aquiferous layer occur very deep and there is no shallow aquiferous layer and the aquifer occurs from an average depth of 300m to 409m. It has high resistivity and yield. Also, the resistivity and the thickness of the weathered layer constitutes the aquifer unit have an average range between $340 \Omega m - 940 \Omega m$ and 50m –134m within Irrua and in Ekpoma it has a resistivity ranging between $2500 \Omega m - 10444 \Omega m$ and 300m – 409m respectively.

Secondly, the study also revealed that the geoelectric sections extracted from the Vertical Electric Sounding results acquired in Irrua and Ekpoma shows that both towns have different geological setting. This dissimilarities in the hydrogeologic settings in the study area shows that there is a variation in the geological setting of Ekpoma and Irrua. The Electric Resistivity Tomography results also showed a sharp transition along the boundary between Ekpoma and Irrua, this observation in the ERT result shows lateral change in facies from Ekpoma axis to Irrua except for area along boundary line within Ekpoma that have replicate of Irrua meaning that the same facies in Irrua also extends to this area.

Thirdly, both the results of the Electrical Resistivity Sounding and the Vertical Electrical Sounding of the study areas revealed clearly that the geology of Ekpoma is different from that of Irrua. Ekpoma is underlain by Bende-Ameki Formation while Irrua is underlain by Ogwashi Asaba Formation. The entire portion of Bende-Ameki Formation is very thick in height but does not carry any aquiferous layer in Ekpoma axis. It is very porous, thus allows rain water to infiltrate easily into the Imo Formation that underlies it and this serves as a medium of recharge for Imo formation.

The nature of the stratigraphic arrangement of geological unit of rock sections in Ekpoma also contributes to occurrence of deep aquifer in Ekpoma. Towards Irrua axis and areas that fall

along the boundary with Irrua, the stratigraphic arrangement of rock units favours shallow occurrence of aquiferous units that majority depend on for source of water. However, at the centre of Ekpoma, groundwater occurs within Imo Formation at a very deep depth while area of Ekpoma that falls within the boundary of Irrua has groundwater from Ogwashi-Asaba Formation In Irrua, groundwater occurs in three stratigraphic units; the thin aquifer (the first and second units) and the thick aquifer (third units) which is the deepest.

The nature of the stratigraphic arrangement of geological unit of rock sections in Ekpoma also contributes to occurrence of deep aquifer in Ekpoma. Towards Irrua axis and areas that fall along the boundary with Irrua, the stratigraphic arrangement of rock units favours shallow occurrence of aquiferous units that majority of the inhabitants depend on for source of water. These results correlate with the borehole data obtained from both areas where the study was conducted.

The result of the Vertical Electrical Sounding of Ekpoma and Irrua showed different resistivity inversion models. This observation suggests that their facies are different and this corroborate the findings of Salufu and Ujuanbi (2015). The change in facies from Ekpoma to Irrua as indicated by VES and ERT results, symbolizes difference in the hydrogeological setting of this two towns.

Electrical Resistivity Tomography results

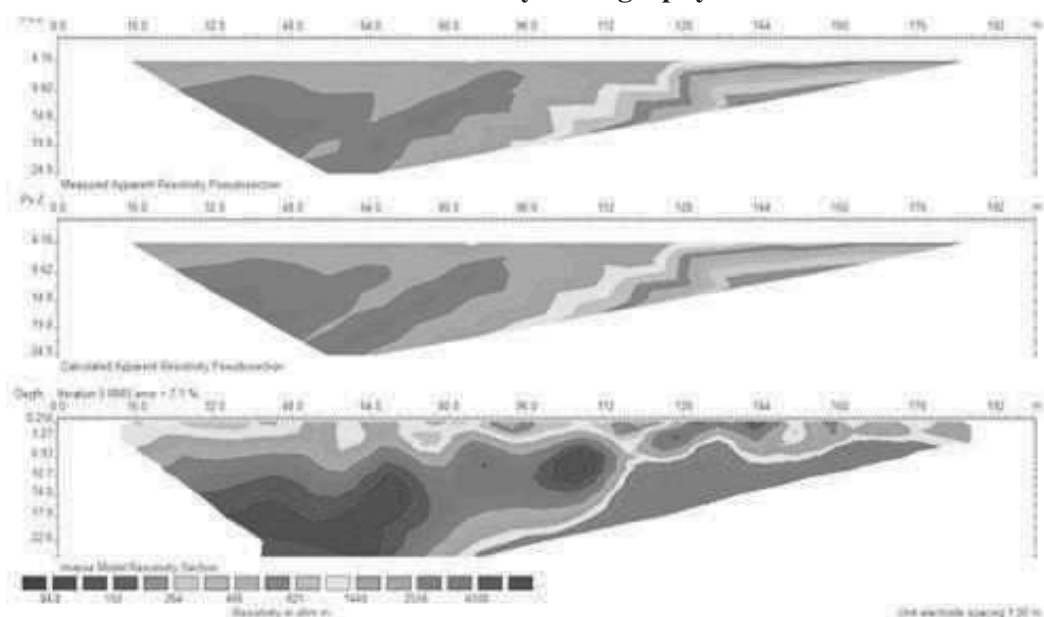


Figure 6: The ERT result acquired along traverse T2 within Ekpoma area

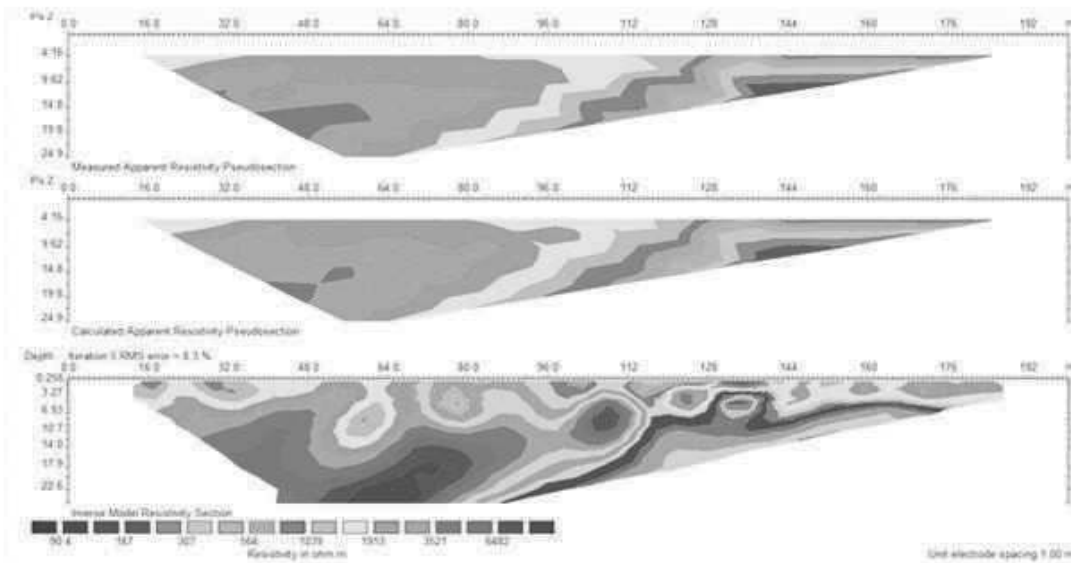


Figure 7: The ERT result acquired along traverse T_3 within Ekpoma area.

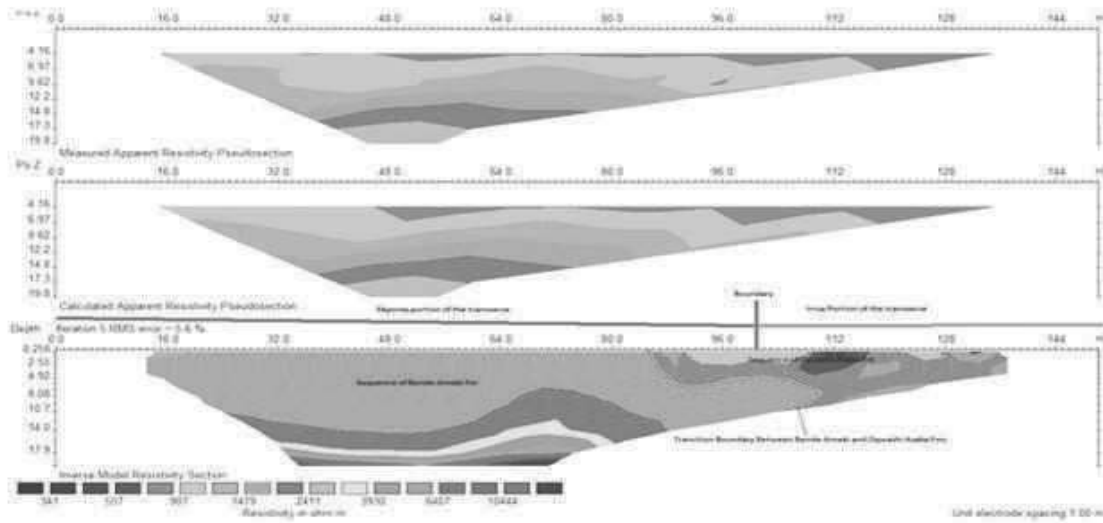


Figure 8: The ERT result acquired along traverse T_4 along the boundary area between Ekpoma and Irrua

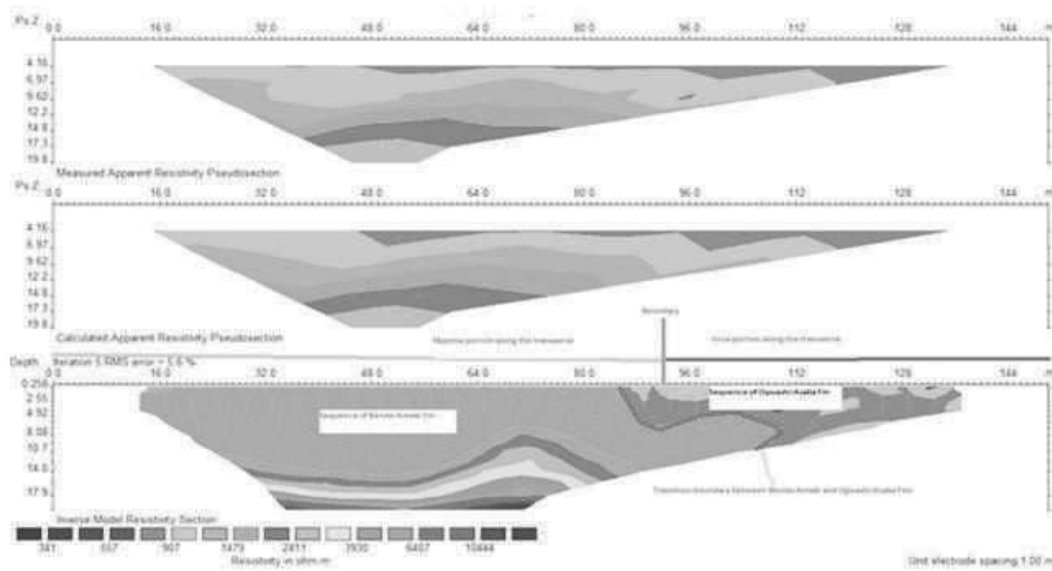


Figure 9: The ERT result acquired along traverse T_1 along the boundary area between Ekpoma and Irrua

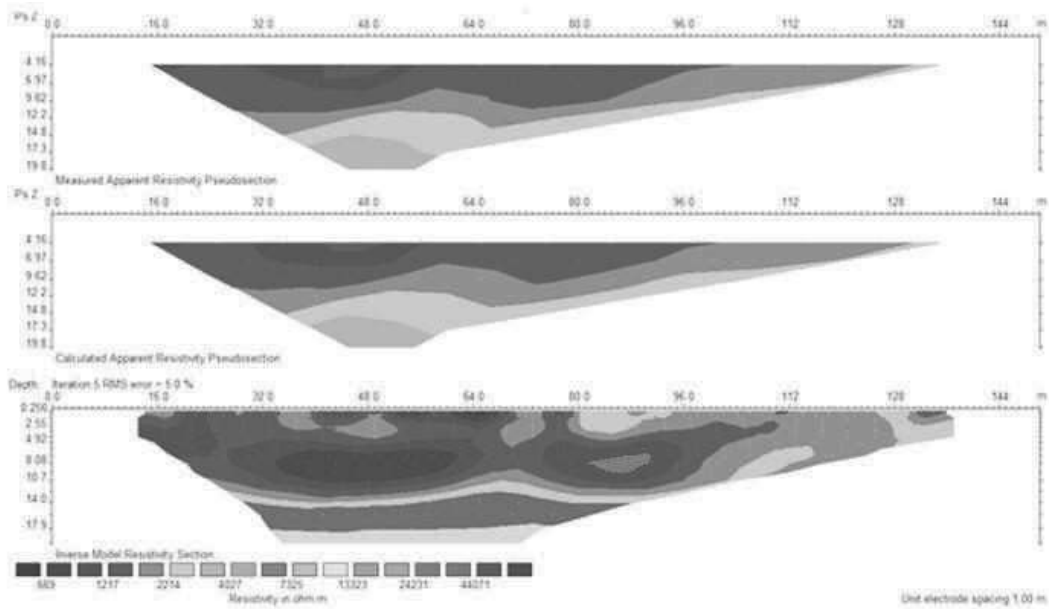


Figure 10: The ERT result acquired along traverse T5 within the Irrua area.

Inverted models for Vertical Electric Soundings acquired from Ekpoma axis

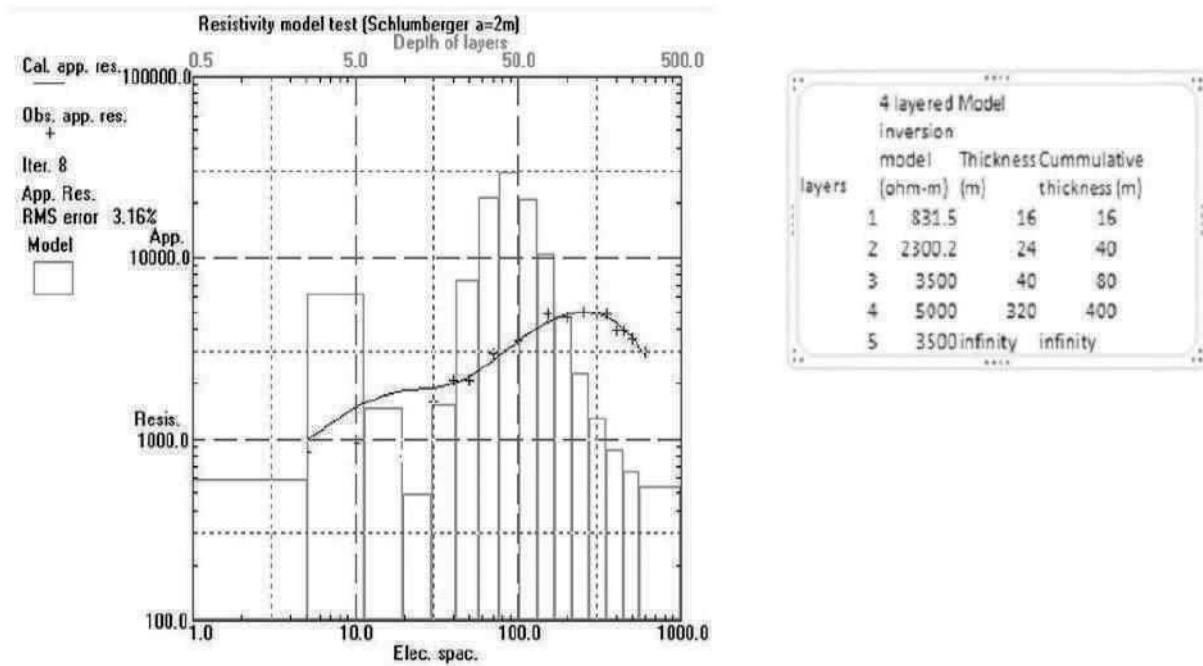


Figure 11: Inverted model for VES 1 acquired in Ekpoma.

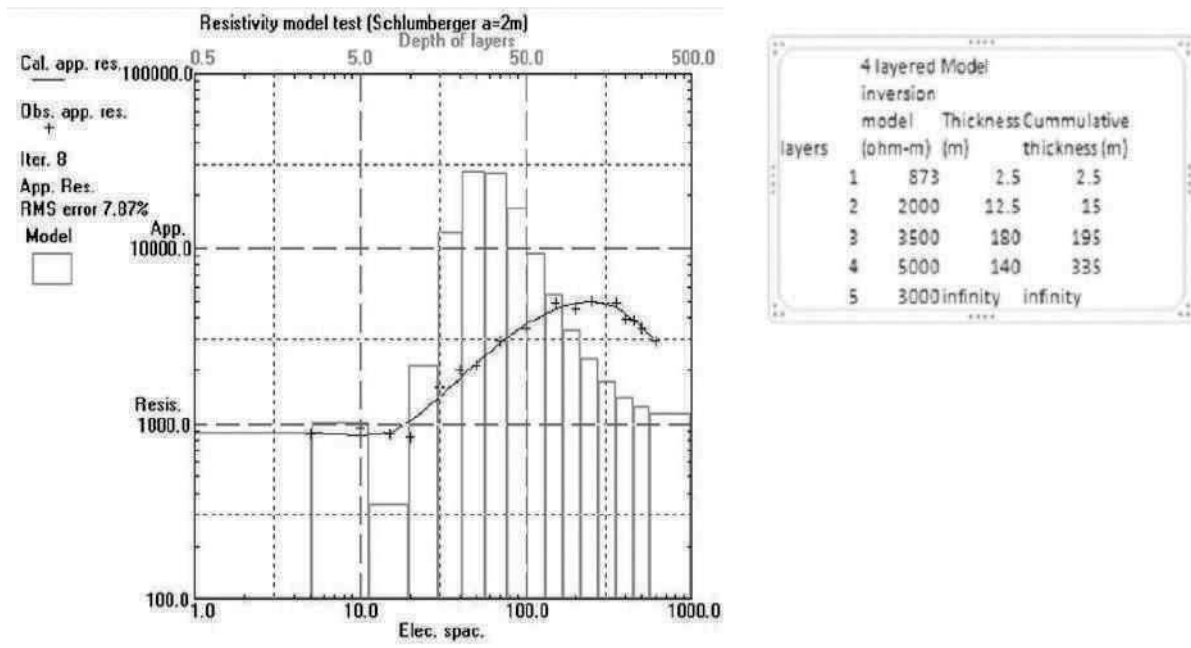


Figure 12: Inverted model for VES 2 acquired in Ekpoma.

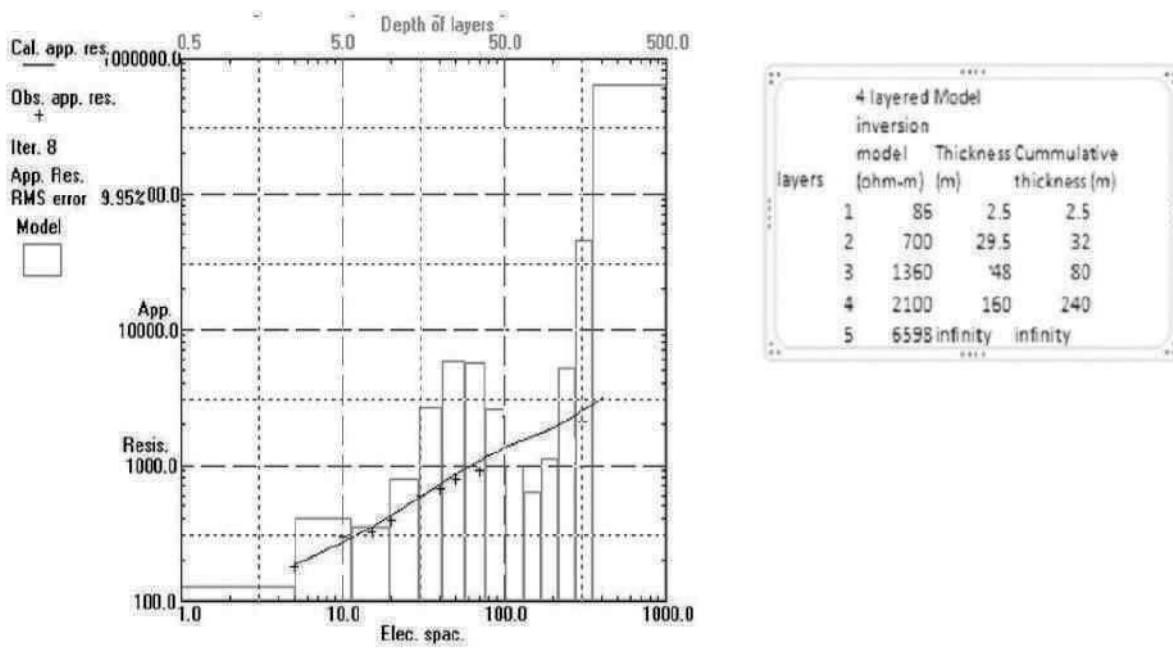


Figure 13: Inverted model for VES 3 acquired in Ekpoma

Inverted models for Vertical Electric Soundings acquired from Irrua axis

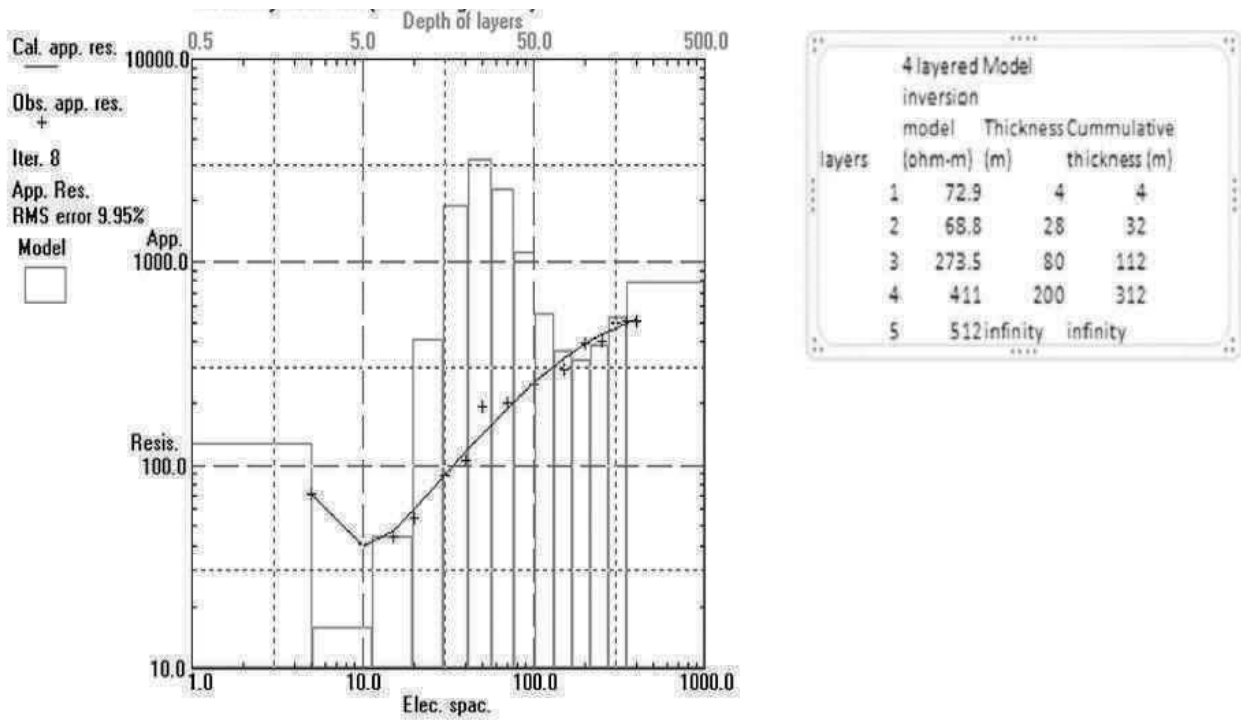


Figure 14: Inverted model for VES 4 acquired in Irrua.

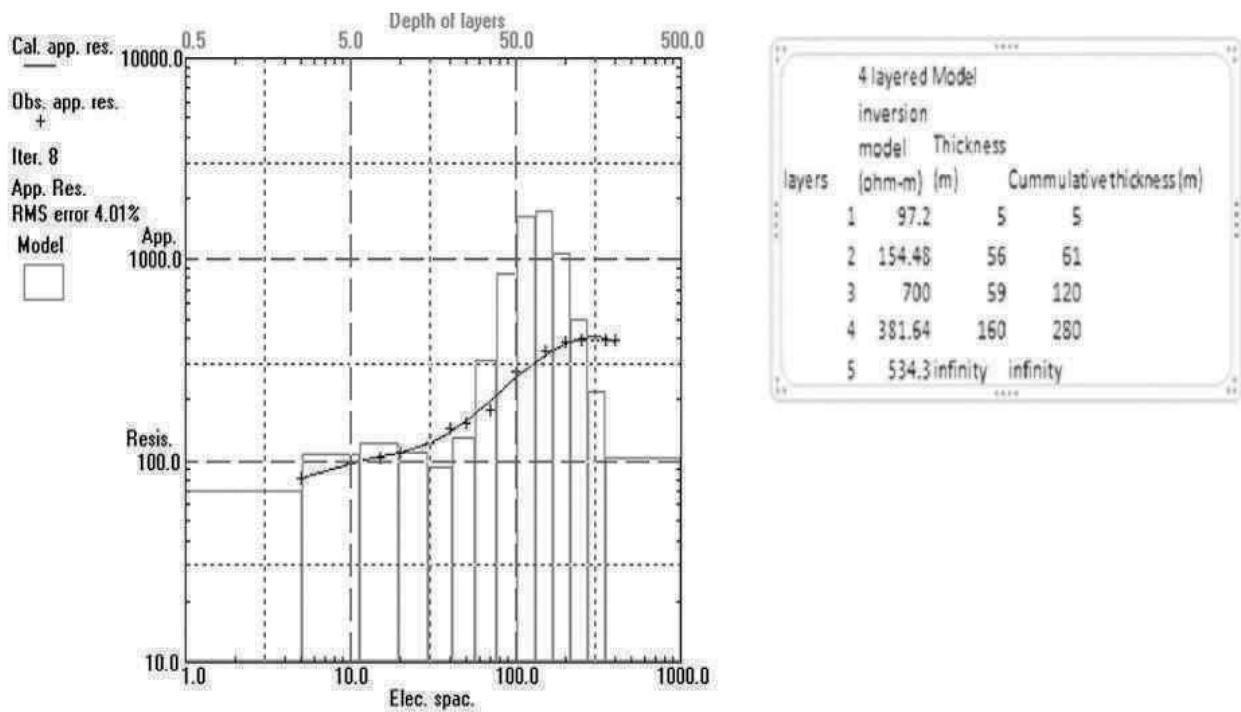


Figure 15: Inverted model for VES 5 acquired in Irrua.

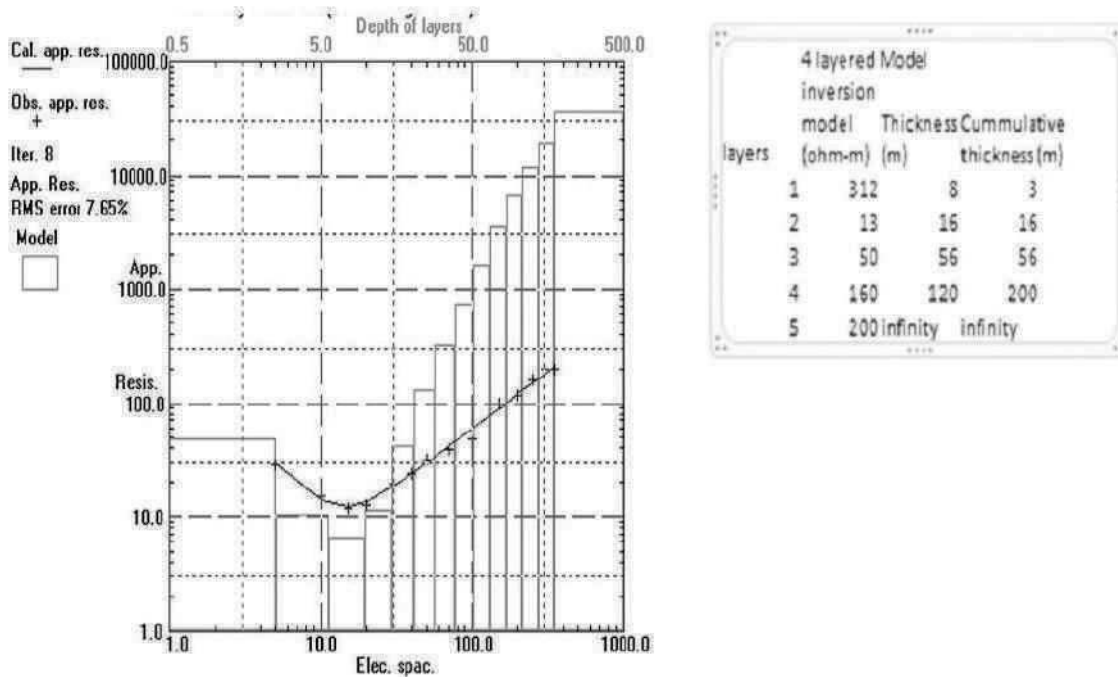


Figure 16: Inverted model for VES 6 acquired in Irrua

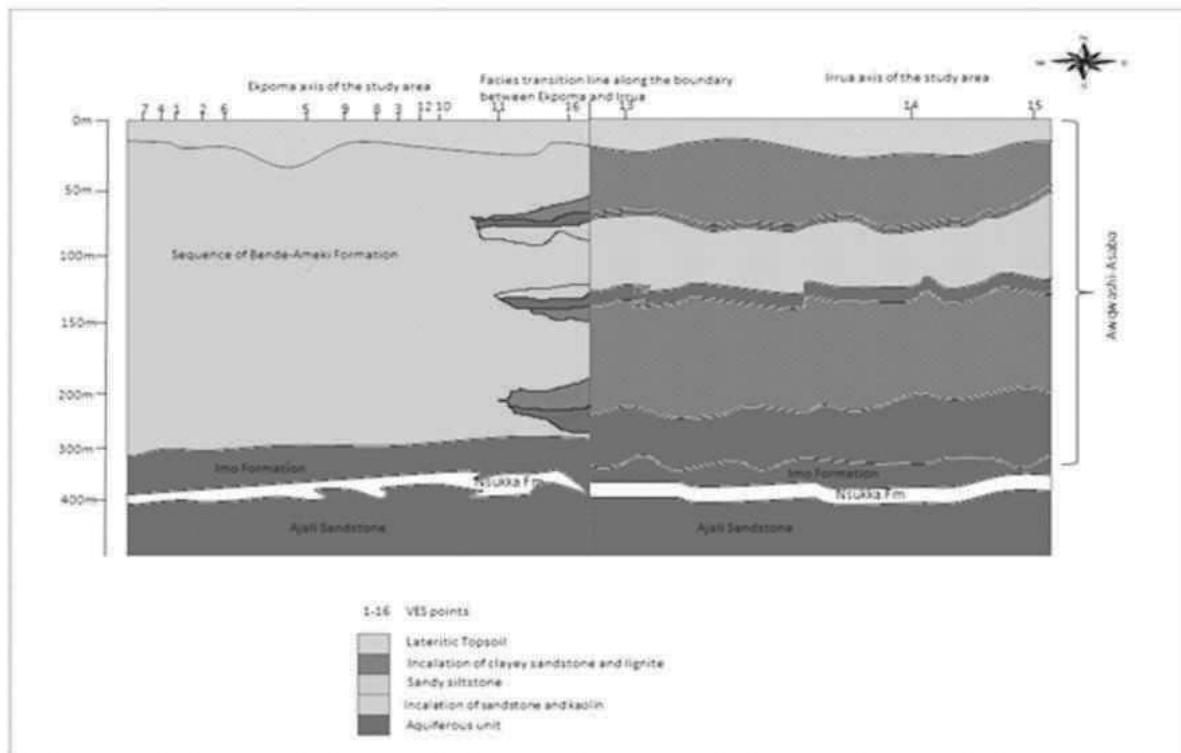


Figure 17: Geoelectric section of the study area (Ekpoma and Irrua).

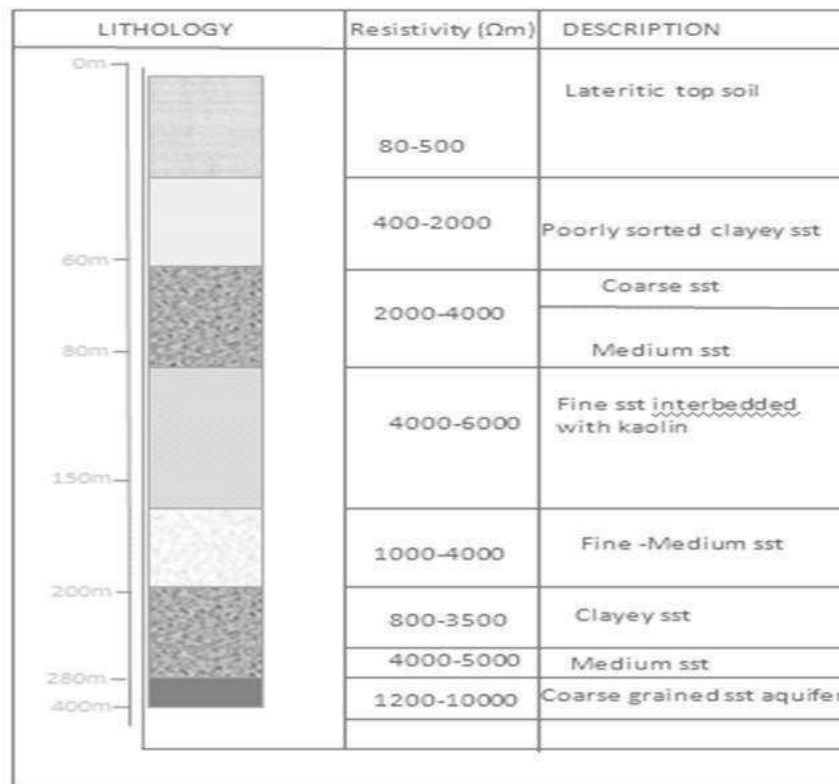


Figure 18: Correlation of borehole data and VES result obtained in Ekpoma (source:Salufu and Ujuanbi 2015).

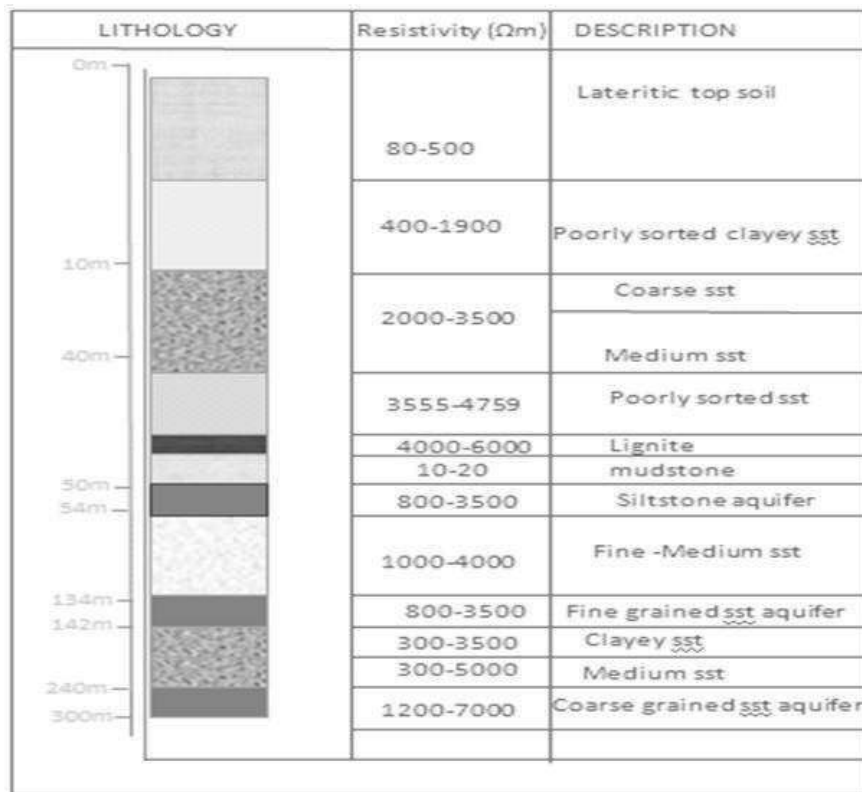


Figure 19: Correlation of borehole data and VES result obtained in Irrua(source:Salufu and Ujuanbi 2015).

References

- Abdullahi, M. G., Toriman, M. E., and Gasim, M. B. (2015). The application of vertical electrical sounding (VES) for groundwater exploration in Tudun Wada Kano State, Nigeria. *Journal Geology and Geoscience*, 4(1): 186–189.
- Abitarin, S. J., Amadi, A. N., Olasehinde, P. I., Ameh, I. M. and Ayeni, J. K. (2016). Geological and structural control of groundwater occurrence in parts of Abuja, North-Central Nigeria. *Nigerian Journal of Pure and Applied Sciences*. 8: 157–165.
- Abdulawal, L., Amidu, S. A., Apanpa, K. A., Adeagbo, O. A., and Akinbiyi, O. A. (2015). Geophysical investigation of subsurface water of Erunmu and its environs, Southwestern Nigeria using electrical resistivity method. *Journal of Applied Sciences*. 15: 741–751.
- Adagunodo, A. A., Akinloye, M. K., Sunmonu, L. A. Aizebeokhai, A. P. Oyeyemi K. D. and Abodunrin F. O. (2018). Groundwater exploration in Aaba residential area of Akure, Nigeria. *Frontiers in Earth Science*. 2(6): 1–12.
- Adeeko, T. O., Samson, D. O., and Umar, M. (2019). Geophysical survey of basement complex terrain using electrical resistivity method for groundwater potential. *World News of Natural Science*. 23:154–165.
- Aigbogun, C. O., Adegbite, J. T., Olorunsola, K., and Ehilenboadiaye, I. J. (2018) Geophysical investigation of Egbeta, Edo State, Nigeria, using electrical resistivity survey to assess the groundwater potential. *International Journal of Scientific Research Engineering and Technology*. 7(4): 368–375.
- Aluko, K. O., Raji, W. O., and Ayolabi, E. A. (2017). Application of 2-D resistivity survey to groundwater aquifer delineation in a sedimentary terrain: A case study of southwestern Nigeria. *Water Utility Journal*. 17: 71–79.
- Anomohanran, O. (2011). Underground water exploration of Oleh, Nigeria using the electrical resistivity method. *Scientific Research and Essays*. 6(20): 4295–4300.
- Bernard, J. 2003. The depth of investigation of electrical methods. IRIS-instruments, France. Pp. 16–44
- Jassim A. S., and Mohammed A. A. (2014). Delineation of groundwater aquifers using VES and 2-D imaging techniques in north Badra area, eastern Iraq. *Iraqi Journal of Science*. 55(1). 174–183.
- Layade, G. O., Adegoke, J. A., and Oladewa, F. C. (2017). Hydrogeophysical investigation for groundwater development at Gbongudu area, Akobo Ojurin, Ibadan, Southwestern Nigeria. *J. Appl. Sci. Environ*. 21(3): 527–535.
- Loke, M.H. (2010). 2D and 3D Electric Imaging Surveys, Geotomo Software SdnBsd, Malaysia. Pp. 23–48
- Loke, M. H. (2001). Electrical imaging surveys for environmental and engineering studies. A Practical guide to 2-D and 3-D surveys. RES2DINV Manual. IRIS Instruments. www.iris-instruments.com. 8–10 pp.
- Loke, M.H. and Lane, J.W. 2004. Inversion of data from electrical resistivity imaging surveys in water covered areas. *Exploration Geophysics*. 35, 266–271.
- Nejad, H. T., Mumipour, M., Kaboli, R. and Najib O. A. (2011). Vertical electrical sounding (VES) resistivity survey technique to explore groundwater in an Arid Region, Southeast Iran. *Journal of Applied Sciences*. 11(23): 3765–3774.
- NGSA (2014). Nigeria Geological Survey Agency: the geological map of Nigeria and Edo state. A publication of Nigeria Geological Survey Agency, Abuja, Nigeria
- Salufu, S. O., and Ujuanbi, O. (2015). The geology and structural geology of Ekpoma and Irrua: Implication for the hydrology and hydrogeologic setting of the areas. *Nigerian annals of Natural Sciences*. 15(1): 131–138.

AN EVALUATION OF THE PHYSICO-CHEMICAL PROPERTIES AFFECTING THE ERODIBILITY OF SOILS IN GULLIES

Okojie Usinomen Victor,

Department of Chemistry, Ambrose Alli University Ekpoma

Isitekhale Harry

Department of Soil Science, Ambrose Alli University Ekpoma.6

Salufu Obomheile Samuel

Department of Physics, Ambrose Alli University Ekpoma

Ufuah Emmanuel

Department of Civil Engineering, Ambrose Alli University Ekpoma

Akhirevbulu Ojeabu Ehijie

Department of Physics, Ambrose Alli University Ekpoma

Onogbosele Oziegbe Cyril

Department of zoology, Ambrose Alli University Ekpoma

Okiti Mohammad Okemukoko

Department of Chemistry, Ambrose Alli University Ekpoma

Abstract

A study of the physico-chemical properties affecting the erodibility of soils in gullies was carried out. Soil samples were collected in selected areas and analyzed for the physico-chemical properties using standard methods. The results showed high exchangeable sodium percentage (ESP) in the soils and increased with increasing soil depth. Deflocculation or dispersion of clay which is the major cause of the erodibility of the soils is facilitated by the low concentrations of organic matter (OM) (11.48–17.28g/kg), calcium (Ca^{2+}) (0.89–1.29cmol/kg) and magnesium (Mg^{2+}) (0.69–1.00cmol/kg) coupled with the increasing concentration of profiled ESP which is above the critical level of 15%. Furthermore, the sandy texture of the soils even at greater depths and the presence of montmorillonite clay further increased the vulnerability of the soils to erosion. The effects of the physico-chemical properties on the soil erodibility were assessed in terms of pH, K^+ , Ca^{2+} , Mg^{2+} , organic matter, exchangeable sodium potential, bulk density exchange acidity, cation ion exchange capacity and base saturation. These properties were correlated with the erodibility factors ($\text{K}_{(\text{fact})}$). The $\text{K}_{(\text{fact})}$ correlated positively with pH, depth, Na^+ and base saturation but correlated negatively with organic matter, Mg^{2+} , Ca^{2+} and K^+ . The regression analysis results indicate that the important properties that contributed to the erodibility of the soils were depth, exchangeable sodium percentage, silt, clay and organic matter.

Keywords: Erodibility, $\text{K}_{(\text{fact})}$, physico-chemical deflocculation, Exchangeable sodium percentage (ESP) montmorillonite clay.

Introduction:

Soil erosion is one of the most important physical and socio-economic problems threatening the environmental settings of Edo State, Nigeria. Apart

from the fact that it constitutes a menace to the environment, soil erosion creates a major problem on our agricultural land thereby interfering seriously with food production, hence the need for predicting the susceptibility of soils to erosion. Although the incipient stage of soil erosion through rill and sheet are common and easily managed by

Corresponding Author: Akhirevbulu Ojeabu Ehijie,
Department of Physics,
Ambrose Alli University Ekpoma.
ojeabu@aauekpoma.edu.ng

the people through recommended soil conservation practice, the gully forms have assumed a different dimension such that settlements, scarce arable land and sustainable road links are threatened. An accurate determination of soil erodibility is important in the design and construction of water, roads and conservative structure management projects. However, this is a difficult task owing to the fact that soil detachment is a complex function of both soil and eroding fluid properties (Egwuonwu and Uzoije, 2008; Akintola, 2001). Soil aggregate stability have been a common soil parameter studied for characterization of soil erodibility. They are commonly used because they can be easily and rapidly obtained, measured incrementally with depth and related to other soil parameters that affect soil erodibility. For a successful characterization of soil erodibility, it is imperative to understand the bonding forces between soil particles and other materials in the soil matrix and by extension some internal and external unquantifiable parameters of the soils. Though some work has been carried out on techniques of assessing erodibility of soils (Okojie *et al.*, 2019, Imeson and Vis, 1984) there is little information on the soil properties that influences erodibility of the soils in the area of study. Aggregate stability and the resistance of aggregates to rain drop impact affect erodibility. Aggregate stability in turn is affected by such characteristics as aggregate size, type, amount of clay and organic carbon (Foster *et al.*, 1985;

Luk1979; Greenland, 1977). In order to manage the soil effectively and combat erosion, the relationship between certain structure building soil properties and soil erodibility needs to be determined.

Though several model for the determination of erodibility factor exist, the ability to utilize them to predict the rate of soil loss is cumbersome (Tran *et al.*, 2002; Mitra *et al.*, 1998). Therefore in this study, the methodology developed by Wischmeier *et al.*, (1971) was modified and implemented. This provides a more flexible and realistic procedure in describing the relationship between the soil erodibility factor and the variables contributing to it.

Local Geology of the Study Area

The study sites comprise of Ibore and Ambrose Alli University (AAU) campus. Ibore is located within the Esan Central Local Government Area of Edo State. It is underlain by Ogwashi-Asaba Formation (Fig. 1). It comprises sequence of well cemented, indurated sandstone. The sequence graded upward to indurated kaolin bed of 1.2m, transits unto indurated coarse sandstone bed and capped with indurated siltstone. The siltstone bed passes upward into a moderately sorted clayey friable sandstone bed of about 14m. The gully site is downhill and it ranges from 1000ft to 1340ft above sea level. The channel meanders through a length of about 200m and with an average depth of 21m. The width of the channel is 25m at the top and narrows down the channel as a result of the indurated nature of the rock at the basal part.

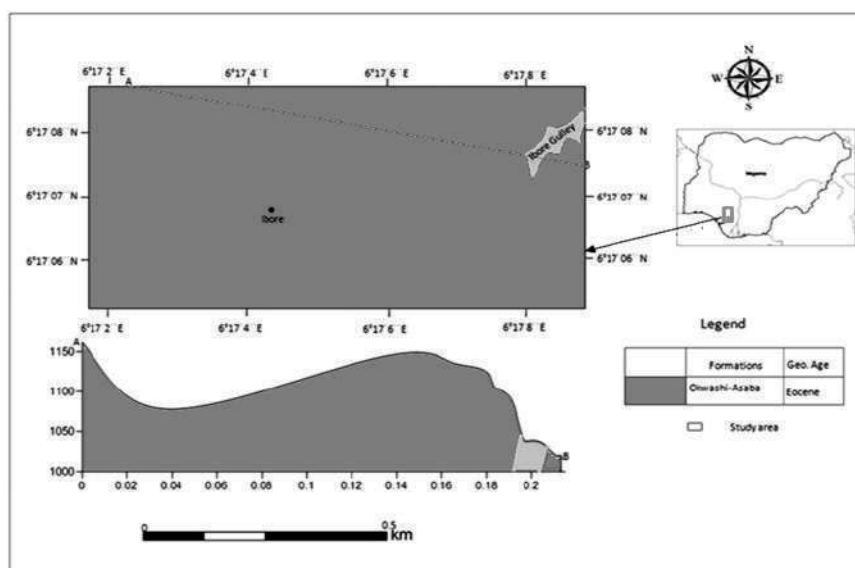


Fig.1: Geologic map of Ibore showing the location of the gully and the geology

Ambrose Alli University campus is located in Ekpoma, Nigeria. Its gully trends from the main Road that passes through the entrance of faculty of Environmental and Management Sciences. The gully meanders from the North West to the South West of the campus. The widest and the deepest portion of the gully occur in the North West of the trend while it becomes shallower and narrower south westward.

AAU is underlain mainly by Bende-Ameki Formation (99%) with minor Imo Formation

(1%)(Fig. 2).The geology sections along the gully showed that the upper portion of the gully comprises friable sandstones while the lower portion of the sections is indurated and clayey. The topography of the area attests to these observations. The shallow and narrow portions are restricted to low elevation (deeper depth; below 1000ft), while the portion that experienced the highest erodibility is restricted to area with higher topography (shallow depth; 1100–1200ft). The gully stretches up to half a kilometer.

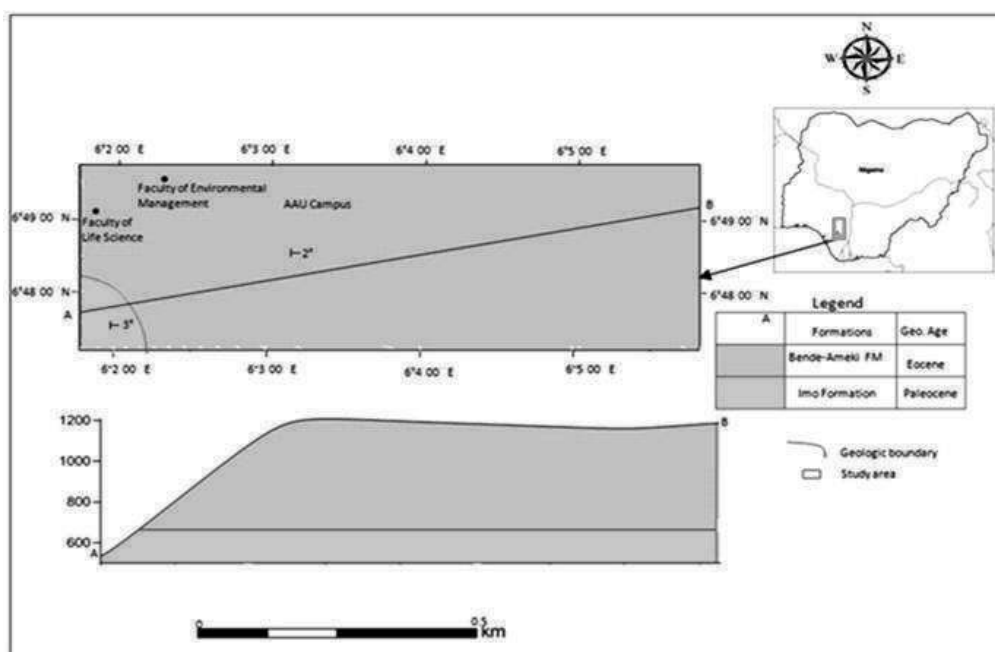


Fig. 2: Geologic map of AAU showing the geology of the area

Materials and Methods

Soil sampling

Surface soil samples were collected from each eroded site at depths of 0 – 15 cm and 15 – 30 cm for the morphological studies. Profile pits were dug in each eroded site and soil samples collected based on Anderson and Ingram (1993) method. Soil morphological properties were collected based on FAO (2006). (Table 1).

Laboratory Analysis

Soil pH was measured in a 1:1 soil-water suspension using glass electrode pH meter (MaClean, 1982). Exchangeable acidity (Al^{3+} , H^+) were extracted with 1N KCL (Thomas, 1982) and determined by titration with 0.05 NaOH using phenophtalin as indicator. Organic carbon (OC) was determined by wet dichromate acid oxidation method (Olsen and Sommers, 1982). Total nitrogen

was determined by the micro-Kjeldahl method (Bremner, 1982). Available phosphorus was extracted with Bray-P1 solution and colour developed by the molybdenum blue method (Olsen and Sommers, 1982) and measured on the technicon auto analyzer. Exchangeable cations (Ca, Mg, Na and K) were extracted with 1N NH_4OAc (pH 7.0), K and Na were determined with flame emission photometer while Ca and Mg were determined with atomic absorption spectrophotometer (Anderson and Ingram, 1993). Effective cation exchange capacity (ECEC) was calculated by the summation of exchangeable bases and exchange acidity (Anderson and Ingram 1993; Okalebo *et al.*, 2002). Particle size distribution was determined by the hydrometer method according to (Okalebo *et al.*, 2002). The soils were dispersed with sodium hexametaphosphate solution and also by distilled water for dispersion determination. The core

method was used to determine the soil bulk density and porosity and estimated according to Rowell (1994). The standard deviation and percent

coefficient of variability was carried out according to Frank and Althoen (1995).

Table 1: Some surface physical and morphological characteristics of the gully sites

| Parameter | University gully Site | Iboregully site |
|---------------------|------------------------------|------------------------------|
| Soil structure | 3 –medium or coarse granular | 3 –medium or coarse granular |
| Aggregate stability | 0.17% | 1.67% |
| Permeability Class | 5 – moderate to rapid | 5 – moderate to rapid |
| Slope Length | 5% | 4% |

Quantifying and estimating soil erodibility (K-factor)

To evaluate the effectiveness of USLE-K model, comparison between the measured (Williams et al., 1984) erodibility data with the (Wischmeier et al.,

1971) and nomograph data was done. The preferred method, according to Goldman *et al.*, (1986), for determining K-factors is the nomograph method based on the work by Wischmeier *et al.*, (1971) and is mathematically represented as follows:

$$K_{fact} = (1.292) \left[2.1 \times 10^{-6} f_p^{1.14} (12 - P_{om}) + 0.0325 (S_{struc} - 2) + 0.025 (f_{perm} - 3) \right] \quad (1)$$

$$(f_p = P_{silt} (100 - P_{clay})) \quad (2)$$

Where;

f_p is the particle size parameter (unit less)

P_{om} is the percentage of organic matter (unit less)

S_{struc} is the soil structure index (unit less)

f_{perm} is the profile-permeability class factor (unit less)

P_{clay} is the percent clay (unit less).

In Equation 1 the factor (1.292) is needed to convert K_{fact} from the English units used in Goldman *et al.* (1986) to the metric units used in this report. The soil structure index, S_{struc} , is equal to: 1 for very fine granular soil; 2 for fine granular soil; 3 for medium or coarse granular soil; 4 for blocky, platy, or massive soil. The profile-permeability class factor, f_{perm} , is equal to: 1 for very slow infiltration; 2 for slow infiltration; 3 for slow

to moderate infiltration; 4 for moderate infiltration; 5 for moderate to rapid infiltration; 6 for rapid infiltration.

Based on the computations from equation 1 and 2 above, the K-factor value for Ibore gully site was 0.01 and 0.14 for University campus gully site. The erodibility indices for the samples of soils from Ibore and University campus sites when compared with standard erodibility indices (Table 2) showed that they fall into group I (permeable outwash well drained soil, slowly permeable substrata) and II (well drained soil in sandy gravel free material) respectively. It is difficult to reduce erodibility once soil has become degraded and lost its organic matter, clay, structure and permeability. K-Factor can rise from 0.1 to 0.2 or 0.35 with the degradation of cropped soils (Roose and Lelong, 1976).

Table 2: Standard erodibility indices.

| GROUP | K-Value | Nature of soil |
|-------|-------------|--|
| I | | Permeable out wash well drained soil, slowly permeable substrata |
| II | 0.11 – 0.17 | Well drained soils in sandy gravel free material |
| III | 0.18 – 0.28 | Graded loams and silt loams |
| IV | 0.29 – 0.48 | Poorly graded moderately fine texture soil |
| V | 0.49 – 0.64 | Poorly graded silt, very fine sandy soil, well and moderately graded |

Source: (Idah *et al.*, 2008)

Results and Discussion

Soil Physical Properties

The soil texture of the University campus gully site ranged from sand to loamy sand, while that of Ibore gully site ranged from sand, loamy sand to sandy clay loam (Table 3 and 4). Based on the texture, soils of the former are more exposed to erosion compared to that of Ibore site. Sand fraction has macropores capable of water movement into the deep layers of the pedon. Sand particles are usually of low transportability (Obi and Asiegbu, 1980). However, deep gullies developed are attributed mainly to the volume of runoff water that enters the site. The dispersion ratio that was very high in both sites (>15%) further accounted for the erodible nature of both sites. The surface soil structure was medium or coarse granular in the University campus and Ibore sites (Table 1). The weak structure is evidenced by the very low organic matter. The sand particles are easily detached and therefore prone to erosion since they form less aggregates (poor soil structure); aggregates are aided by organic matter, clays, iron oxides and aluminum oxides. Aggregate breakdown and soil dispersion may affect soil porosity, decreasing water infiltration and hydraulic conductivity and increasing surface sealing and susceptibility to erosion (Raine and So, 1994; Fuller *et al.*, 1995).

Bulk density ranged from 0.99 to 2.00 g/cm³ in the University campus site and 0.97 to 2.88 g/cm³ in Ibore site and increased down the profile (Table 3

and 4). Surface bulk density was very low in both sites. Porosity is directly proportional to the bulk density and was almost of similar value with mean porosity of 41% and 43.2% for AAU university campus and Ibore sites respectively. Abu-Hamdeh and Al-Jalil (1999) reported that as soil particles are eroded, soil materials become loose, therefore reducing the bulk density and increasing the porosity. Soil density increases with compaction at depth and very compact subsoils (Cresswell and Hamilton, 2002). At higher depths, higher bulk density values is often attributed to high clay content, and were it exist, makes the soil to be less susceptible to erosion as the case of Ibore sites. However, in University campus site the sandy texture of the profile even at higher depths further increases its vulnerability to erosion (Idah *et al.*, 2008).

As measured, the permeability of both sites was 5 (moderate to rapid) (Table 1). Slope angles of the sites are high (4° and 5°) with high slope lengths. No other variable affects the stability of slopes with regard to surficial erosion and mass wasting as does topography or slope morphology i.e. inclination and degree of slope (Gray, 2016). It should be noted that despite slope angle of 10%, runoff will not only carry fine particles but can also attack the soil, digging out stratified channels in which speed quality build up, and thus becoming linear erosion (grooves, rills and gullies).

Table 3: Textural and physical properties of Ambrose Alli University gully site

| Depth (cm) | Sand | Silt % | Clay → | Silt/Clay | Bulk density g/cm ³ | Porosity ← | Dispersion % → |
|------------|-------|-----------|-----------|-----------|--------------------------------------|---------------|-------------------|
| 0 - 10 | 93.02 | 1.98 | 5.00 | 0.40 | 0.99 | 63 | 64 |
| 10 - 25 | 92.30 | 1.69 | 6.01 | 0.32 | 1.23 | 54 | 60 |
| 25 - 55 | 91.67 | 1.00 | 7.33 | 0.14 | 1.56 | 41 | 42 |
| 55 - 74 | 88.17 | 2.88 | 8.95 | 0.32 | 1.67 | 37 | 56 |
| 74 - 122 | 85.67 | 2.10 | 12.23 | 0.17 | 1.70 | 36 | 57 |
| 122 - 157 | 82.67 | 4.00 | 13.33 | 0.30 | 1.87 | 29 | 55 |
| 157 - 200 | 80.19 | 1.61 | 18.20 | 0.09 | 2.00 | 25 | 45 |
| X | 87.67 | 2.18 | 10.22 | 0.25 | 1.57 | 41 | 54 |
| SD | 5.02 | 0.98 | 4.84 | 0.11 | 0.35 | 13.49 | 7.90 |
| %CV | 6 | 45 | 47 | 46 | 23 | 33 | 15 |

Where;

X = average value

SD = Standard deviation

% CV = percentage coefficient variance

Table 4: Textural and physical properties of Ibore gully site

| Depth (cm) | Sand | Silt % | Clay → | Silt/Clay | Bulk density g/cm ³ | Porosity ← | Dispersion % → |
|------------|-------|-----------|-----------|-----------|--------------------------------------|---------------|----------------------|
| 0 – 10 | 97.23 | 0.22 | 2.55 | 0.09 | 0.97 | 63 | 43 |
| 10 – 30 | 96.58 | 0.42 | 3.00 | 0.14 | 1.10 | 59 | 50 |
| 30 – 60 | 94.88 | 0.12 | 5.00 | 0.02 | 1.20 | 55 | 50 |
| 60 – 95 | 92.86 | 0.61 | 6.53 | 0.09 | 1.23 | 54 | 46 |
| 95 – 120 | 88.67 | 1.03 | 10.10 | 0.10 | 1.28 | 52 | 59 |
| 120 – 160 | 75.77 | 3.57 | 20.66 | 0.17 | 2.50 | 6 | 39 |
| 160 – 200 | 70.23 | 3.20 | 26.57 | 0.12 | 2.88 | 9 | 34 |
| X | 88.05 | 1.31 | 10.63 | 0.10 | 3.00 | 432 | 46 |
| SD | 10.78 | 1.45 | 9.37 | 0.05 | 3.60 | 24.24 | 8.19 |
| %CV | 12 | 111 | 88 | 47 | 120 | 57 | 18 |

Soil Chemical Properties

The soil chemical properties of the two eroded sites are given in Tables 5 and 6. The eroded soils are strongly acidic and low in organic matter (OM). The sites are of low nutrient status and retention due to low total nitrogen, exchangeable cations (Ca²⁺, Mg²⁺ and K⁺), effective cation exchange capacity (ECEC) and high exchangeable Na percentage (ESP). The ratio of exchangeable sodium to the total of exchangeable cations – the exchangeable sodium

percentage or ESP – is a good indicator of soil structural stability. Structural stability is encouraged by high organic matter, clay, calcium and Mg elements; their low contents coupled with increasing profile ESP could result in clay dispersion or deflocculation. However, soil dispersion problems may occur at a higher or lower ESP depending upon clay type. Kalonitic clay type is most affected and constitutes about 80% of our tropical soils.

Table 5: Chemical properties of Ibore gully site

| Depth (cm) | Ph | OC ← | OM g/kg | N → | Na ← | Mg | Ca cmol/kg | K | Ech. Acidity | ECEC → | BS ← % | ESP → | Ca/Mg |
|------------|------|---------|------------|--------|---------|------|---------------|------|-----------------|-----------|--------------|----------|-------|
| 0 – 10 | 5.0 | 10.00 | 17.24 | 0.80 | 0.58 | 1.00 | 1.25 | 0.15 | 0.25 | 3.23 | 92 | 20 | 1.25 |
| 10 – 30 | 4.9 | 7.89 | 13.60 | 0.60 | 0.67 | 0.99 | 1.29 | 0.11 | 0.38 | 3.23 | 86 | 24 | 1.30 |
| 30 – 60 | 5.0 | 7.65 | 13.19 | 0.60 | 0.78 | 0.89 | 1.03 | 0.09 | 0.45 | 3.24 | 86 | 28 | 1.16 |
| 60 – 95 | 5.1 | 6.78 | 5.08 | 0.50 | 0.89 | 0.67 | 0.98 | 0.06 | 0.39 | 2.99 | 87 | 34 | 1.46 |
| 95 – 120 | 5.2 | 5.66 | 3.94 | 0.30 | 0.95 | 0.78 | 0.90 | 0.04 | 0.50 | 3.17 | 84 | 36 | 1.15 |
| 120 – 160 | 4.9 | 5.01 | 3.29 | 0.40 | 0.87 | 0.60 | 0.88 | 0.02 | 0.40 | 2.77 | 86 | 38 | 1.47 |
| 160 – 200 | 4.9 | 4.98 | 3.26 | 0.20 | 0.99 | 0.56 | 0.78 | 0.02 | 0.44 | 2.79 | 84 | 42 | 1.39 |
| X | 5 | 6.85 | 8.51 | 0.49 | 0.82 | 0.79 | 1.02 | 0.07 | 0.40 | 3.06 | 86 | 31.71 | 1.31 |
| SD | 0.12 | 1.82 | 5.94 | 0.20 | 0.15 | 0.18 | 0.19 | 0.05 | 0.08 | 0.21 | 2.74 | 7.95 | 0.13 |
| %CV | 2 | 27 | 70 | 42 | 18 | 23 | 19 | 70 | 2 | 7 | 3 | 25 | 10 |

Table 6: Chemical properties of Ambrose Alli University gully site

| Depth (cm) | pH | OC ← | OM % | N → | Na ← | Mg | Ca | K | Ech. Acidity | ECEC → | BS ← % | ESP → | Ca/Mg |
|---------------|------|---------|---------|--------|---------|------|---------|------|-----------------|-----------|--------------|----------|-------|
| | | | | | | | cmol/kg | | | | | | |
| 0 – 10 | 4.6 | 6.66 | 11.48 | 0.40 | 0.58 | 0.69 | 0.89 | 0.09 | 0.85 | 2.25 | 96 | 27 | 1.29 |
| 10 – 25 | 4.6 | 5.70 | 9.82 | 0.40 | 0.60 | 0.26 | 0.65 | 0.06 | 0.87 | 2.45 | 64 | 38 | 2.50 |
| 25 – 55 | 4.4 | 5.69 | 9.81 | 0.39 | 0.77 | 0.24 | 0.43 | 0.06 | 0.88 | 2.38 | 63 | 51 | 1.79 |
| 55 – 74 | 4.5 | 5.30 | 9.13 | 0.41 | 0.89 | 0.21 | 0.44 | 0.05 | 0.99 | 2.48 | 64 | 56 | 2.10 |
| 74 – 122 | 4.4 | 4.98 | 8.59 | 0.34 | 0.97 | 0.18 | 0.39 | 0.04 | 1.11 | 2.10 | 47 | 98 | 2.17 |
| 122 – 157 | 4.6 | 4.66 | 8.03 | 0.20 | 0.99 | 0.11 | 0.30 | 0.02 | 1.12 | 2.54 | 56 | 68 | 2.73 |
| 157 – 200 | 4.9 | 4.30 | 7.41 | 0.20 | 1.05 | 0.11 | 0.35 | 0.02 | 1.08 | 2.71 | 60 | 64 | 3.18 |
| X | 4.57 | 5.33 | 9.18 | 0.33 | 0.84 | 0.26 | 0.49 | 0.05 | 0.99 | 2.42 | 64 | 58 | 2.25 |
| SD | 0.17 | 0.78 | 1.34 | 0.09 | 0.19 | 0.20 | 0.21 | 0.02 | 0.12 | 0.19 | 15.24 | 22.93 | 0.62 |
| %CV | 4 | 15 | 15 | 29 | 23 | 77 | 42 | 50 | 12 | 8 | 24 | 40 | 28 |

The statistical relationship between the soil properties and the indices of erodibility (K_{fact}) was determined using the correlation and multiple regression technique. Tables 7 and 8 shows how results of the various soils physical and chemical properties correlate with each other and with the erodibility factor (K_{fact}). The negative correlation value between (K_{fact}) and organic matter (-0.759 , -0.881) and between the k_{fact} and calcium (-0.767 , -0.598) for Ibore and Ekpoma sites respectively, indicate that organic matter and calcium may have possible binding effect on the soil but, the negative coefficient is significant in that it impacts negatively on soil aggregates stability. OM and Ca bind soil particles together to form stable aggregates which can withstand the disruptive effect of rain drops. Therefore the low concentration of these materials in the soil results in the low stability of the aggregates. Published works also showed that organic matter help to bind soil aggregates together and hence reduce disruptive effect of rain drops (Forster *et al.*, 1975; Luk 1979; Greenland, 1977). There was also negative correlation value between pH and K fact result (-0.389) for Ibore site, but positive (0.829) for Ekpoma sites. The influence of pH on erodibility in this study is indirect, probably due to some aggregate stabilizing materials (Fe and Al) in the soil, the concentration of which decreases with increase in pH. This reduction in the concentration of these materials results in the building of less stable aggregates. The soil pH of the Ekpoma site had a greater effect on erodibility as shown from the magnitude of the correlation coefficient. K_{fact} correlated positively with depth,

silt and clay for both sites except for sand (-0.960) for Ibore gully and (-0.691) for Ekpoma sites respectively. However, the high correlation coefficient for depth (0.889), silt (0.995), clay (0.950) and sand (0.990) for Ibore gully site appear to indicate that these parameters may not be playing appreciable roles in aggregate stability which greatly influences erodibility. Depth of sampling can only influence erodibility indirectly as a result of certain aggregates building properties of the soil for example Fe oxide, which are depth dependent. Clay help to increase the binding capacity of the soil which is responsible for aggregate stability which influence erodibility. There was a positive correlation between K_{fact} and Na (0.638) for Ibore and (0.678) for Ekpoma gully sites. Na plays a role in the dispersion of soil particles and thus influences erodibility of soils. The negative correlation between K_{fact} and Ca, Mg and K in both sites is significant as shown by the magnitude of the correlation coefficient. These aggregates stabilizing materials played an insignificant role in aggregate stability, because the concentration of these ions in soils decreases with pH. This reduction in the concentration of these ions results in the building of less stable aggregates. However, the high negative correlation coefficient had a greater negative effect on erodibility as shown in table 7 and 8.

Table 7: Correlation Matrix Showing Correlation Coefficients (R) among Soil Properties and the Correlation Coefficient (K_{fact}) for Ibore gully site

| | Depth | Sand | Silt | Clay | pH | OM | Na | Mg | Ca | K | K_{fact} |
|------------|----------|----------|----------|----------|-------|----------|----------|----------|----------|----------|------------|
| Depth | 1 | -0.945** | 0.874* | 0.949** | 0.806 | -0.912** | 0.901** | -0.947** | -0.945** | -0.955** | 0.889** |
| Sand | -0.945** | 1 | -0.967** | -0.999** | — | — | — | — | — | — | -0.960** |
| Silt | 0.874* | -0.967** | 1 | 0.957** | — | — | — | — | — | — | 0.995** |
| Clay | 0.949** | -0.999** | 0.957** | 1 | — | — | — | — | — | — | 0.950** |
| pH | — | — | — | — | 1 | 0.708 | 0.588 | 0.892 | 0.784 | 0.950 | -0.389 |
| OM | -0.912** | — | — | — | 0.708 | 1 | -0.942** | 0.925** | 0.897** | 0.969** | -0.759* |
| Na | 0.901** | — | — | — | 0.588 | -0.942** | 1 | -0.875** | -0.945** | -0.944** | 0.638 |
| Mg | -0.947** | — | — | — | 0.892 | 0.925** | -0.875** | 1 | 0.918** | 0.925** | -0.849* |
| Ca | -0.945** | — | — | — | 0.784 | 0.897** | -0.945** | 0.918** | 1 | 0.933** | -0.767 |
| K | -0.955** | — | — | — | 0.950 | 0.969** | -0.944** | 0.925** | 0.933** | 1 | -0.823* |
| K_{fact} | 0.889** | -0.960** | 0.995** | 0.950** | — | -0.759* | 0.638 | -0.849 | -0.767 | -0.823* | 1 |
| | | | | | 0.389 | | | | | | |

Table 8: Correlation Matrix Showing Correlation Coefficients (R) among Soil Properties and the Correlation Coefficient (K_{fact}) for AAU Ekpoma gully Site

| | Depth | Sand | Silt | Clay | pH | OM | Na | Mg | Ca | K | K_{fact} |
|------------|----------|----------|---------|----------|---------|----------|----------|----------|----------|----------|------------|
| Depth | 1 | -0.990** | 0.478 | 0.991** | 0.494 | -0.945** | 0.942** | -0.735** | -0.835* | -0.938** | 0.638 |
| Sand | -0.990** | 1 | -0.418 | -0.982** | — | — | — | — | — | — | -0.691 |
| Silt | 0.478 | -0.418 | 1 | 0.237 | — | — | — | — | — | — | 0.897** |
| Clay | 0.991** | -0.982** | 0.237 | 1 | — | — | — | — | — | — | 0.551 |
| pH | 0.494 | — | — | — | 1 | -0.387 | 0.616 | 0.830 | 0.845 | 0.419 | 0.829 |
| OM | -0.945** | — | — | — | -0.387 | 1 | -0.925** | 0.907** | 0.921** | 0.989** | -0.881 |
| Na | 0.942** | — | — | — | -0.616 | -0.926** | 1 | -0.781* | -0.910** | -0.909** | 0.678 |
| Mg | -0.735 | — | — | — | 0.830 | 0.907** | -0.781* | 1 | -0.940** | 0.902** | -0.620 |
| Ca | -0.835** | — | — | — | 0.845 | 0.921** | -0.910** | 0.940** | 1 | 0.907** | -0.598 |
| K | -0.938** | — | — | — | 0.419 | 0.989** | -0.909** | 0.902** | 0.907** | 1 | -0.762* |
| K_{fact} | 0.638 | 0.990** | 0.990** | 0.478 | 0.991** | -0.681 | 0.678 | -0.620 | -0.598 | -0.762 | 1 |

Conclusion

The soil texture for the studied gully sites ranged from sandy to loamy sand with a dispersion ratio of more than 15% and accounts for the erodible nature of the sites. In addition, the weak structure is evidenced by the very low organic matter coupled with high exchangeable sodium potential even at greater depth, hence the soil particles are easily detached and therefore prone to erosion. However, the deep gullies that developed were mainly facilitated by the volume of run-off water that enters the sites.

Acknowledgement

The financial support granted by the Tertiary Education Trust Fund (TETFund) is appreciated.

References

Abu-Hamdeh N and Al-jalil HF (1999). Hydraulically powered soil core sampler and its application to soil density and porosity estimation. *Soil. Tillage Res.*

52:(1-2):113-120.

Akintola, J.O., (2001). Determination of rainfall erosivity for different agro-ecological zones in Nigeria. Unpublished M.Sc. Thesis, Department of Agric. Engrg, University of Ibadan.

Anderson, J. M. and Ingram, J.S.I. (1993). *Tropical soil biology and fertility. A handbook of methods.* Information Press Eynsham.

Bremner, J.M. (1982). Inorganic nitrogen. In Page A.L, Miller, R.H and Keeney, D.R. (eds). *Methods of soil analysis. Part II* 2nd edition. *America Society of Agronomy.* Madison, Wisconsin. p1142.

Bruce-okine E. and Lal, R.(1975). Soil erodibility as determined by rain drop techniques soil Sci. **119** (2) 149-157

Cresswell, H.P and Hamilton, (2002). Particles size analysis. In soil physical

- measurements and interpretation for evaluation. (eds. N.J. Mackenzie, H.P. Cresswell and K.J. Coughlan) CSIRO Publ. Collingwood, Victoria. 224-239.
- Egwuonwu, C. and Uzoije, A.P. (2008). A Comparative Analysis of Coconut, Palm Frond and Palm Stem Fibres As Erosion Control Materials On Embankments. *J. Agric. Sci. Env.*, 9 (2):1-7.
- FAO (2006). Guidelines of soils description, 4th ed. Rome. United Nations. p97.
- Foster G.R., Young, R.A., Romkens M.J.M., and Onstad, C.A. (1985). Processes of soil Erosion by water in R. F. Follet and B.A Steward ed soil erosion and crop Productivity ASA – CSSA –SSSA, Madison. Pp 137–162.
- Frank, H and Althoen, S.C. (1995). *Statistics concepts and applications*. Low price (ed). Cambridge University Press. 539 – 554.
- Fuller, L.G.; Goh, T.B. and Oscarson, D.W. (1995). Cultivation effects on dispersible clay of soil aggregates. *Canadian Journal of Soil Science*. 75: 101-107.
- Goldman, R.C; T.J. Bolling; W.E. Kohlbrenner; Y. Kim and J.L. Fox. (1986). Primary structure of CTP: CMP-3-deoxy-D-manno-octulosonate cytidyltransferase (CMP-KDO synthetase) from *Escherichia coli*. *J. Biol. Chem.* 261:15831-15835.
- Gray, D. (2016). Effect of slope shape on soil erosion. *Journal of Civil Environmental Engineering*. 6: 231.
- Greenland D.J (1977). Soil structure and Erosion hazards in soil conservation and management in humid tropics, Greenland P.J and Lal R. editors pp. 17-23 John Wiley and Sons New York.
- Idah, P.A., H. I. Mustapha; J. J. Musa and Dike, J. (2008). Determination of Erodibility Indices of Soils in Owerri West Local Government Area of Imo State, Nigeria. *Australian Journal of Technology*. 12 (2): 130-133.
- Imeson, A.C, and Vis M. (1984). Assessing soil aggregate stability by water-drop impact and ultrasonic dispersion. *Geoderma* 34: 185-200.
- Luk S.H. (1979). Effect of soil properties on erosion by wash and splash Earth surf Process 4 (3): 241-255.
- MacClean, E. O. (1982). Aluminium. In C. A. Black (ed), *Methods of soil analysis Part II. Agron 9: American Society of Agronomy* Madison, Wisconsin, USA. p927.
- Mitra, B., Scott, H.D., Dixon, J.C. and McKimmey, J.M., (1998). Applications of fuzzy logic to the prediction of soil erosion in a large watershed, *Geoderma*. 86: 183-209.
- Obi, M.E and Asiegbu, B.O. (1980). The physical properties of some eroded soils southwestern Nigeria. *Soil Science*. 130: 39-48.
- Okalebo, J.R; Gathua, K.W and Woomer, P.L. (2002). *Laboratory methods of soil and plant analysis. A working manual*. 2nd edition. Sacred Africa, Nairobi, Kenya. 22-77.
- Okojie, V.U., Isitekhale, H., Salufu, O.S., Ufuah, E., Akhirevbulu, O.E and Okiti, M.O (2019). A three pronged technique for determination of erodibility of soils in gullies of Ibore. *ASUU journal of science*. 5 (1 and 2): 58-76.
- Olsen, S.R and Sommers, L.E. (1982). Phosphorus. In: Page, A.L., Ed., *Methods of Soil Analysis Part 2 Chemical and Microbiological Properties*, American Society of Agronomy, Soil Science Society of America, Madison, 403-430.
- Raine, S.R. and So, H.B. (1994). Ultrasonic dispersion of soil in water: the effect of suspension properties on energy dissipation and soil dispersion. *Australian Journal of Soil Research* 32: 1157-1174.
- Roose, E.J. and Lelong, F. (1976). Factors in water erosion in tropical Africa studies using small experimental soil plots. *Rev. Geogr. Phys. Geol. Dynam.* 18, 365-374.
- Rowell, D. L (1994). *Soil science: Methods & Applications*. Addison Wesley Longman Singapore Publishers (Pte) Ltd., England, UK. 350 p.
- Thomas, G.W. (1982). Exchangeable cations, Pgs 159-165 In: *Methods of soil analysis. Part*

- II (page A. L Miller. R. H., and Keeney. D. R., eds),. 2nd edition. America Society of Agronomy and Soil Science of America. Madison. Wisconsin, USA.
- Tran, L.T., Ridgley, M. A., and Duckstein, L. (2002). Application of Fuzzy Logic-based on the Revised Universal Soil Loss Equation. *Catena*, 47: 203–226.
- Williams J.R., Jones C.A and Dyke P.T. (1984). A Modeling Approach to Determining the Relationship between erosion and productivity. Transactions of the ASAE 27(1):129–144.
- Wischmeier, W.H., Johnson, C.B and Cross, B.V., (1971). A soil erodibility nomograph for farmland and construction sites *.J. Soil Water Conserv.* 26: 189–193.